METAL DECORATED POLYMERIC MEMBRANES FOR LOW TRANS PARTIAL HYDROGENATION OF SOYBEAN OIL

by

DEVINDER SINGH

B.E., Panjab University, 2000
M.S., University of North Dakota, 2005

AN ABSTRACT OF A DISSERTATION

submitted in partial fulfillment of the requirements for the degree

DOCTOR OF PHILOSOPHY

Department of Chemical Engineering
College of Engineering

KANSAS STATE UNIVERSITY
Manhattan, Kansas

2009

Abstract

Multiphase reactions are often constrained by mass transfer limitations which in many cases lead to low reaction rates and undesirable product distribution. Here we fabricate integral-asymmetric polymeric membranes decorated with metal catalysts, to supply hydrogen directly at or near the surface of the catalyst, thus minimizing mass-transfer limitations. The metal decorated polymeric membranes were used for partial hydrogenation of soybean oil with the goal to minimize trans fatty acid (TFA) formation. It was discovered that polymeric membranes with "defective" metal coatings are well suited to achieve low-TFA hydrogenation of soybean oil at quite moderate process conditions.

The metal decorated polymeric membranes studied produced significantly lower trans fatty acid as compared to traditional reactors (3.5 wt% at an Iodine Value of 95 as compared to 8 wt% in slurry reactor), at pressures and temperatures which are compatible with the existing systems. The process concept is simpler than some of the alternatives being studied and no catalyst recovery from the oil is needed since the catalyst is immobilized on the membrane.

Metal decorated polymeric membranes having a variety of hydrogen fluxes, skin defects, and catalyst loadings were evaluated. All the metal decorated polymeric membranes evaluated produced low TFA. Membranes with high hydrogen fluxes resulted in higher hydrogenation rates but had little influence on TFA formation. Membranes with higher catalyst loadings resulted in lower TFA but increased saturate formation.

Metal decorated polymeric membranes behaved differently to changes in temperature and pressures when compared to traditional slurry reactors. They showed a minor increase in TFA with temperature (50-90 °C) as compared to traditional slurry reactors. The hydrogenation rate and cis-trans isomerization also showed a modest dependence on pressure.

Due to the defective nature of the metal layer on the polymeric membrane skin and the low temperatures (50-90 °C) at which the reactor is operating, the hydrogen permeability of metals has a minor influence on hydrogenation reaction. A range of metal catalysts can be used for the given system.

Repeat runs using the same membrane showed a decrease in hydrogenation activity, without any change in isomerization or hydrogenation selectivity. Initial results indicate the decreased activity may not be from leaching of catalyst from membrane surface nor from sulfur poisoning.

METAL DECORATED POLYMERIC MEMBRANES FOR LOW TRANS PARTIAL HYDROGENATION OF SOYBEAN OIL

by

DEVINDER SINGH

B.E., Panjab University, 2000
M.S., University of North Dakota, 2005

A DISSERTATION

submitted in partial fulfillment of the requirements for the degree

DOCTOR OF PHILOSOPHY

Department of Chemical Engineering
College of Engineering

KANSAS STATE UNIVERSITY
Manhattan, Kansas

2009

Approved by:

Co-Major Professor
Dr. Peter H. Pfromm

Approved by:

Co-Major Professor
Dr. Mary E. Rezac

Copyright

Abstract

Multiphase reactions are often constrained by mass transfer limitations which in many cases lead to low reaction rates and undesirable product distribution. Here we fabricate integral-asymmetric polymeric membranes decorated with metal catalysts, to supply hydrogen directly at or near the surface of the catalyst, thus minimizing mass-transfer limitations. The metal decorated polymeric membranes were used for partial hydrogenation of soybean oil with the goal to minimize trans fatty acid (TFA) formation. It was discovered that polymeric membranes with "defective" metal coatings are well suited to achieve low-TFA hydrogenation of soybean oil at quite moderate process conditions.

The metal decorated polymeric membranes studied produced significantly lower trans fatty acid as compared to traditional reactors (3.5 wt% at an Iodine Value of 95 as compared to 8 wt% in slurry reactor), at pressures and temperatures which are compatible with the existing systems. The process concept is simpler than some of the alternatives being studied and no catalyst recovery from the oil is needed since the catalyst is immobilized on the membrane.

Metal decorated polymeric membranes having a variety of hydrogen fluxes, skin defects, and catalyst loadings were evaluated. All the metal decorated polymeric membranes evaluated produced low TFA. Membranes with high hydrogen fluxes resulted in higher hydrogenation rates but had little influence on TFA formation. Membranes with higher catalyst loadings resulted in lower TFA but increased saturate formation.

Metal decorated polymeric membranes behaved differently to changes in temperature and pressures when compared to traditional slurry reactors. They showed a minor increase in TFA with temperature (50-90 °C) as compared to traditional slurry reactors. The hydrogenation rate and cis-trans isomerization also showed a modest dependence on pressure.

Due to the defective nature of the metal layer on the polymeric membrane skin and the low temperatures (50-90 °C) at which the reactor is operating, the hydrogen permeability of metals has a minor influence on hydrogenation reaction. A range of metal catalysts can be used for the given system.

Repeat runs using the same membrane showed a decrease in hydrogenation activity, without any change in isomerization or hydrogenation selectivity. Initial results indicate the decreased activity may not be from leaching of catalyst from membrane surface nor from sulfur poisoning.

Table of Contents

List of Figures

List of Tables

Acknowledgements

I would like to express my deepest appreciation to my advisors, Dr. Peter Pfromm and Dr. Mary Rezac, for their invaluable guidance, continued encouragement and never-ending patience over the course of my doctoral studies. I feel fortunate to have had the opportunity to work with them.

I thank all the members of my advisory committee, Dr. Koushik Adhikari, Dr. Stefan H. Bossmann, and Dr. Keith Hohn, for taking time to serve on my PhD committee, and for their valuable suggestions, comments and guidance.

I am grateful to Dr. Chundi Cao and Myles Ikenberry for performing XPS experiments; Kabeer Jasuja for help with spin coating; Dr. Dan Boyle for performing TEM, Kent Hampton for SEM and for changing the sputtering targets whenever I needed; and Dr. Vikas Berry and Namrita for their guidance, friendship and support.

I also wish to thank former and current members of the research group, especially Juan Cruz, Mohammed Hussain, Ronald Michalsky, Alison Young, and Fan Zhang for their support, suggestions and enjoyable time shared in lab.

I want to express gratitude to the faculty and staff members in the Department of Chemical Engineering: Florence Sperman, Cindy Barnhart, Alison Hodges and David Threewit for their activities related to this research.

The project was supported by the National Research Initiative of the USDA Cooperative State Research, Education and Extension Service, grant number 2005-35503-15398. Their support is greatly appreciated.

Finally, no words will suffice for the endless support, love, and sacrifice from my parents and wife throughout my educational career. I also want to thank my sister and brother for their love and encouragement.

Dedication

To mom and dad, Gurjeet, Ravinder, and Sarabjit for their endless love, support and encouragement.

CHAPTER 1 - Introduction

1.1 Research Motivation

Three phase reactions (liquid-gas-solid) which are widely used in the chemical, petrochemical, biotechnology, and food process industries pose numerous challenges to reactor design, one of them being the slow mass transfer of reactants to the active sites. This causes a scarcity of one or more of the reactants at the catalyst surface and may often lead to lower reaction rates or in some cases [1, 2] have a detrimental effect on the final product composition. The situation is exacerbated if the liquid phase is highly viscous and/or has a low solubility for the gas phase.

Partial hydrogenation of vegetable oil is an important reaction in the food industry, used for the production of base stocks for margarines and shortenings. In the U.S. alone, the annual production of margarines and shortenings was around 8 billion pounds in 2007[3]. It is a three phase (gas-liquid-solid) reaction with hydrogen as a gas, oil as a liquid and the catalyst as a solid. The traditional approach to hydrogenation of vegetable oil is in a batch autoclave over nickel based catalyst in slurry. This approach leads to the formation of high amounts of trans fatty acids[4,5] , which have come under intense scrutiny with regard to human health [6-12]. The amount of TFAs in partially hydrogenated vegetable oil while using traditional reactors can be as high as 40 weight percent [4, 13].

The high amounts of TFA results from low concentration of hydrogen at the surface of the catalyst due to significant gas-liquid mass transfer limitations encountered in conventional industrial hydrogenation reactors[14]. The TFA formed in conventional slurry reactors can be minimized by increasing pressure, decreasing temperature, and increasing agitation to reduce detrimental mass transfer limitations[14]. These process changes increase the hydrogen availability at the surface of the catalyst and lead to lower TFAs. However, there are practical limits to which pressure and agitation can be increased and thereby TFAs reduced in conventional industrial reactors.

1.2 Objective of research

The research will focus on the development of a membrane contactor to allow gas and liquid reactant to come in direct contact with each other without the need for dispersion of one phase into another as is practiced traditionally. More specifically the work will focus on the development of a membrane contactor to allow the hydrogen and vegetable oil to come in direct contact with each other at/near the surface of the catalyst. This will minimize the mass transfer limitations that are prevalent in conventional slurry reactors. The high concentration of hydrogen attained at catalyst surface using this approach should minimize the formation of TFAs. In the course of the research answers to the following questions will be explored:

- Does the supply of hydrogen using a membrane as proposed reduce the amount of TFA formation as compared to traditional slurry reactors?
- Does the proposed catalytic membrane reactor system apply to a wide range of catalysts?
- How does the hydrogen supply rate and nature of hydrogen supplied affect hydrogenation rate and selectivity?
- Does the catalytic membrane reactor system behave similar to conventional reactor systems as far as changes in process conditions like temperature and pressure are concerned?
- Is the catalytic membrane reactor system stable?

1.3 Outline of thesis

The thesis comprises of chapters that are published papers or in the process for publications. These chapters are reproduced here as they were prepared for publication. Some of the other chapters may be developed into publishable papers at a later stage. The details of the chapters are listed below:

Chapter 2 gives a general overview of molecular architecture of vegetable oil, vegetable oil hydrogenation process, and the traditional slurry reactor system for the hydrogenation of vegetable oil. It also gives a theoretical background on polymeric membranes and metal-polymer composite membranes. Some part of this information may be repeated in chapters that are

prepared for publication. The reader may skip this chapter depending on his familiarity with this topic.

Chapter 3 is a published paper that investigates if the supply of hydrogen as proposed reduces the amount of TFA as compared to traditional slurry reactor [15]. The hydrogenation run performed using platinum catalytic membrane are compared with the traditional slurry reactor, and other novel reactor configurations like hydrogenation in supercritical conditions, porous membrane reactors, and electrochemical reactor for vegetable oil hydrogenation.

Chapter 4 explores the applicability of catalytic membranes to various precious metal catalysts and alloys. Hydrogenation results are presented for platinum, palladium, and palladium-lead alloy. These different catalysts are compared in terms of hydrogenation rate, hydrogenation selectivity, and cis-trans isomerization.

Chapter 5 is a paper submitted for publication[16]. It focuses on the properties of the composite membranes that have a significant impact on the hydrogenation rate and cis-trans isomerization. These properties include: the hydrogen flux of the membrane, the presence/absence of defects in the membrane skin, and the catalyst loading on the membrane surface.

Chapter 6 is a paper prepared for publication and is reproduced as is. It explores the behavior of the catalytic membrane reactor as far as changes in temperature and pressure are concerned. The behavior is compared to what is observed in slurry reactors for hydrogenation of vegetable oil.

Chapter 7 evaluates the stability of catalytic membranes for partial hydrogenation of vegetable oil.

Finally, the conclusions and recommendations for future work are made in Chapter 8.

1.4 References:

1. Veldsink JWB, Martin J.; Schoon, Nils-H.; Beenackers, Antonie A. C. M. Heterogeneous hydrogenation of vegetable oils: a literature review. Catalysis Reviews - Science and Engineering. 1997;39(3):253-318.

2. Guettel R, Kunz U, Turek T. Reactors for Fischer-Tropsch synthesis. Chemical Engineering & Technology. May 2008;31(5):746-754.

3. Bureau USC. Current industrial reports. M311K, Fats and oils production, consumption, and stocks. In: Bureau USC, ed; 2007.

4. Musavi A, Cizmeci M, Tekin A, Kayahan M. Effects of hydrogenation parameters on trans isomer formation, selectivity and melting properties of fat. European Journal of Lipid Science and Technology. Mar 2008;110(3):254-260.

5. Dejonge A, Coenen JWE, Okkerse C. Selective Hydrogenation of Linolenate Groups in Soya-Bean Oil. Nature. 1965;206(4984):573-574.

6. Mozaffarian D, Katan MB, Ascherio A, Stampfer MJ, Willett WC. Medical progress - Trans fatty acids and cardiovascular disease. New England Journal of Medicine. Apr 13 2006;354(15):1601-1613.

7. Koletzko B. Trans-Fatty-Acids May Impair Biosynthesis of Long-Chain Polyunsaturates and Growth in Man. Acta Paediatrica. Apr 1992;81(4):302-306.

8. Salmeron J, Hu FB, Manson JE, et al. Dietary fat intake and risk of type 2 diabetes in women. American Journal of Clinical Nutrition. Jun 2001;73(6):1019-1026.

9. Willett WC, Stampfer MJ, Manson JE, et al. Intake of Trans-Fatty-Acids and Risk of Coronary Heart-Disease among Women. Lancet. Mar 6 1993;341(8845):581-585.

10. Oomen CM, Ocke MC, Feskens EJM, van Erp-Baart MAJ, Kok FJ, Kromhout D. Association between trans fatty acid intake and 10-year risk of coronary heart disease in the Zutphen Elderly Study: a prospective population-based study. Lancet. MAR 10 2001;357(9258):746-751.

11. Hunter JE. Dietary levels of trans-fatty acids: basis for health concerns and industry efforts to limit use. Nutrition Research. 2005;22(5):499-513.

12. Hu FB, Manson JE, Willett WC. Types of dietary fat and risk of coronary heart disease: A critical review. Journal of the American College of Nutrition. Feb 2001;20(1):5-19.

13. Coenen JWE. Catalytic-Hydrogenation of Fatty Oils. Abstracts of Papers of the American Chemical Society. 1985;189(Apr-):51-Inde.

14. Dijkstra AJ. Revisiting the formation of trans isomers during partial hydrogenation of triacylglycerol oils. European Journal of Lipid Science and Technology. 2006;108(3):249-264.

15. Singh D, Pfromm PH, and Rezac ME, Partial Hydrogenation of Soybean Oil with Minimal Trans Fat Production Using a Pt-Decorated Polymeric Membrane Reactor. Journal of American Oil Chemists' Society 86 (2009) 93.

16. Singh D, Pfromm PH, Rezac ME. Partial hydrogenation of soybean oil using metal polymer composite membranes: effect of catalyst dispersion and membrane properties. Journal of Membrane Science, submitted, 2009.

CHAPTER 2 - Background

This chapter focuses on the background and literature review of topics relevant to this research. This chapter is divided into two parts; the first section focuses on vegetable oil and its hydrogenation. The second part focuses on membranes and membrane reactors.

2.1 Vegetable oil

Vegetable oils are mixtures of triglycerides which consist of one molecule of glycerol combined with three molecules of fatty acids. Frequently, the three fatty acids have different chemical structures, which are also termed as mixed triglycerides (refer to Figure 2-1). The major fatty acids present in vegetable oils are palmitic acid (nomenclature C16:0, nomenclature: 16 carbon atoms with zero double bonds), stearic acid (C18:0, m.p. 70°C), oleic acid (C18:1), linoleic acid (C18:2), linolenic acid (C18:3, m.p. -11°C), and minor amounts of other fatty acids (C14:0 to C24:0).

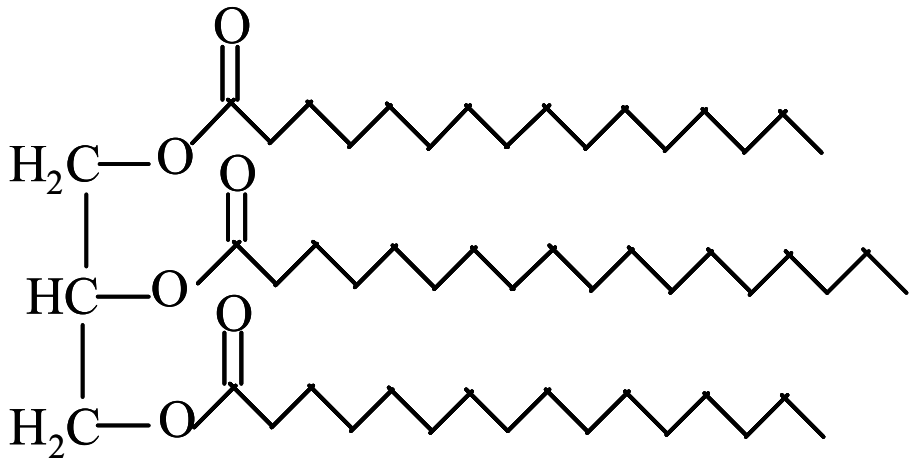

Figure 2-1: Structure of a mixed triglyceride with two palmitic and one stearic acid attached to the glycerol backbone.

It is the composition of the major fatty acids in oil that determines the bulk physical and chemical properties of fats and oils. The properties like melting characteristics and oxidative stability depend on the amount and type of fatty acids on the glycerol molecule. The oxidative stability of different fatty acids follow the following order: C18:1> C18:2 >C18:3. Unsaturation

is associated with lower melting points, greater solubility, and chemical reactivity[1]. Table 2-1 lists the relative oxidation rates and melting points of some common fatty acids. Depending on the fatty acid compositions, the properties of natural oils can vary widely. A triglyceride with one stearic and two oleic acids is 15 times more oxidativly stable as compared to a triglyceride with three linoleic acids. So by modifying the fatty acids attached to the glycerol, the behavior of fat as a whole can be modified.

Table 2-1: Relative oxidation rates and melting points of fatty acids[2,3].

Fatty acid	Relative oxidation rate	Melting point, °C
Stearic	1	70
Oleic	10	14
Linoleic	100	-5
Linolenic	150	-11
α-eleostearic	800	49

The unsaturated bonds in naturally occurring oils are essentially all in the cis configuration meaning that both of the missing hydrogen atoms lie on the same side of the chain. Alternatively, the two hydrogen atoms may be positioned on the opposite side of the chain, which is known as the trans configuration. Trans fatty acids in vegetable oils are formed only during processing of oils like deodorization and hydrogenation.

Figure 2-2 shows the molecular structures of some common cis and trans fatty acids found in processed vegetable oil. Cis isomers are relatively asymmetric in structure and pack poorly in the crystal lattice due to a kink in the structure. Trans double bonds, on the other hand, are relatively symmetric with structure similar to that of saturated fats. These fatty acids pack better in the crystal lattice, thereby increasing their melting points, which falls between the melting temperatures of cis unsaturated and saturated fatty acids. Trans fatty acids have also been associated with adverse health effects[4].

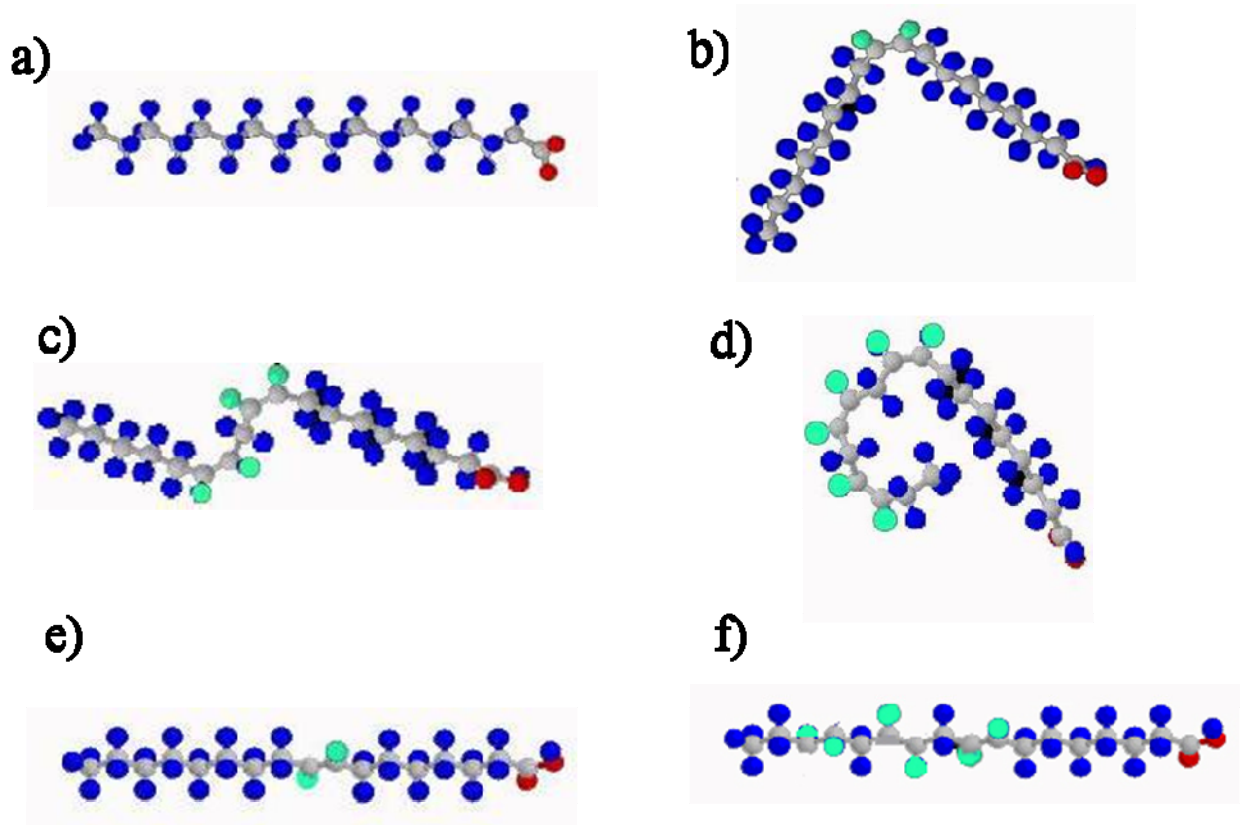

Figure 2-2: Structures of fatty acids commonly present in processed vegetable oil: a) Stearic acid (C18:0), b) Oleic acid (C18:1 9c), c) Linoleic acid (C18:2 9c 11c), d) Linolenic acid (C18:3 9c 11c 13c) e) Elaidic acid (C18:1 9t) f) . All cis unsaturated fatty acids have a kink in their structure while all the trans unsaturated acids have straight structures similar to saturated fats.

2.1.1 *Health effects of trans fatty acids and FDA rules*

There has been health concern that high intake of TFA could adversely affect the risk of coronary heart disease (CHD), partly because the straight configuration of TFA resembles that of saturated fatty acids[4]. Recent studies indicate that increased intake of TFA can contribute to increased risk of CHD because of the following reasons[5]:

- TFA raise LDL cholesterol levels and lower HDL cholesterol levels relative to cis isomers and the increase in the ratio of HDL cholesterol is twice of what is observed for saturated fat[6].
- TFA increases lipoprotein and plasma triglyceride levels which are associated with increased risk of CHD[7, 8].

- TFA can adversely affect essential fatty acid metabolism and may promote thrombogenesis [9].

Increased intake of TFA also promotes inflammation which is associated with increased risk of atherosclerosis, sudden death from cardiac causes, diabetes, and heart failure[10]. Several studies also suggest that TFA cause endothelial dysfunction [11].

Due to the risk factors outlined above, TFA consumption should be kept as low as possible. TFA consumption of less than 0.5 percent of the total energy intake may be necessary to avoid adverse effects [10].

Due to the adverse effects associated with TFA intake, the US Food and Drug Administration (FDA) requires the listing of TFA content on nutritional labels of food products. For the purpose of nutritional labeling, TFA are defined as all unsaturated fatty acids that contain one or more isolated (i.e. nonconjugated) double bonds in a trans configuration[12]. The declaration of trans fats is to be expressed as grams per serving to the nearest 0.5 gram increment below 5 grams and to the nearest gram increment above 5 grams[12]. The amount of TFA can be declared zero if it is less than 0.5 gram per serving.

2.1.2 Vegetable oil hydrogenation

Hydrogenation involves the modification of fatty acids present in vegetable oil to obtain a fatty acid composition profile that has a high oxidative stability and solid fat content most suited for a particular application. The main goals are to minimize C18:3 because of its poor oxidative stability, maintaining C18:2 since it forms a valuable part of the human diet, and minimizing the formation of saturated C18:0. Recent health concerns [4, 13, 14] regarding TFA have added avoiding TFA formation to the list of requirements for vegetable oil hydrogenation. Therefore hydrogenation selectivity is important. Most commonly used definitions of selectivity have been formulated presuming first order reaction scheme as outlined in Equation 2-1[15], where k_1, k_2, k_3, are pseudo-first-order rate constants.

$$C18:3(Ln) \xrightarrow{k_1} C18:2(L) \xrightarrow{k_2} C18:1(O) \xrightarrow{k_3} C18:0(S) \qquad \text{Equation 2-1}$$

The selectivities can now be defined as:

$$S_{Ln} = \frac{k_1}{k_2}$$ Equation 2-2

$$S_L = \frac{k_2}{k_3}$$ Equation 2-3

Linolenic selectivity (S_{Ln}) represents the preferential saturation of trienes over monoenes and linoleic selectivity (S_L) represents the preferential saturation of dienes over monoenes. High values of linoleic and linolenic selectivity are desirable in hydrogenation because at equivalent conversion levels, high value of S_{Ln} and S_L indicate lower level of linolenic and stearic acid, respectively. Since hydrogenation is also accompanied by cis-trans isomerization, and high selectivity towards cis configuration is preferred, a specific isomerization index is used and is defined as:

$$S_i = \frac{\text{Trans double bond formed}}{\text{Double bonds hydrogenated}}$$ Equation 2-4

The conventional hydrogenation of vegetable oil is carried out in a batch autoclave over nickel based catalyst in slurry at 110-190ºC, 30-70 psi hydrogen pressure, with 0.01-0.15wt% Ni catalyst[15] (supported on kieselguhr, silica-alumina, or carbon [3]). The traditional slurry approach to vegetable oil hydrogenation relies on the dissolution of hydrogen in the oil to supply hydrogen to the catalytic sites by diffusion though stagnant liquid boundary layers surrounding the particles. A batch autoclave (typically capable of handling 30,000-90,000 pound batch sizes [17]) equipped with a hydrogen gas distributor, agitator, and heating/cooling coils is generally used and supported Ni catalyst is dispersed in oil.

The vegetable oil hydrogenation process can be described by the Horiuti-Polanyi mechanism [18, 19]. The hydrogen diffuses through the liquid oil and is adsorbed on the catalyst surface where it dissociates into two adsorbed hydrogen atoms. The adsorbed hydrogen atom reacts with the adsorbed fatty acid molecule to form an unstable half-hydrogenated intermediate complex. Depending on the concentration of hydrogen at the catalyst surface, this half-hydrogenated intermediate complex can gain a hydrogen atom and hydrogenate or lose a hydrogen atom and in the process may isomerize. Figure 2-3 shows the hydrogenation and

isomerization reactions involved in the hydrogenation of linolenic fatty acid (C18:2) to oleic acid (C18:1).

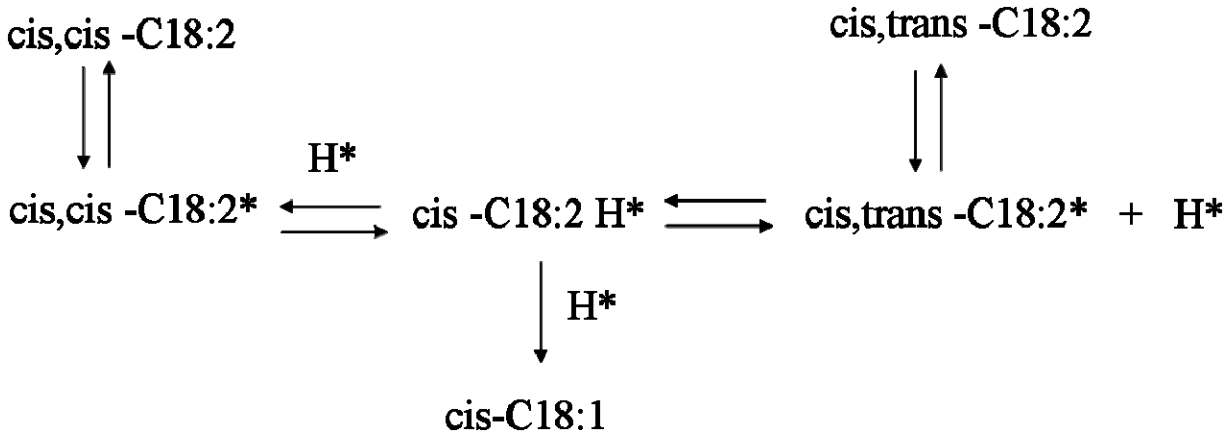

Figure 2-3: Reactions involved in the hydrogenation of Linoleic fatty acid (C18:2) to Oleic acid (C18:1) (* indicates species adsorbed on the catalyst surface).

Due to the low solubility of hydrogen in oils, the conventional industrial hydrogenation slurry reactors suffer from significant gas-liquid mass transfer limitations[15]. This may often lead to the surface of the catalyst being hydrogen starved and result in increased amount of TFAs. The relatively high temperature used in these reactors also promotes the formation of TFAs by increasing the hydrogen consumption rate which exacerbates hydrogen starvation of the catalyst.

2.1.3 Minimizing TFA formation

According to the mechanism discussed above, the formation of TFAs will be encouraged if the steps involving the formation or dissociation of half-hydrogenated intermediate are encouraged. This can be attained by lowering the hydrogen concentration at the catalyst surface. This provides these intermediates time to dissociate and isomerize while doing so[18]. However, if the addition of a hydrogen atom to such an intermediate is encouraged, it will promote hydrogenation and minimize the formation of TFAs. This can be attained by having a high hydrogen concentration at the catalyst surface.

In the industrial hydrogenation process, a high concentration of hydrogen at the catalyst surface can be attained by changes in the process conditions as outlined in Table 2-2. However there are practical limits to which changes in process conditions can decrease the amount of TFAs. Increased pressure and agitation can only be achieved at considerable expense and

reducing the amount of catalyst drastically will render the process unstable[18], so reducing the temperature might be the only viable option.

Table 2-2:Influence of process conditions on hydrogenation selectivity and isomerization [18].

Increase of	Effect upon		
	$[H_2]_{bulk}$	S_L	S_i
Pressure	+	-	-
Agitation	+	-	-
Temperature	-	+	+
Amount of catalyst	-	+	+
Activity of catalyst	-	+	+
Reactivity of oil	-	+	+

Although nickel is the catalyst of choice for industrial hydrogenation of vegetable oils, several studies have focused on the use of precious metals for edible oil hydrogenation [20-27]. Precious metal catalysts are active at considerably lower temperatures and can thus produce less TFA as compared to conventional Ni catalysts. The order of catalytic activity of precious metal catalysts is Pd > Rh > Pt > Ru. The cis-trans isomerization follows the order Pd > Rh > Ru > Pt. Due to the low selectivity of Pt towards cis-trans isomerization, it may be the most interesting metal for future hydrogenation catalysts[15]. A disadvantage of using metal catalysts in slurry systems is the difficult recovery of the catalyst particles from the reaction mixture which results in some loss of precious metal catalyst.

Other modifications which have been studied in an attempt to decrease the amount of TFA formation include using a solvent to increase hydrogen solubility in oil under supercritical conditions [20, 28], using novel reactors like an electrochemical hydrogenation cell [29-32], or other novel reactor configurations [33-35].

2.2 Polymeric membranes

A membrane is a discrete, thin interface that moderates the permeation of chemical species in contact with it[36]. Based on the materials used membranes can be classified broadly as organic (polymeric) membranes and inorganic membranes such as metallic, molecular sieving carbon, zeolites, and ceramics. Polymeric membranes are generally less expensive, easier to process, and more mechanically tunable than their inorganic counterparts[37]. The principal types

of polymeric membranes classified according to their morphology are shown in Figure 2-4 and described briefly below:

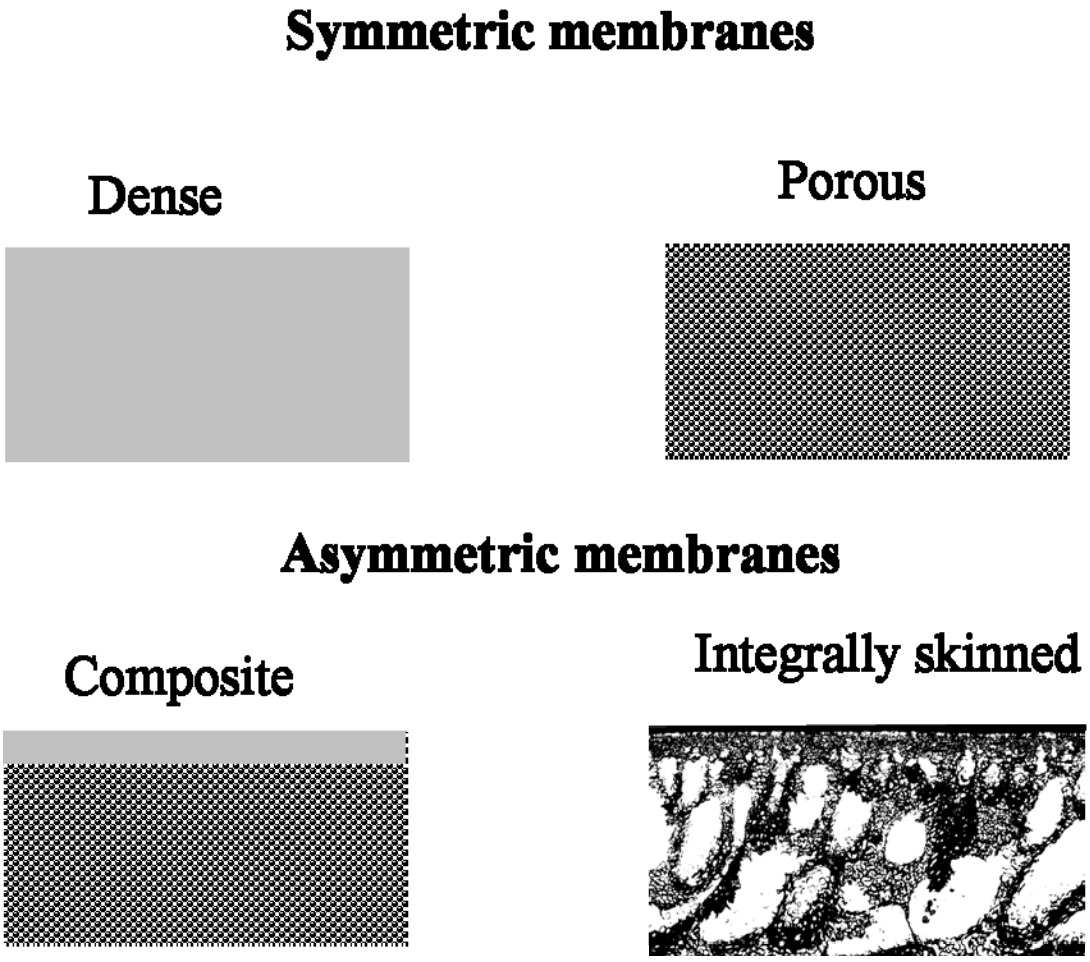

Figure 2-4: Classification of polymeric membranes according to their morphology.

Dense homogeneous polymer membranes have thickness larger than 10 μm and can be prepared from solution by solvent evaporation or extrusion of the melted polymer. The permeant flow across these membranes is quiet low which makes them practical only for highly permeable polymers like silicone.

Porous symmetric membranes can be made by irradiation, stretching, or vapor phase precipitation of a polymer solution and find applications in microfiltration, ultrafiltration, and dialysis[38, 39]. The pores in these membranes are on the order of 0.01 to 10 μm in diameter[36] and particles larger than the pores are completely rejected.

Due to economic reasons a high flow of permeant is desirable which can be attained by having a membrane as thin as possible. However, thin membranes lack mechanical strength.

Asymmetric membranes allow for high flow rates as well as reasonable mechanical strength by having a thin selective layer on a porous support. In *composite membranes* the selective layer and the porous support are made from different polymers. *Integral asymmetric* membranes prepared mostly by the "phase-inversion" process have a dense skin layer supported by a porous support of the same material[37]. These types of membranes find applications in microfiltration, ultrafiltration, reverse osmosis, gas separation, and pervaporation.

2.2.1 Transport through polymeric film/membrane

Transport of gases through a dense polymeric film or the selective layer of an integral asymmetric membrane occurs via solution-diffusion mechanism[36]. It is believed to occur in three steps: sorption of penetrant on the upstream face of the film; diffusion of the penetrant through the polymer; and finally desorption from the downstream face of the film at the permeate side. So the flux of a penetrant will not only depend on its solubility and diffusion in the polymeric material, but also on the driving force and thickness For the same driving force, the permeation rate through these membranes depends on the thickness of the selective layer:

$$J_i = P_i \frac{\Delta p}{l} \qquad \text{Equation 2-5}$$

where J_i is the flux of the gas through the membrane, P_i is the permeability coefficient (product of diffusion and sorption coefficient and is usually expressed in terms of Barrrer, 1 Barrer $=10^{-10}$ cc(STP) cm cm^{-2} s^{-1} $cmHg^{-1}$), Δp is the pressure difference across the membrane, and l is the thickness of the membrane. Permeability is the property of the polymer whereas flux is the property of a membrane.

2.2.2 Membrane characterization

The asymmetric membranes used here are characterized by the ideal gas selectivity, α and gas permeation properties which are excellent indicators of membrane integrity. The ideal gas selectivity is the ratio of the gas permeation rate of two gases at identical feed pressure and is a measure of the potential separation characteristics of the membrane material. For example, $\alpha_{H2/N2}$ values for poly (vinyl fluoride), polyisobutylene, polysulfone and polyetherimide (PEI) are 60[40], 19, 15[41], and 179[42], respectively. Any defects in the membrane skin will result in selectivities that are lower than the ideal value. As the defects become larger, the transport mechanism changes from diffusion process to a pore-flow mechanism. If the defect size is such

that it is smaller than the mean free path of the gas (500-2000 Å at atmospheric pressure) then permeation occurs through Knudsen diffusion and the separation is based on inverse square root of the molecular weights (then $\alpha_{H2/N2}$, Knudsen=3.7)[36]. The different mechanisms for permeation of gases through membranes are shown in Figure 2-5.

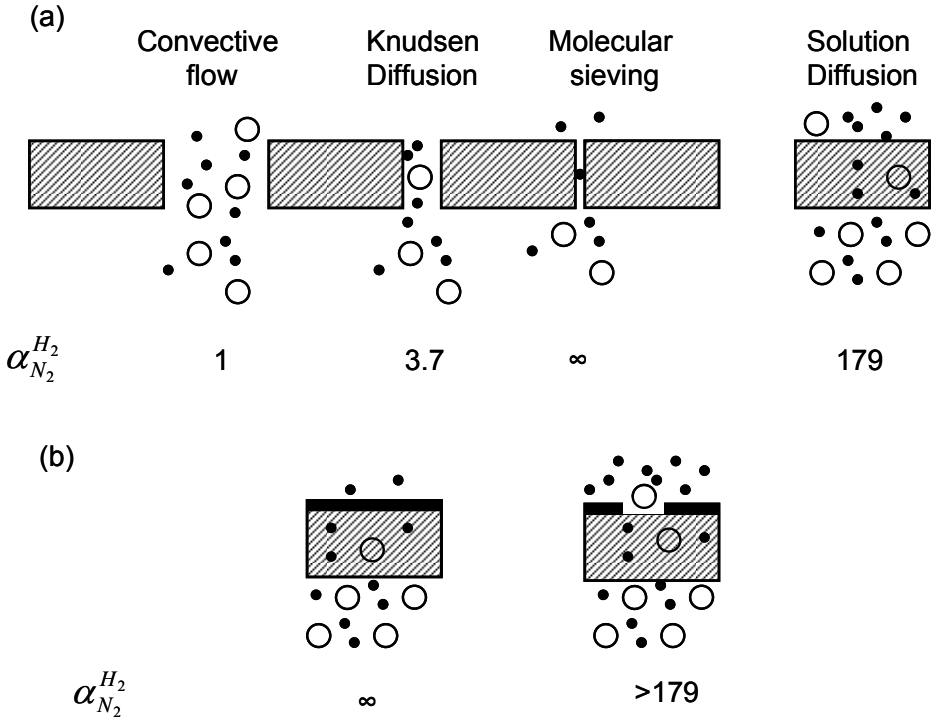

Figure 2-5: Schematic of mechanisms and selectivities for permeation of gases through (a) membrane (PEI) (b) metal-polymer composite membrane (PEI).

The gas permeation rates and selectivity of metal-polymer composite membranes will depend both on the properties of the polymer membrane skin and the metal layer. The diffusion of hydrogen through metals also occurs by the solution-diffusion mechanism due to the difference in chemical potential on the two sides of the membranes. The permeation of hydrogen through metals involves the following steps: dissociative chemisorption on the surface of the metal; absorption into the bulk metal; diffusion to the opposite face through the metal lattice; associative desorption; and diffusion away from the surface into bulk gas. A defect-free metal layer would result in infinite selectivity to hydrogen but pinholes and cracks present in the metal layer result in loss of the ultrahigh selectivity for hydrogen. Baker et al.[43] reported $\alpha_{H2/N2}$ as high as 700 using composite membranes produced by sputtering polyetherimide membranes with Pd-Ag alloy. A defect-free film and high metal loading would also result in very low hydrogen fluxes through the composite membrane.

2.2.3 Membranes as reactors

A membrane as or inside a reactor can serve a variety of functions. Some of the different functions a membrane reactor could perform are: selective product removal for increased conversion; selective reactant supply to increase selectivity; act as an interphase contactor; reactant distribution for better control and facilitating stoichometric feed rates of reactants. Several studies have focused on membranes as reactors to serve the above mentioned functions[44-47]. More recent studies [33-35, 48, 49] have also focused on using membranes for hydrogenation of vegetable oil. The objective has been to minimize mass-transfer limitations for the production of low TFAs [33, 48] or to obtain high reaction selectivities[49]. These studies and their reactor configurations will be discussed in more detail in Chapter 5 of the thesis.

2.3 References

1. Patterson, H. B. W., Hydrogenation of fats and oils. 1983 ed.; Applied Science Publishers Ltd.: 1983.
2. Formo, M. W., General physical and chemical properties of fatty acids. In Fatty acids and their industrial applications, Pattison, E. S., Ed. Marcel Dekker, Inc., New York: 1968.
3. Grau, R. J.; Cassano, A. E.; Baltanas, M. A., Catalysts and Network Modeling in Vegetable Oil Hydrogenation Processes. Catalysis Reviews-Science and Engineering 1988, 30, (1), 1-48.
4. Willett, W. C.; Stampfer, M. J.; Manson, J. E.; Colditz, G. A.; Speizer, F. E.; Rosner, B. A.; Sampson, L. A.; Hennekens, C. H., Intake of Trans-Fatty-Acids and Risk of Coronary Heart-Disease among Women. Lancet 1993, 341, (8845), 581-585.
5. Hu, F. B.; Manson, J. E.; Willett, W. C., Types of dietary fat and risk of coronary heart disease: A critical review. Journal of the American College of Nutrition 2001, 20, (1), 5-19.
6. Zock, P. L.; Katan, M. B., Hydrogenation Alternatives - Effects of Trans-Fatty-Acids and Stearic-Acid Versus Linoleic-Acid on Serum-Lipids and Lipoproteins in Humans. Journal of Lipid Research 1992, 33, (3), 399-410.
7. Sundram, K.; Ismail, A.; Hayes, K. C.; Jeyamalar, R.; Pathmanathan, R., Trans (elaidic) fatty acids adversely affect the lipoprotein profile relative to specific saturated fatty acids in humans. Journal of Nutrition 1997, 127, (3), S514-S520.
8. Utermann, G., The Mysteries of Lipoprotein(a). Science 1989, 246, (4932), 904-910.

9. Kinsella, J. E.; Bruckner, G.; Mai, J.; Shimp, J., Metabolism of Trans Fatty-Acids with Emphasis on the Effects of Trans,Trans-Octadecadienoate on Lipid-Composition, Essential Fatty-Acid, and Prostaglandins - an Overview. American Journal of Clinical Nutrition 1981, 34, (10), 2307-2318.

10. Mozaffarian, D.; Katan, M. B.; Ascherio, A.; Stampfer, M. J.; Willett, W. C., Medical progress - Trans fatty acids and cardiovascular disease. New England Journal of Medicine 2006, 354, (15), 1601-1613.

11. De Roos, N. M.; Bots, M. L.; Katan, M. B., Replacement of dietary saturated fatty acids by trans fatty acids lowers serum HDL cholesterol and impairs endothelial function in healthy men and women. Arteriosclerosis Thrombosis and Vascular Biology 2001, 21, (7), 1233-1237.

12. Moss, J.; Wilkening, V., Trans Fat-New FDA Regulations. In Trans Fat Alternatives, Kodali, D. R.; List, G. R., Eds. AOCS Press: 2005.

13. Hunter, J. E., Dietary levels of trans-fatty acids: basis for health concerns and industry efforts to limit use. Nutrition Research 2005, 22, (5), 499-513.

14. Salmeron, J.; Hu, F. B.; Manson, J. E.; Stampfer, M. J.; Colditz, G. A.; Rimm, E. B.; Willett, W. C., Dietary fat intake and risk of type 2 diabetes in women. American Journal of Clinical Nutrition 2001, 73, (6), 1019-1026.

15. Veldsink, J. W. B., M.J.; Schoon, N.H.; Beenackers, Antonie A. C. M., Heterogeneous hydrogenation of vegetable oils: a literature review. Catalysis Reviews - Science and Engineering 1997, 39, (3), 253-318.

16. Coenen, J. W. E., Hydrogenation of Edible Oils. Journal of the American Oil Chemists Society 1976, 53, (6), 382-389.

17. Farr, W. E., Hydrogenation: processing technologies. In Bailey's Industrial Oil and Fat Products, Shahidi, F., Ed. John Wiley & Sons: 2005; Vol. 5.

18. Dijkstra, A. J., Revisiting the formation of trans isomers during partial hydrogenation of triacylglycerol oils. European Journal of Lipid Science and Technology 2006, 108, (3), 249-264.

19. Horiuti, I.; Polanyi, M., Exchange reactions of hydrogen on metallic catalysts. Trans. Faraday Soc. 1934, 30, 1164 - 1172.

20. Piqueras, C. A.; Tonetto, G.; Bottini, S.; Damiani, D. E., Sunflower oil hydrogenation on Pt catalysts: Comparison between conventional process and homogeneous phase operation using supercritical propane. Catalysis Today 2008, 133, 836-841.

21. Piqueras, C. M.; Fernandez, M. B.; Tonetto, G. M.; Bottini, S.; Damiani, D. E., Hydrogenation of sunflower oil on Pd catalysts in supercritical conditions: Effect of the particle size. Catalysis Communications 2006, 7, (6), 344-347.

22. Nohair, B.; Especel, C.; Marecot, P.; Montassier, C.; Hoang, L. C.; Barbier, J., Selective hydrogenation of sunflower oil over supported precious metals. Comptes Rendus Chimie 2004, 7, (2), 113-118.

23. Santana, A.; Larrayoz, M. A.; Ramirez, E.; Nistal, J.; Recasens, F., Sunflower oil hydrogenation on Pd in supercritical solvents: Kinetics and selectivities. Journal of Supercritical Fluids 2007, 41, (3), 391-403.

24. Ahmad, M. M.; Priestley, T. M.; Winterbottom, J. M., Palladium-Catalyzed Hydrogenation of Soybean Oil. Journal of the American Oil Chemists Society 1979, 56, (5), 571-577.

25. Hsu, N.; Diosady, L. L.; Rubin, L. J., Catalytic Behavior of Palladium in the Hydrogenation of Edible Oils. Journal of the American Oil Chemists Society 1988, 65, (3), 349-356.

26. Hsu, N. Catalytic hydrogenation of canola and soybean oils using transition metal complexes and supported/unsupported palladium. University of Toronto, Toronto, 1987.

27. Maki-Arvela, P.; Kuusisto, J.; Sevilla, E. M.; Simakova, I.; Mikkola, J. P.; Myllyoja, J.; Salmi, T.; Murzin, D. Y., Catalytic hydrogenation of linoleic acid to stearic acid over different Pd- and Ru-supported catalysts. Applied Catalysis a-General 2008, 345, (2), 201-212.

28. King, J. W.; Holliday, R. L.; List, G. R.; Snyder, J. M., Hydrogenation of vegetable oils using mixtures of supercritical carbon dioxide and hydrogen. Journal of the American Oil Chemists Society 2001, 78, (2), 107-113.

29. Pintauro, P. N. Synthesis of a low-trans content edible oil, non-edible oil, or fatty acid in a solid polymer electrolyte reactor. 6218556 B1, 2001.

30. Pintauro, P. N.; Gil, M. P.; Warner, K.; List, G.; Neff, W., Electrochemical hydrogenation of soybean oil with hydrogen gas. Industrial & Engineering Chemistry Research 2005, 44, (16), 6188-6195.

31. An, W. D.; Hong, J. K.; Pintauro, P. N.; Warner, K.; Neff, W., The electrochemical hydrogenation of edible oils in a solid polymer electrolyte reactor. II. Hydrogenation selectivity studies. Journal of the American Oil Chemists Society 1999, 76, (2), 215-222.

32. Mondal, K.; Lalvani, S., Low temperature soybean oil hydrogenation by an electrochemical process. Journal of Food Engineering 2007, 84, (4), 526-533.

33. Fritsch, D.; Bengtson, G., Development of catalytically reactive porous membranes for the selective hydrogenation of sunflower oil. Catalysis Today 2006, 118, (1-2), 121-127.

34. Schmidt, A.; Haidar, R.; Schomacker, R., Selectivity of partial hydrogenation reactions performed in a pore-through-flow catalytic membrane reactor. Catalysis Today 2005, 104, (2-4), 305-312.

35. Schmidt, A.; Schomacker, R., Partial hydrogenation of sunflower oil in a membrane reactor. Journal of Molecular Catalysis a-Chemical 2007, 271, (1-2), 192-199.

36. Baker, R. W., Membrane technology and applications. 2nd ed.; John Wiley & Sons, Ltd: 2004.

37. Nenoff, T. M.; Spontak, R. J.; Aberg, C. M., Membranes for hydrogen purification: An important step toward a hydrogen-based economy. Mrs Bulletin 2006, 31, (10), 735-741.

38. Strathmann, H., Membrane Separation Processes. Journal of Membrane Science 1981, 9, (1-2), 121-189.

39. Pinnau, I. Skin formation of integral-asymmetric gas separation membranes made by dry/wet phase inversion. PhD Thesis, The University of Texas at Austin, 1991.

40. Kesting, R. E.; Fritzsche, A. K., Polymeric gas seperation membranes. John wiley & Sons, Inc.: 1993.

41. Adhikari, S.; Fernando, S., Hydrogen membrane separation techniques. Industrial & Engineering Chemistry Research 2006, 45, (3), 875-881.

42. Barbari, T. A.; Koros, W. J.; Paul, D. R., Polymeric Membranes Based on Bisphenol-a for Gas Separations. Journal of Membrane Science 1989, 42, (1-2), 69-86.

43. Baker, R. W., Louie, J., Pfromm, P. H., Wijmans, J. G Ultrathin Metal Composite Membranes for Gas Separation. 4,857,080, 1989.

44. Uemiya, S., Brief review of steam reforming using a metal membrane reactor. Topics in Catalysis 2004, 29, (1-2), 79-84.

45. Vankelecom, I. F. J., Polymeric membranes in catalytic reactors. Chemical Reviews 2002, 102, (10), 3779-3810.

46. Rezac, M. E.; Koros, W. J.; Miller, S. J., Membrane-Assisted Dehydrogenation of N-Butane Influence of Membrane-Properties on System Performance. Journal of Membrane Science 1994, 93, (2), 193-201.

47. Ozdemir, S. S.; Buonomenna, M. G.; Drioli, E., Catalytic polymeric membranes: Preparation and application. Applied Catalysis a-General 2006, 307, (2), 167-183.

48. Fritsch, D.; Bengtson, G., Catalytic polymer membranes for high temperature hydrogenation of viscous liquids. Advanced Engineering Materials 2006, 8, (5), 386-389.

49. Veldsink, J. W., Selective hydrogenation of sunflower seed oil in a three-phase catalytic membrane reactor. Journal of the American Oil Chemists Society 2001, 78, (5), 443-446

CHAPTER 3 - Partial Hydrogenation of Soybean Oil with Minimal Trans Fat Production using a Pt-decorated Polymeric Membrane Reactor

3.1 Introduction

The partial hydrogenation of vegetable oil to improve its oxidative stability and increase its solid fat content has been practiced since the early 19th century. Improved oxidative stability increases the shelf life of the product and the solid fat content makes it more suitable for margarines, shortenings, and baking applications. Recent health concerns regarding trans fatty acids (TFAs) formed during partial hydrogenation of oil have led to a renewed interest in hydrogenation technologies and process modifications that minimize TFAs. Ideally, the technology being considered should be easy to commercialize and compatible with the existing hydrogenation facilities. Processing temperatures and hydrogen pressures compatible with existing capital equipment are especially important.

The vegetable oil hydrogenation process can be described by the Horiuti-Polanyi mechanism in which hydrogen dissociates on the catalyst surface and forms an unstable half-hydrogenated intermediate complex with the adsorbed fatty acid molecule. The half-hydrogenated intermediate formed can isomerize, or add or loose additional hydrogen, depending on the concentration of hydrogen at the surface of the catalyst. A high concentration of hydrogen at the surface of the catalyst would favor hydrogenation while a lower concentration of hydrogen at the surface of the catalyst would favor isomerization and thus the formation of TFAs [1].

Industrial hydrogenation of vegetable oil is a three-phase (gas-solid-liquid) process generally carried out in a batch autoclave over nickel based catalyst as a slurry at 110-190 ºC, 30-70 psi hydrogen pressure, with 0.01-0.15 weight percent Ni [2]. Due to low solubility of hydrogen in oils, the conventional industrial hydrogenation slurry reactors suffer from significant gas-liquid mass transfer limitations. This may often lead to the surface of the catalyst being hydrogen starved and result in increased formation of TFAs. The relatively high

temperature used in these reactors also promotes the formation of TFAs by increasing the hydrogen consumption rate which exacerbates hydrogen starvation of the catalyst surface. TFA formation can be minimized by increasing pressure, decreasing temperature, and increasing agitation to address mass transfer limitations[3]. These changes increase the hydrogen availability at the surface of the catalyst and lead to lower TFA. However, there are practical limits to which pressure and agitation can be increased and thereby TFA reduced in conventional industrial reactors.

Precious metal catalysts are active at considerably lower temperatures and can thus produce less TFA as compared to conventional Ni catalysts. The order of catalytic activity of precious metal catalysts is Pd > Rh > Pt > Ru. The cis-trans isomerization follows the order Pd > Rh > Ru > Pt[1]. Due to the low selectivity of Pt towards cis-trans isomerization, it may be the most interesting metal for future hydrogenation catalysts [2]. Several studies focus on the use of precious metal catalysts for partial hydrogenation of vegetable oil[4]. A disadvantage of using metal catalysts in slurry systems is the difficult recovery of the catalyst particles from the reaction mixture which results in loss of precious metal catalyst.

Other modifications which have been reported to lead to low TFA include using a solvent to increase hydrogen solubility in oil under supercritical conditions[5], using novel reactors like electrochemical hydrogenation cell [6], or other novel reactor configurations[7-9].

Here we demonstrate the hydrogenation of soybean oil over metal/polymer composite asymmetric membrane with platinum catalyst deposited on the "skin" side of an integral-asymmetric polymeric membrane and hydrogen being supplied directly at or near the surface of the catalyst. The concept of supplying hydrogen at the catalyst surface was studied by Gryaznov et al.[10] for the hydrogenation of cyclopentadiene. A polydimethylsiloxane film was covered with a dense layer of Pd-Ru alloy which supplied atomic hydrogen at the surface of the catalyst for the hydrogenation reaction. The very low hydrogen permeability of metals, however, does limit the efficiency of this process. The Pt catalyst layer in our case is imperfect and has defects which are beneficial for the process as is discussed below. The hydrogenation results obtained are compared with conventional slurry system and other developing technologies.

3.1.1 Concept

The metal/polymer composite catalytic membrane used here consists of an integral asymmetric membrane with high flux and selectivity for hydrogen and negligible permeability to vegetable oil. The polymeric membrane consists of a highly porous substructure with a thin (approximately 0.2 microns) dense and defect-free layer known as the membrane skin which results in high hydrogen selectivity and flux for defect-free membranes. Gases permeate through the thin skin by the well-known solution/diffusion mechanism while the porous substructure allows for convection. These solution diffusion polymeric membranes have no continuous passages but rely on the thermally agitated motion of chain segments comprising the polymer matrix to generate penetrant scale transient gaps in the matrix, thereby allowing diffusion through the membrane [11]. The membrane skin is coated with a very thin layer of platinum using a magnetron sputter. Hydrogen would emerge only as atomic hydrogen at the oil side of the metal coating if the platinum layer was defect free. This would result in quite low hydrogen fluxes [12]. The platinum layer on the membrane used in our case has defects which results in significant hydrogen fluxes with our sputtered membranes (see below). This, however, is neither unexpected nor detrimental to our concept.

Figure 3-1 shows a proposed schematic of our vegetable oil hydrogenation process. In the concept studied, hydrogen is supplied from the porous side of the membrane and oil is pumped across the skin/platinum side of the membrane where it comes in contact with the catalytic metal. A positive hydrostatic pressure is maintained on the oil side to prevent the membrane from being mechanically destroyed. We assume that the hydrogen diffuses mainly through the defect-free polymeric skin under the driving force of a hydrogen partial pressure difference maintained by consumption of hydrogen by hydrogenation reaction near the membrane surface. Since the hydrogen is supplied near or at the catalytic sites and in part as atomic hydrogen permeating metal-coated portions of the membrane we expect that TFAs will be reduced since hydrogen starvation of the catalytic surface can be avoided. If hydrogen builds up in the oil then the driving force for hydrogen permeation will diminish which represents a type of self-limiting mechanism for hydrogen transport through the membrane to the oil phase.

Thus, we propose to minimize TFA formation by avoiding hydrogen starvation of the catalyst surface by directly supplying hydrogen to the catalytic sites via "reverse permeation”

(from substructure to skin) of a high-flux thin film asymmetric metal/polymer composite membrane with a perfect polymer skin and a "defective" metal coating.

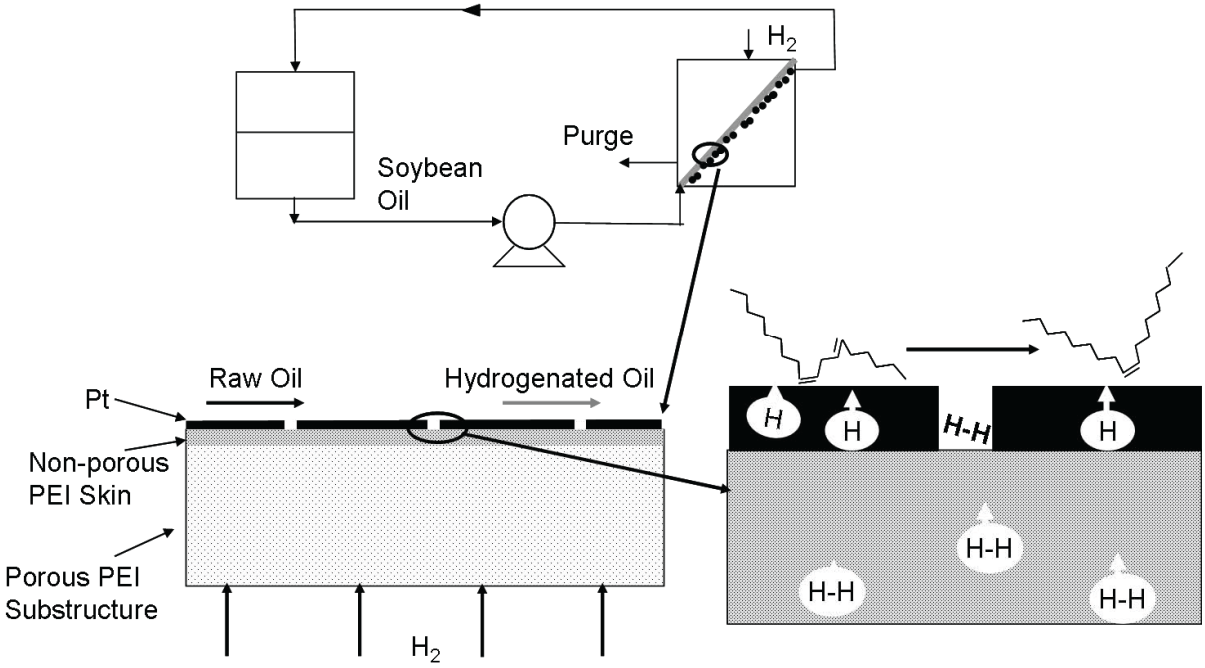

Figure 3-1: Schematic of vegetable oil hydrogenation as it would take place in the catalytic membrane reactor.

3.2 Experimental procedure

3.2.1 Materials

Soybean oil (Iodine Value IV = 129-131) was obtained from MP Biomedicals (Solon, OH). Table 3-1 gives the composition of soybean oil used for hydrogenation experiments. PEI to cast asymmetric membranes was obtained from General Electric (Huntersville, NC, Ultem-1000). Acetic acid (HPLC grade), acetone (99.5%), p-xylene (99.9%), and dicholoromethane (99.9%), used in membrane casting were obtained from Fisher Scientific (Rochester, NY), 1,1,2,2-tetrachloroethane (98%), and, a 5 wt% Platinum on activated carbon catalyst used in hydrogenation experiments were from Sigma Aldrich (St. Louis, MO). Platinum target (99.95wt% platinum) for membrane sputtering was from Ted Pella Inc. (Redding, CA).

Table 3-1: Composition of soybean oil used in hydrogenation experiments

Component	Content, weight percent
C16:0	11.6-12.0
C18:0	4.3-4.4
C18:1	21.6-23.8
C18:2	51.6-53.3
C18:3	7.1-7.8
Total trans fatty acids	0.7-1.2
C18:1 trans	0
14:0-24:0	0.9-1.5

3.2.2 Membrane preparation

The integral asymmetric PEI membranes used in this study were fabricated using the phase inversion process as described by Peinemann [13]. About 170 ml of a solution containing 15.9 weight percent polyetherimide, 54.6 weight percent dichloromethane, 4.8 weight percent 1,1,2,2-tetrachloroethane, 17.6 weight percent xylene (swelling/pore forming agent) and 7.1 weight percent acetic acid (swelling/pore forming agent) was prepared. The polymer solution was cast onto a pre-cooled glass plate (11x8.5 inch, 16-18 °C) as a film of approximately 350 micrometer thickness using a Gardner knife. After 3-4 seconds evaporation in air by free convection the nascent membrane is submerged in an acetone bath at 12-16ºC for 30 minutes. The nascent membranes are then air dried overnight. Circular stamps (4.6 cm diameter) are cut and tested in a filter holder (see below) for their gas flux using a constant-volume variable-pressure apparatus similar to the one described elsewhere [14]. All evaluations were completed at 25 °C with a feed pressure of 65 psi. The normalized gas flux and the ideal gas selectivity (H_2/N_2) are calculated as a quality control. The ideal gas selectivity $\alpha_{H2/N2}$ is the ratio of the normalized gas fluxes for gas H_2 and N_2 at a given temperature and feed pressure.

The hydrogen flux of these membranes can be as high as 100 GPU (one gas permeation unit or GPU equals 10^{-6} $cm^3(STP)$ $cm^{-2}s^{-1}cmHg^{-1}$) and ideal gas selectivities measured by single gas permeation of $\alpha_{H2/N2}$ up to 179 at 35 °C(ideal $\alpha_{H2/N2}$ for PEI) [15]. Any defects in the membrane skin result in ideal gas selectivities that are lower than 179. Membranes

were deemed acceptable with a hydrogen flux of at least 20 GPU before sputtering and $\alpha_{H2/N2}$ of at least 40 before sputtering with platinum.

Acceptable membranes were stored in air. Before use in hydrogenation experiments the membranes were sputtered on the skin side with platinum using a DESK II magnetron sputter (Denton Vacuum, Moorestown, NJ, 3 seconds at 45 mA, 100 mtorr) and were re-tested for their gas transport properties. The gas flux of the membranes is reduced by on the order of 4-5 fold after sputtering as can be expected from coverage of the membrane with a metal layer containing defects. Gas selectivities after sputtering also change and the change depends on factors such as initial $\alpha_{H2/N2}$, and the defects on the platinum sputtered layer.

The loading of the platinum on the membrane was determined by sputtering platinum on a quartz crystal under the same sputtering conditions as used for sputtering the membrane and measuring the weight of the deposited ($\mu g\ cm^{-2}$) platinum using a quartz crystal microbalance.

Figure 3-2a shows an SEM image of an integral asymmetric PEI membrane manufactured in our laboratory using the method [13] discussed above. As shown in Figure 3-2a, the membrane consists of a highly porous substructure with a thin dense layer known as the membrane skin. Figure 3-2b shows SEM of the membrane surface after sputtering with platinum. As shown in Figure 3-2b, the platinum layer has defects which result in high hydrogen fluxes through the sputtered membrane. Table 3-2 gives the properties of the catalytic membrane used in the hydrogenation experiment. The high value of $\alpha_{H2/N2}$ means that the membrane skin was defect-free but the platinum layer was not. The final flux of the membrane used in hydrogenation experiment was 15 GPU with a Pt catalyst loading of 0.86 $\mu g\ cm^{-2}$.

3.2.3 Experimental setup and procedure

The platinum sputtered membrane was installed in a stainless steel 47 mm filter holder (model XX4404700, Millipore Corp., Billerica. MA). Figure 3-3 shows the schematic of the experimental setup used for hydrogenation with the catalytic membrane. Before the start of the hydrogenation reaction the Pt catalyst on the membrane was reduced using hydrogen at 60 ºC for 15 hours applied to the platinum (skin) side of the membrane with the permeate side open to the atmosphere. About 13.7-13.8 grams of oil were added to the system. To avoid oil oxidation, air was removed from the system with a nitrogen purge before heating the oil. The oil was circulated with a flow rate of about 25 grams/min across the platinum sputtered side of the

membrane using a gear pump (series GA, Micropump Inc., Vancouver, WA). The oil side pressure was maintained at 75 psi using ultra high purity (UHP) nitrogen applied to the headspace of the reactor. UHP hydrogen was supplied from the porous substructure side of the membrane at 65 psi after the reaction temperature of 70 °C was attained. The hydrogenation reaction was allowed to proceed for 8 hours with oil sample taken after every 2 hours and analyzed. The conventional slurry reactor run was performed in a Parr Reactor (model number 4565) using 50 grams of soybean oil and 0.05 gram of 5 wt% Pt on activated carbon as catalyst. The reaction was performed at 70 °C, 65 psi hydrogen pressure with a stirring speed of 300 rpm (standard four blade turbine type impeller).

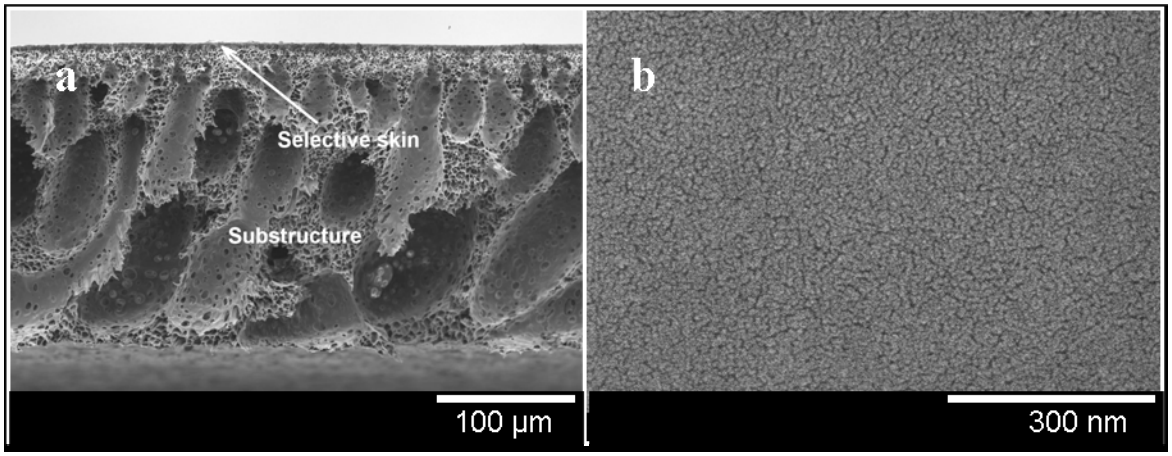

Figure 3-2: SEM images of Pt sputtered integral asymmetric PEI membrane. a) Cross-section of membrane showing the porous substructure and the dense selective skin. b) Surface of the membrane showing the defective platinum layer.

Table 3-2: Properties of catalytic membrane used in soybean oil hydrogenation experiment.

	Before Pt sputtering	After Pt sputtering
H_2 flux, GPU	35	15
H_2/N_2 selectivity	170	200
Catalyst loading, µg cm^{-2}	-	0.86

3.2.4 Analysis

Oil samples were converted to their corresponding fatty acid methyl esters (FAMEs) following the alternate method in AOCS official method Ce 2-66. FAMEs thus obtained were analyzed by gas chromatography (GC) using a 100 m CP-Sil 88 column in a Hewlett-Packard 6890 series gas chromatograph. AOCS official method Ce 1h-05 was followed for the analysis of fatty acids. The injection port and column were maintained at 250 ºC and 181 ºC, respectively, helium carrier gas at 1 ml/min and split injection (split ratio 1:100) was used. The IV of hydrogenated oil was calculated from the composition obtained by GC analysis using Equation 3-1[16].

$$IV = (\%C16{:}1 \times 0.9502) + (\%C18{:}1 \times 0.8598) + (\%C18{:}2 \times 1.7315) + (\%C18{:}3 \times 2.6152) \quad \text{Equation 3-1}$$

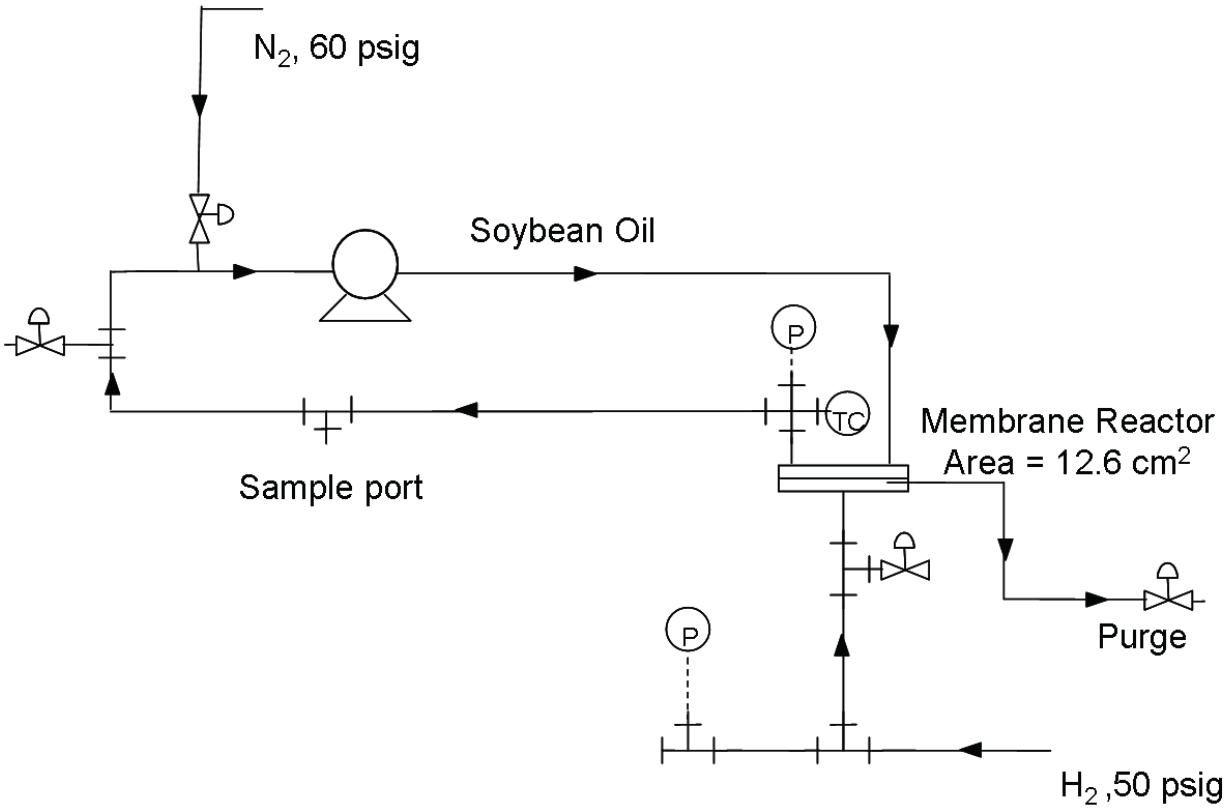

Figure 3-3: Schematic of the experimental setup used for hydrogenation runs with catalytic membrane (all oil containing lines heat traced, membrane reactor insulated with glass wool).

3.2.5 Hydrogenation selectivity calculation

If the hydrogenation of soybean oil is represented by the first-order irreversible reaction scheme as shown in Equation 3-2, then it is possible to calculate hydrogenation selectivities using the experimental composition data from our experiments [17].

$$C18:3(Ln) \xrightarrow{k_1} C18:2(L) \xrightarrow{k_2} C18:1(O) \xrightarrow{k_3} C18:0(S) \qquad \text{Equation 3-2}$$

$$S_{Ln} = \frac{k_1}{k_2} \qquad \text{Equation 3-3}$$

$$S_L = \frac{k_2}{k_3} \qquad \text{Equation 3-4}$$

$$S_O = \frac{k_1}{k_3} \qquad \text{Equation 3-5}$$

Integrating the appropriate rate equations based on Equation 3-2 for the mol% of linolenate [Ln], linoleate [L], and oleate [O] fatty acids and rearranging yields [17]:

$$[Ln]_t = [Ln]_{t=0}\, e^{-k_1 t} \qquad \text{Equation 3-6}$$

$$[L]_t = [Ln]_{t=0}\left(\frac{k_1}{k_2 - k_1}\right)\left(e^{-k_1 t} - e^{-k_2 t}\right) + [L]_{t=0}\, e^{-k_2 t} \qquad \text{Equation 3-7}$$

$$[O]_t = [Ln]_{t=0}\left(\frac{k_1}{k_2 - k_1}\right)\left(\frac{k_2}{k_3 - k_1}\right)\left(e^{-k_1 t} - e^{-k_3 t}\right) \quad - \quad [Ln]_{t=0}\left(\frac{k_1}{k_2 - k_1}\right)\left(\frac{k_2}{k_3 - k_2}\right)\left(e^{-k_2 t} - e^{-k_3 t}\right) +$$

$$[L]_{t=0}\left(\frac{k_2}{k_3 - k_2}\right)\left(e^{-k_2 t} - e^{-k_3 t}\right) + [O]_{t=0}\, e^{-k_3 t} \qquad \text{Equation 3-8}$$

The selectivities reported here were calculated using our experimentally determined oil composition and then solving equations [6-8] to obtain k_1, k_2, and k_3 using a computer code as described in AOCS official method Tz 1b-79 . The code was rewritten in Java with a convergence criterion of 0.01%.

3.3 Results and discussion

An improved soybean oil hydrogenation process must not only significantly reduce the formation of TFA at comparable levels of hydrogenation as represented by the target IV number

but the process must ideally do so at hydrogen pressures, operating temperatures, and stirring speeds that do not require major modifications to existing facilities. The need for costly catalyst materials must be minimized and long catalyst life is desirable. Below we show a comparison of the metal/polymer catalytic integral-asymmetric membrane process with conventional and other novel approaches.

Figure 3-4 compares the TFA vs. IV profile obtained for hydrogenation experiments using platinum membrane, Pt/C slurry reactor, Pt/TiO_2 slurry reactor[18] and conventional Ni slurry reactor[19]. It should be kept in mind that for the same catalyst hydrogen starvation of the catalyst surface results in increased TFA formation. As expected the conventional Ni slurry reactor produced the most TFA, 24.5 weight percent at an IV of 95 [19]. The extremely high amount of TFA produced using Ni slurry reactor is due to the high selectivity of Ni catalysts for TFA formation as compared to Pt catalysts and also due to higher reaction temperatures used that result in the catalyst surface being hydrogen starved. The hydrogenation run using the platinum membrane (70 °C, 65 psi H_2, membrane H_2 flux =15 GPU, membrane $\alpha H_2/N_2$ = 200) produced the least amount TFA, 3.5 weight percent at an IV of 95. Hydrogenation run under similar conditions of temperature and pressure with Pt/C slurry reactor produced significantly higher TFA as compared to the catalytic membrane reactor (more than 8 weight percent TFA at an Iodine Value of 95). Conventional slurry hydrogenation runs reported with Pt/TiO_2[18] (100 °C, 60 psi H_2) produced much higher TFA 12.5 weight percent at an IV of 95, possibly due to the higher temperature used for the reaction. We hypothesize that our concept of supplying hydrogen from the substructure of the metal/polymer composite membrane directly at or near the catalytic sites reduces TFA formation due to alleviating hydrogen starvation of the catalyst surface when compared to supplying hydrogen by diffusion from the bulk oil phase.

Due to the different metal/oil ratios, metal dispersion, and type of reactors used, it may be inappropriate to directly compare the reaction rates for all the above cases. However, in order to provide an insight into the hydrogenation rates obtained in catalytic membrane reactor, the secondary x-axis in Figure 3-4 gives the time corresponding to the iodine values for the catalytic membrane reactor.

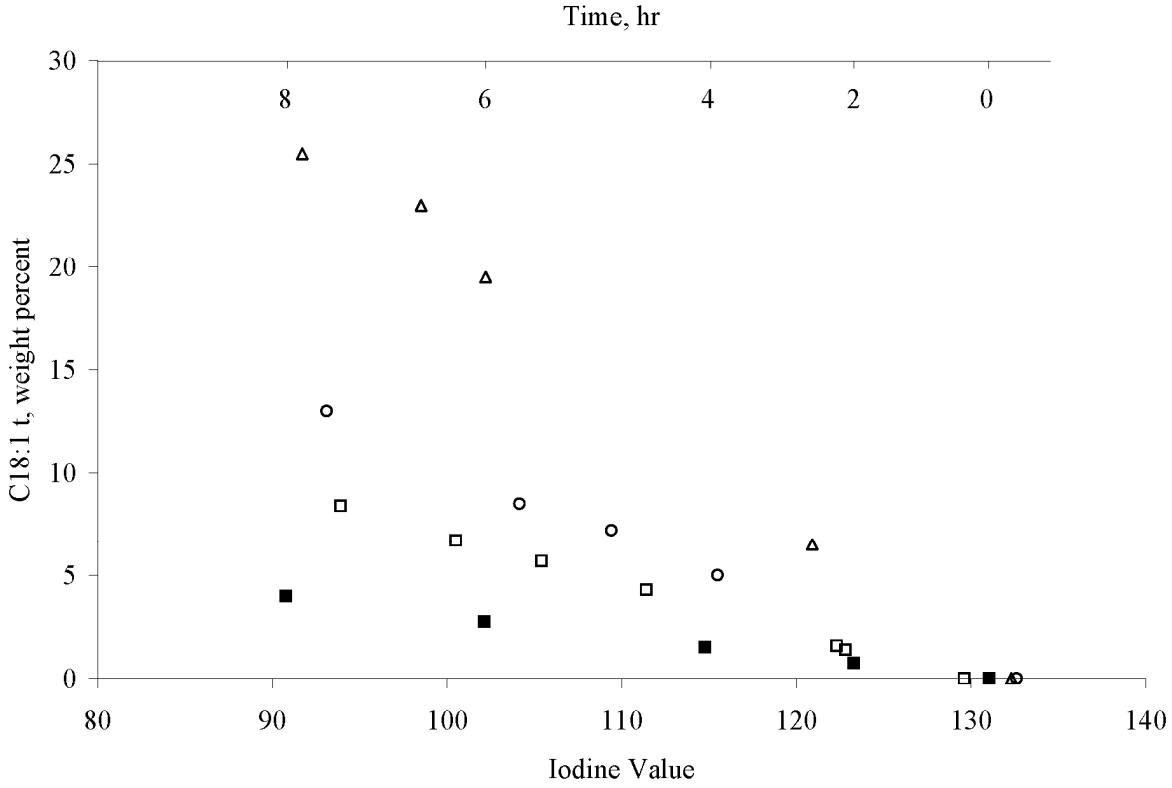

Figure 3-4: Trans fatty acid content as a function of Iodine Value during hydrogenation of vegetable oil. Pt catalytic membrane (■, secondary x-axis gives the time for corresponding iodine values, only for Pt catalytic membrane), Pt/C slurry reactor(□) at 70 °C, 65 psi, Pt/TiO_2 slurry reactor at 100 °C, 60 psi (○) (18), and Ni slurry reactor at 140 °C, 15 psi (Δ) [19].

Figure 3-5 compares the composition profiles (C18:0, C18:1, C18:2, C18:3) of hydrogenation using the Pt catalytic membrane, the Pt/C catalyst as a slurry at 70 °C, 65 psi, and the conventional Ni/Si catalyst at 140º C[19]. The Ni slurry reactor produced significantly higher C18:1 and lower C18:0 as compared to the platinum catalysts. The S_{LN}, S_L, S_O fatty acid selectivities were 2.0, 18.5, and 37.4, respectively. The significant differences in composition profiles with increasing hydrogenation for the conventional Ni catalysts are characteristics of Ni catalysts and are consistent with the literature. The platinum membrane produced very similar composition profile for all the components as compared to the conventional Pt/C slurry reactor. The S_{LN}, S_L, S_O fatty acid selectivities were 1.5, 2.6, and 3.8, for the platinum membrane reactor and 1.6, 2.4, 3.9 for Pt/C slurry reactor. Although an increase in hydrogen concentration at the catalyst surface is also generally accompanied by a decrease in hydrogenation selectivities, they

are also affected by the physical characteristics of the catalyst as it controls the diffusion of reactants in and out of the catalyst pores. Selectivities are higher when triglyceride molecules can move freely in and out of the catalyst pores [20]. Conventional slurry reactors use catalyst supported on a porous support, which increases diffusion limitation of triglyceride molecules and decreases the hydrogenation selectivity. Due to the non-porous and structured nature of the platinum catalyst on the membranes, higher selectivities may have been expected but because of the high hydrogen concentration at the catalyst surface the selectivities were ultimately very similar to Pt/C slurry reactors with lower TFAs being produced while using platinum membrane reactor.

Several authors have studied novel reactor configurations for the partial hydrogenation of vegetable oil. Figure 3-6 compares TFA and C18:0 saturates (at IV=90 except where specified) from some of these reports with that obtained in the present study. Schmidt et al. [8] hydrogenated sunflower oil using membrane reactor in the pore-flow-through mode where the reaction mixture was pumped through catalytic active porous membranes (using both Pt and Pd catalyst). The aim was to prevent TFA formation by eliminating mass transfer limitations. However hydrogen scarcity at the catalyst surface promoted the isomerization to TFA as compared to the conventional process. The amount of TFAs formed using these membranes with platinum catalyst was 15 weight percent at an IV of around 98 (80 °C, 290 psi H_2). Fritsch et. al [7] developed microporous polymer membranes with very high oil fluxes (1000-2000 L $m^{-2}hr^{-1}bar^{-1}$) and the membranes were activated with platinum. The membranes were then used for hydrogenation of sunflower oil at 100 °C and 58 psi. The amount of TFA and C18:0 saturates formed at an IV of 90 were 22 weight percent and 12.5 weight percent, respectively, which is very high and may not satisfy the specifications established.

Piqueras et. al[18] reported the hydrogenation of sunflower oil on Pt/TiO_2 catalyst using supercritical propane to eliminate gas-liquid interface and increase the hydrogen solubility in oil by creating a homogeneous phase. This led to an increase in hydrogen concentration at the surface of the catalyst as compared to the conventional process and thus resulted in very low TFA formation. At an IV of 90 the TFA formed were 4 weight percent as compared to 13 weight percent formed in the conventional slurry process under similar conditions. The decrease in TFA was also accompanied by an increase in C18:0 saturates from around 10 weight percent in conventional reactor to 20 weight percent when using supercritical propane. However the

pressure used to achieve the homogeneous phase is extremely high (2300 psi) which would require special equipment designed to handle high pressures. Pintauro et. al [6] reported the hydrogenation of soybean oil using a solid polymer electrolyte reactor where hydrogen is generated in situ by the electro-reduction of protons at the anode and migrate through the ion exchange membrane to Pt-black cathode where the reaction takes place. The low amount of trans fatty acids and high saturates obtained (3 weight percent total TFA, 21 weight percent saturates at IV 92) using solid polymer electrolyte electrochemical cell also indicates hydrogenation carried out at high hydrogen concentration. The membranes studied in this work produced the same low amount of TFA (4 weight percent at IV of 90) and less saturates (14.5 weight percent at an IV of 90) at temperatures and pressures which are compatible with the existing equipment. In addition, the process is much simpler than operating the reactor as an electrochemical cell.

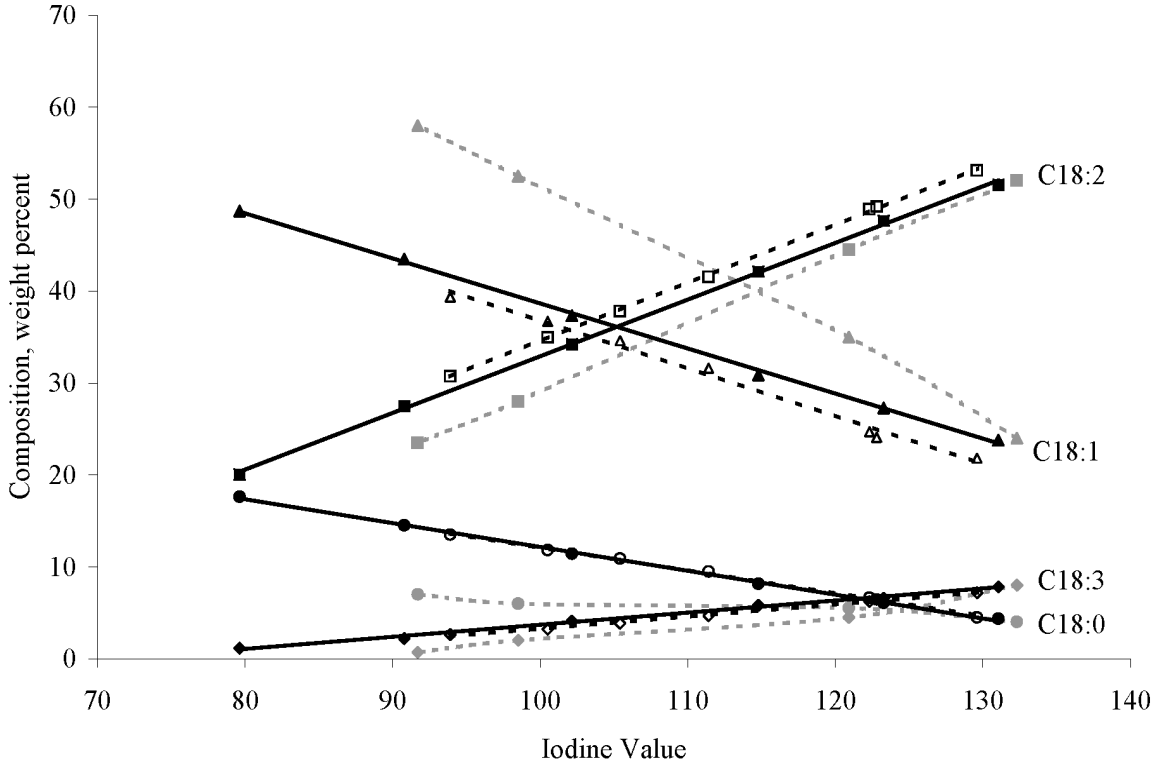

Figure 3-5: Fatty acid composition as a function of IV during hydrogenation of soybean oil using Pt catalytic membrane (——), Pt/C slurry reactor (– – –), and Ni slurry reactor (– – –) [19]. Reaction conditions: temperature= 70 °C (140 °C for Ni slurry reactor [19]), hydrogen pressure= 65 psi (15 psi for Ni slurry reactor [19]).

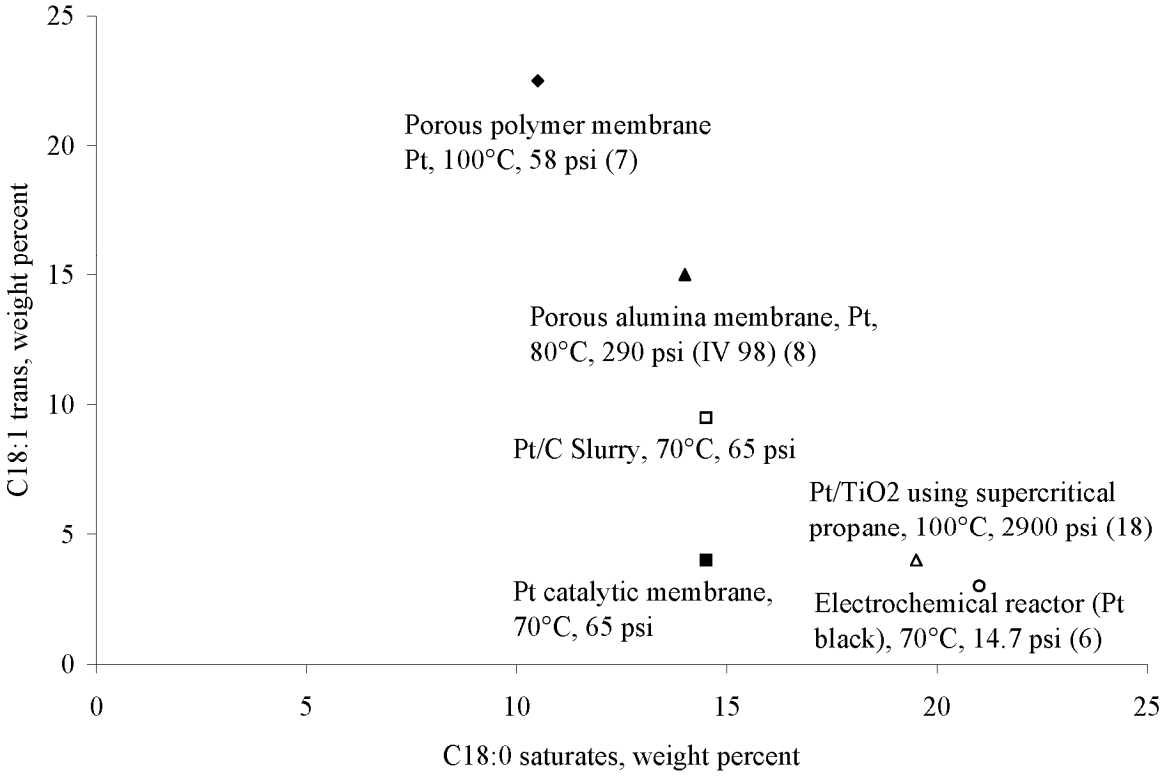

Figure 3-6: Comparison of the amount of C18:1 trans and C18:0 saturates formed for our platinum catalytic membranes and other novel processes being studied for the hydrogenation of vegetable oil (At IV = 90).

3.4 Conclusion

This study demonstrates a novel integral-asymmetric metal-polymer composite catalytic membrane approach for low trans fatty acid hydrogenation of soybean oil. Hydrogen is supplied directly at or near the surface of an integral-asymmetric polymeric membrane sputtered with platinum by pressurizing the porous substructure of the membrane with hydrogen. The oil flows over the platinum-sputtered feed (skin) side of the membrane. The process is simpler than some of the alternatives being studied and no catalyst recovery from the oil is needed since the catalyst is immobilized on the membrane. The system is compatible with existing commercial hydrogenation facilities as far as temperatures (~70 °C) and hydrogen pressure (~65 psi). Our approach shows significantly lower TFA values at comparable hydrogenation levels. We hypothesize that this is due to avoiding hydrogen starvation of the catalyst surface by rapid hydrogen permeation through a high performance asymmetric membrane.

3.5 References

1. Dijkstra, A.J., Revisiting the formation of trans isomers during partial hydrogenation of triacylglycerol oils, European Journal of Lipid Science and Technology 108:249-264 (2006).

2. Veldsink, J.W.B., Martin J.; Schoon, Nils-H.; Beenackers, Antonie A. C. M., Heterogeneous hydrogenation of vegetable oils: a literature review., Catalysis Reviews - Science and Engineering 39:253-318 (1997).

3. Musavi, A., M. Cizmeci, A. Tekin, and M. Kayahan, Effects of hydrogenation parameters on trans isomer formation, selectivity and melting properties of fat, European Journal of Lipid Science and Technology 110:254-260 (2008).

4. Nohair, B., C. Especel, P. Marecot, C. Montassier, L.C. Hoang, and J. Barbier, Selective hydrogenation of sunflower oil over supported precious metals, Comptes Rendus Chimie 7:113-118 (2004).

5. King, J.W., R.L. Holliday, G.R. List, and J.M. Snyder, Hydrogenation of vegetable oils using mixtures of supercritical carbon dioxide and hydrogen, Journal of the American Oil Chemists Society 78:107-113 (2001).

6. Pintauro, P.N., Synthesis of a low-trans content edible oil, non-edible oil, or fatty acid in a solid polymer electrolyte reactor, U.S. Patent 6218556 B1 (2001).

7. Fritsch, D., and G. Bengtson, Catalytic polymer membranes for high temperature hydrogenation of viscous liquids, Adv Eng Mater 8:386-389 (2006).

8. Schmidt, A., and R. Schomacker, Partial hydrogenation of sunflower oil in a membrane reactor, Journal of Molecular Catalysis a-Chemical 271:192-199 (2007).

9. Veldsink, J.W., Selective hydrogenation of sunflower seed oil in a three-phase catalytic membrane reactor, Journal of the American Oil Chemists Society 78:443-446 (2001).

10. Gryaznov, V.M., M.M. Ermilova, and N.V. Orekhova, Membrane-catalyst systems for selectivity improvement in dehydrogenation and hydrogenation reactions, Catal Today 67:185-188 (2001).

11. Baker, R.W., Membrane technology and applications, John Wiley & Sons, Ltd, 2004.

12. Baker, R.W., Louie, J., Pfromm, P. H., Wijmans, J. G, Ultrathin Metal Composite Membranes for Gas Separation, U.S. Patent 4,857,080 (1989).

13. Peinemann, K.V., Method for producing an integral, asymmetric membrane and the resultant membrane, U.S. Patent 4,673,418 (1987).

14. Obrien, K.C., W.J. Koros, T.A. Barbari, and E.S. Sanders, A New Technique for the Measurement of Multicomponent Gas-Transport through Polymeric Films, Journal of Membrane Science 29:229-238 (1986).

15. Barbari, T.A., W.J. Koros, and D.R. Paul, Polymeric Membranes Based on Bisphenol-a for Gas Separations, Journal of Membrane Science 42:69-86 (1989).

16. Petursson, S., Clarification and expansion of formulas in AOCS recommended practice Cd 1c-85 for the calculation of iodine value from FA composition, Journal of the American Oil Chemists Society 79:737-738 (2002).

17. Albright, L.F., Quantitative Measure of Selectivity of Hydrogenation of Triglycerides, Journal of the American Oil Chemists Society 42:250-253 (1965).

18. Piqueras, C.A., G. Tonetto, S. Bottini, and D.E. Damiani, Sunflower oil hydrogenation on Pt catalysts: Comparison between conventional process and homogeneous phase operation using supercritical propane, Catal Today 133:836-841 (2008).

19. Dejonge, A., J.W.E. Coenen, and C. Okkerse, Selective Hydrogenation of Linolenate Groups in Soya-Bean Oil, Nature 206:573-574 (1965).

20. Patterson, H.B.W., Hydrogenation of fats and oils, Applied science publishers ltd., 1983.

CHAPTER 4 - Precious metal polymer membranes for partial hydrogenation of soybean oil

4.1 Introduction

An important area to address for the metal decorated polymeric membranes is if the high permeability of metal is an essential criterion for the hydrogenation to occur. As can be seen in Figure 4-1 there is an order of magnitude difference in hydrogen permeation coefficients of various metals[1]. The application of metal polymer composite membranes may be limited to high permeability metals or could be used for a range of metal catalysts depending upon if the permeability of the metal is an essential criterion for hydrogenation to occur.

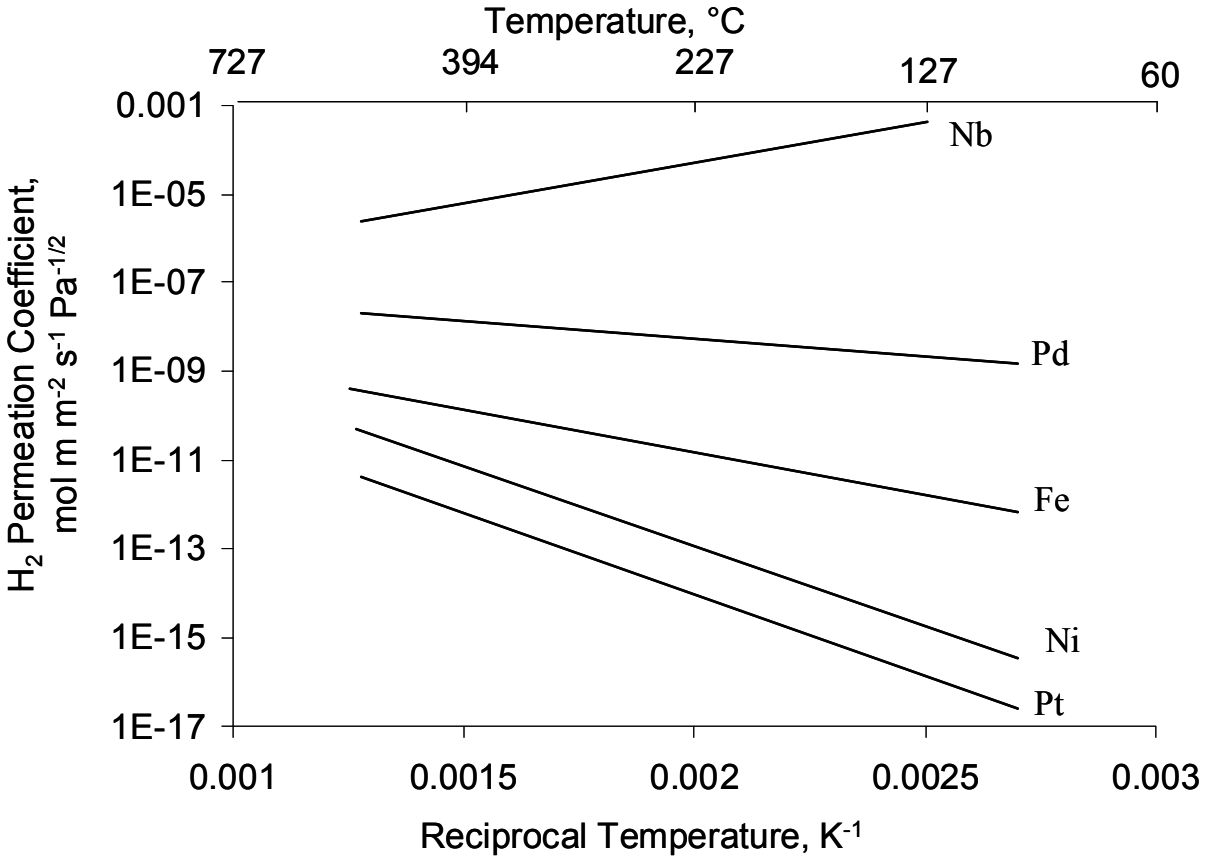

Figure 4-1: Hydrogen permeation coefficients of various metals [1].

For the experiments presented here platinum was chosen as a metal with low hydrogen permeability and palladium was chosen as a metal with high hydrogen permeability.

Additionally palladium-lead alloy was chosen because it is reported to promote the selectivity towards cis oleic isomers[2].

4.2 Experimental procedure

The metal polymer membranes were prepared and characterized as described in section 3.2.2. Different polymeric membranes were sputter coated with platinum, palladium, and palladium-lead alloy. All the metals were sputtered using a DESK II magnetron sputter (Denton Vacuum, Moorestown, NJ, 9 seconds at 45 mA, 100 mtorr). The metal loading on the membrane was estimated by sputtering the metal on a quartz crystal at the same conditions as used to sputter metal on polymeric membranes. The change in weight was measured using a quartz crystal microbalance (QCM, model RQCM, Maxtek Inc., East Syracuse, New York). The properties of the membranes used for hydrogenation experiments are given in Table 4-1.

The morphology of the metal layer on the membrane was studied using transmission electron microscopy (TEM). TEM's were taken from a perspective perpendicular to the polymer surface. For this purpose, a thin layer (< 100 nm) of PEI was spin coated on a TEM grid (2000 mesh copper grid, Electron Microscopy Sciences, Hatfield, PA) followed by sputtering under the same conditions (25 °C, 100 mTorr air, 45 mA for 9 seconds) .

The hydrogenation runs were performed using the hydrogenation setup and procedure as explained in section 3.2.3 and analyzed as explained in section 3.2.4.

Table 4-1: Properties of membranes used for hydrogenation runs.

Metal	Metal loading, ($\mu g\ cm^{-2}$)	H_2 flux after sputtering (GPU)	H_2/N_2 selectivity
Platinum	3.4	10	5
Palladium	1.4	81	6
Palladium-lead alloy (Pd90Pb10)	2.7	5	102

4.3 Results and discussion

The polymeric membranes were sputter coated with metals that have very high permeability to hydrogen and metals that have relatively low permeability to hydrogen. The hydrogen permeability of the metal will have a significant impact if the metal-composite

membranes produced have nearly defect-free PEI skin and metal layer. If the metal layer is defective then a significant portion of hydrogen will permeate through the defects and hydrogen permeability of metals may be less important. Figure 4-2 shows the TEM of the membrane surface after sputtering with platinum, palladium, and palladium-lead alloy for 9 seconds. All the three metals appear to be in the form of interconnected network of metal islands with significant defects and the metal area coverage for all the cases in the range of 60-70%.

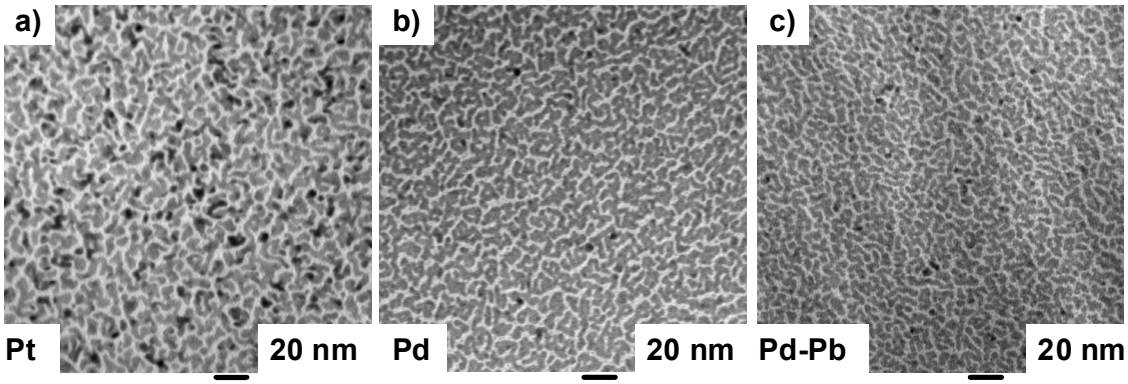

Figure 4-2: TEMs of the surface of PEI films sputtered with platinum, palladium, and palladium-lead alloy. An interconnected network of metal islands on the polymer surface is seen for all the cases.

With the metal coverage as in Figure 4-2 and the low temperatures at which we are operating, a significant portion of the hydrogen will permeate through the defects and all the metals should show hydrogenation activity irrespective of their intrinsic hydrogen permeation coefficients. Figure 4-3 shows the hydrogenation of soybean oil with time for polymer membranes sputtered with platinum, palladium, and palladium-lead alloy. As expected all the metals showed catalytic activity towards hydrogenation. Of all the metals tested palladium showed the most activity followed by platinum and then palladium-lead alloy. The hydrogenation rates were 1.0, 7.2, 10.4 IV hr^{-1} for palladium, platinum, and palladium-alloy respectively. This order of activity is consistent with the literature[2, 3]. Palladium is more active than platinum for the hydrogenation of vegetable oil. Nohair et al.[2] observed during hydrogenation of ethyl esters of sunflower oil that addition of lead or copper to palladium promoted the selectivity towards cis oleic isomers but decreased the activity of the catalyst.

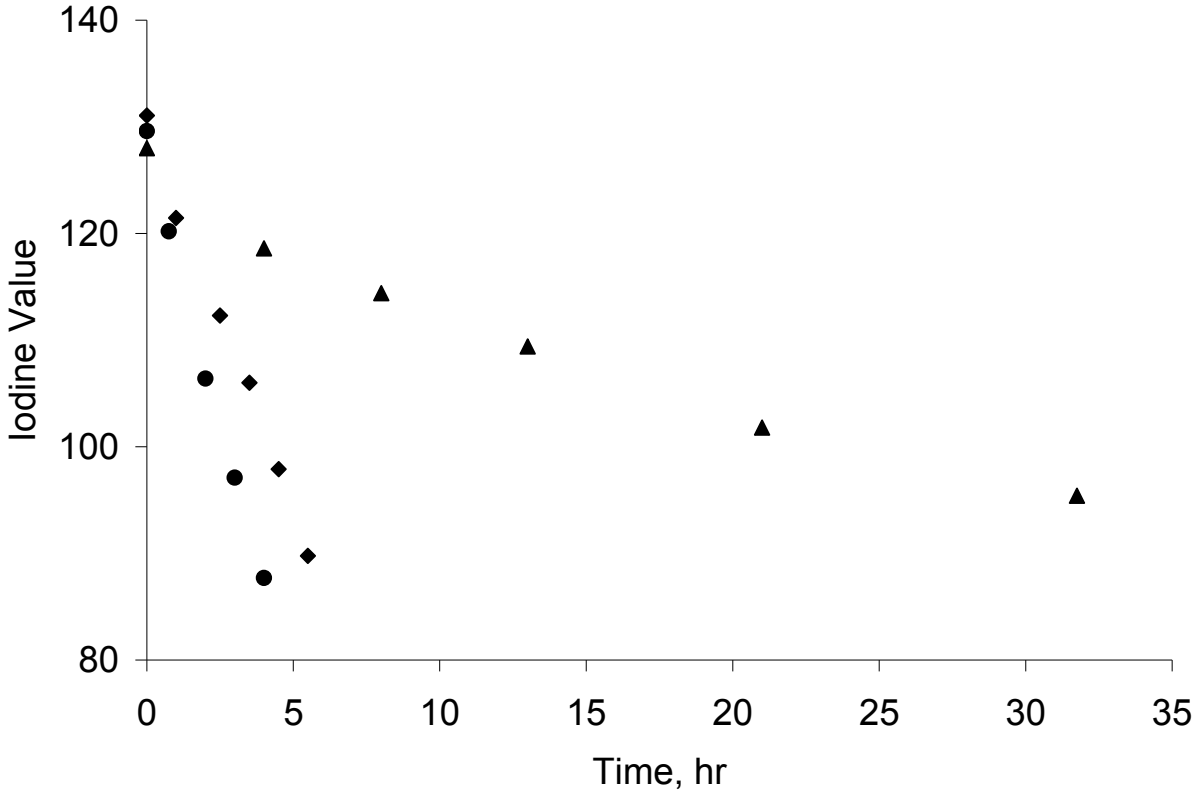

Figure 4-3: Iodine value with time for hydrogenation of soybean oil using palladium (●), platinum (♦), and palladium-lead (▲) decorated polymeric membranes.

The palladium-lead alloy showed the highest linolenic, and linoleic hydrogenation selectivities while platinum showed minimum hydrogenation selectivity towards the formation of TFA. Figure 4-4 compares the hydrogenation and isomerization selectivities obtained while using platinum, palladium, and palladium-lead alloy sputtered membranes. As can be seen in Figure 4-4, addition of lead to palladium not only promoted selectivity towards cis isomers but also showed higher linolenic acid selectivity. The high linolenic acid selectivity obtained while using palladium-lead alloy means that at similar hydrogenation levels, palladium-lead alloy will have less linolenic acid and thus will be more oxidative stability. At an iodine value of 100, the composition of partially hydrogenated oil using the palladium sputtered membrane was: C18:3, 3.3 mol%; C18:2, 33.0 mol%; C18:1, 39.1 mol%; and C18:0, 11.0 mol%. While the composition of partially hydrogenated oil using palladium-lead alloy sputtered membrane was (IV=100): C18:3, 1.3 mol%; C18:2, 34.3 mol%; C18:1, 41.4 mol%; and C18:0, 7.9 mol%.

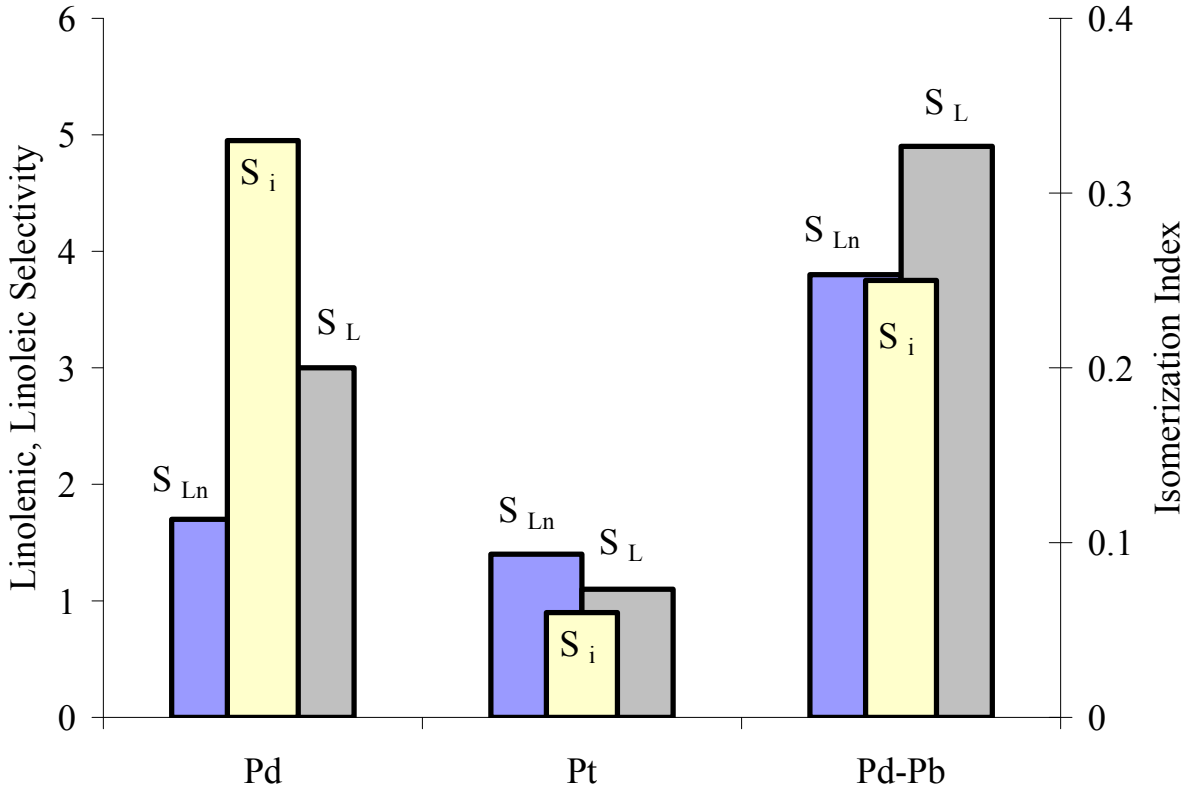

Figure 4-4: Hydrogenation and isomerization selectivities obtained using palladium, platinum, and platinum-lead alloy sputtered PEI membranes. Hydrogen pressure=50 psig, Temperature=70°C.

4.4 Conclusion

Metal polymer membranes sputtered with high hydrogen permeability metal and low hydrogen permeability metal showed activity towards the hydrogenation of soybean oil. Due to the large number of defects in the metal layer and relatively low permeation rate of hydrogen through metals at the reaction temperature as compared to polymeric membrane, a significant portion of hydrogen will permeate through the defects, which allows both high permeability and low permeability metals to be used as catalysts on the membrane surface. Palladium showed the highest activity. Adding lead to palladium decreased the isomerization selectivity and activity but increased linolenic selectivity. Platinum showed the lowest selectivity towards formation of TFA but also resulted in lower linolenic and linoleic acid selectivities. However, due to recent

health concerns about TFAs, platinum may be one of the most interesting metals for future hydrogenations.

4.5 Reference

1. Uemiya, S., Brief review of steam reforming using a metal membrane reactor. Topics in Catalysis 2004, 29, (1-2), 79-84.

2. Nohair, B.; Especel, C.; Marecot, P.; Montassier, C.; Hoang, L. C.; Barbier, J., Selective hydrogenation of sunflower oil over supported precious metals. Comptes Rendus Chimie 2004, 7, (2), 113-118.

3. Veldsink, J. W. B., M.J.; Schoon, N.H.; Beenackers, Antonie A. C. M., Heterogeneous hydrogenation of vegetable oils: a literature review. Catalysis Reviews - Science and Engineering 1997, 39, (3), 253-318.

CHAPTER 5 - Partial hydrogenation of soybean oil using metal decorated integral-asymmetric polymer membranes: effects of morphology and membrane properties

5.1 Introduction

Reactions involving a liquid, a solid catalyst, and a reactant that is gaseous at reaction conditions pose many challenges to reactor design, one of them being the slow mass transfer of reactants from a gas phase through a liquid to the active catalyst sites. This liquid-phase mass transfer resistance frequently causes a scarcity of one or more of the reactants at the catalyst surface. This may lead to lower reaction rates and in some cases have a detrimental effect on the composition of the final product. The situation is exacerbated if the liquid phase is viscous and/or has a low solubility for the gas phase reactant as is the case with hydrogen and vegetable oil.

Partial hydrogenation of vegetable oils is an important reaction in the food industry, used for the production of base stocks for margarines and shortenings. In the U.S. alone, the annual production of margarines and shortenings was around 8 billion pounds in 2007[1]. The traditional approach to hydrogenation of vegetable oil is bubbling hydrogen through oil in a stirred batch autoclave and hydrogenating over a nickel based catalyst that is supported on particles suspended in the oil. This slurry reactor approach leads to the formation of relatively high amounts of TFA[2, 3] generally attributed to low availability of hydrogen at the catalyst due to significant hydrogen mass transfer limitations in the oil phase[4].

In this paper, we study metal-decorated integral-asymmetric polymer membranes for partial hydrogenation of vegetable oil. The concept is to alleviate hydrogen starvation of the catalyst surface by supplying dissolved hydrogen near or at the catalytic sites. This should promote the desired hydrogenation and reduce the undesirable TFA formation based on the literature on catalyzed hydrogenation of oils. After initial successful proof-of-concept of the process at pressures and temperatures compatible with the existing hydrogenation processes [5] we focus here on the membrane morphology and the impact of the membrane properties on the hydrogenation results.

5.2 Background

5.2.1 Molecular architecture of vegetable oil

Vegetable oils are mixtures of triglycerides which consist of one molecule of glycerol combined with three molecules of fatty acid residues. The major fatty acids present are palmitic acid (C16:0, nomenclature: 16 carbon atoms with zero double bonds), stearic acid (C18:0, m.p. 70°C), oleic acid (C18:1), linoleic acid (C18:2), linolenic acid (C18:3, m.p. -13°C), and minor amounts of other fatty acids (C14:0 to C24:0). It is the composition of the major fatty acids that determines the bulk physical and chemical properties of fats and oils. The melting characteristics and oxidative stability depend on the fatty acid residues attached to the glycerol backbone. The oxidative stability of different fatty acids follows the order: C18:1> C18:2 >C18:3. A triglyceride with one stearic and two oleic acid residues is 15 times more oxidatively stable than a triglyceride with three linoleic acids [6].

5.2.2 Vegetable oil hydrogenation

Hydrogenation involves adding hydrogen to double bonds of fatty acids present in vegetable oil to obtain a fatty acid composition profile that has a high oxidative stability and a melting point most suited for a particular application. The main goals are to minimize C18:3 because of its poor oxidative stability while maintaining C18:2 since it forms a valuable part of the human diet, and minimizing the formation of saturated C18:0. Recent health concerns regarding TFA [7, 8] have added avoiding TFA formation to the list of requirements for vegetable oil hydrogenation.

The conventional hydrogenation of vegetable oil is carried out in a stirred batch autoclave (typically 30,000-90,000 pounds of oil [11]) over nickel based catalyst in a slurry at 110-190ºC, 30-70 psi hydrogen pressure, with 0.01-0.15wt% Ni catalyst [9] (supported on Kieselguhr, silica-alumina, or carbon [10]). This approach (Figure 1a) relies on the dissolution of hydrogen in the oil followed by convective (supported by stirring) and diffusive (in the particle boundary layer) hydrogen transport to the catalytic sites. The various reactions occurring during hydrogenation of vegetable oil can be described by the Horiuti-Polanyi mechanism [4, 12]. The hydrogen diffuses through the liquid oil and is adsorbed on the catalyst surface where it dissociates into two adsorbed hydrogen atoms which react with the adsorbed fatty acid molecule to form an unstable half-hydrogenated intermediate. Depending on the concentration of hydrogen at the catalyst

surface, this intermediate complex can gain a hydrogen atom and thereby hydrogenate or lose a hydrogen atom and in the process may isomerize. Figure 5-1 shows the hydrogenation and isomerization reactions of linolenic fatty acid (C18:2) to oleic acid (C18:1) [4]. Details about hydrogenation kinetics are available elsewhere [13-15].

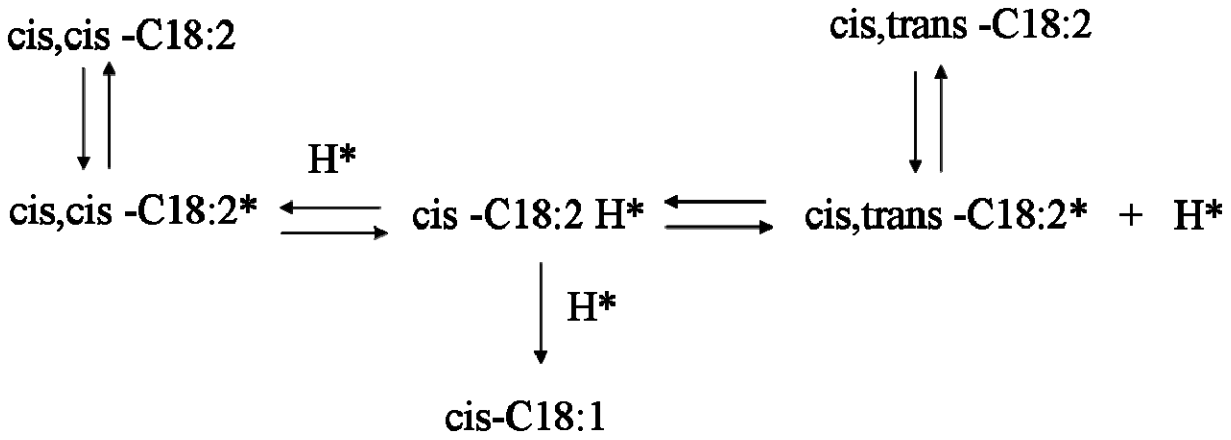

Figure 5-1: Reactions involved in the hydrogenation of Linoleic fatty acid (C18:2) to Oleic acid (C18:1) (* indicates species adsorbed on the catalyst surface).

The overall hydrogenation rate depends strongly on the concentration of hydrogen in the bulk oil [4]. However, the low solubility of hydrogen in oils leads to hydrogen starvation of the catalytic sites and promotes isomerization to TFA. Decreased temperature, increased agitation, and increased hydrogen pressure reduce detrimental hydrogen mass transfer limitations [3, 16]. However, the reaction conditions must be kept in an operating window that does not render the process uneconomical. Excessive hydrogen pressure, for example, could only be used at considerable capital expense.

5.2.3 Published novel catalytic membrane approaches

Recent studies [17-20] report novel reactor designs for hydrogenation of vegetable oils to maximize the delivery of hydrogen to the catalyst surface and minimize TFA production. Most of these studies [17, 19, 20] use porous membranes as gas-liquid-solid contactors to alleviate mass transfer issues

Schmidt and Schomacker [19] describe the development of a porous membrane with catalyst particles on the surface (Figure 5-2b). A mixture of oil and gaseous hydrogen is pumped through the pores [19]. The mass-transfer limitations where hoped to be reduced.

However, the TFA generated in this system was unfortunately higher than that achieved in the conventional system [19].

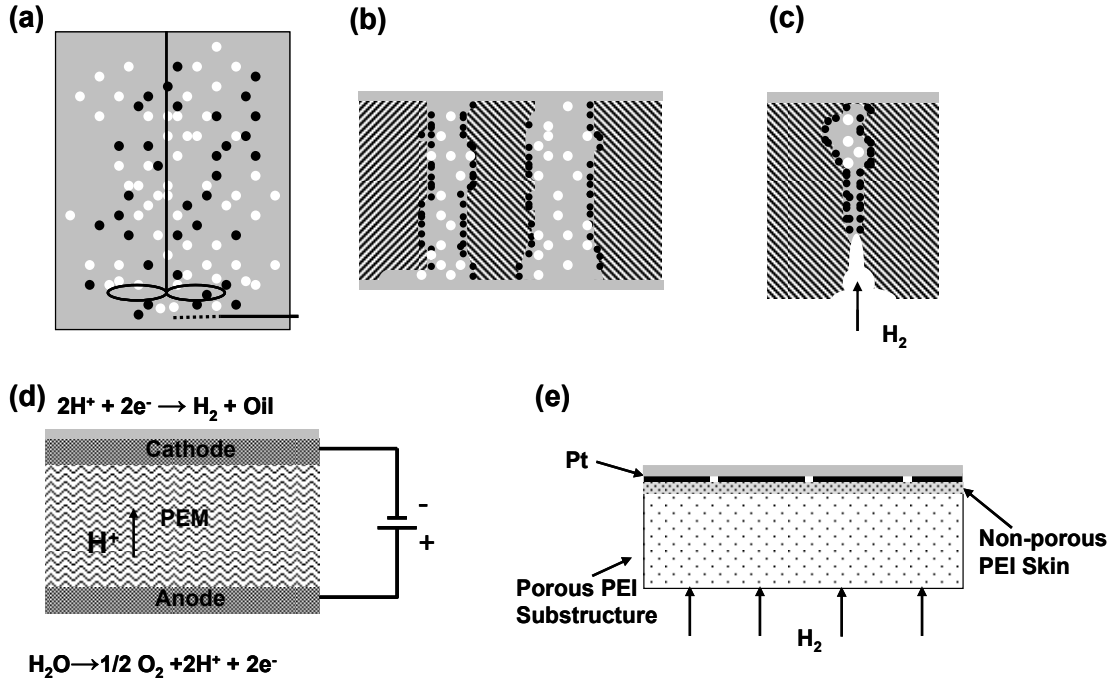

Figure 5-2: Hydrogenation of vegetable oils: a) traditional slurry reactor b) flow-through contactor mode c) diffuser mode with liquid on the catalyst side d) Hydrogenation combined with water electrolysis to supply hydrogen e) metal decorated integral-asymmetric polymer membrane (this work).

An alternative approach (Figure 5-2c) employed a porous membrane used in "diffuser mode" with catalyst deposited on a part of the pore walls and oil filling that part of the pore. Veldsink et al. [20] used porous zirconia membranes (20 nm pore size) and Pd catalyst impregnated on the pore walls. The aim was to increase the hydrogenation selectivity by eliminating intraparticle diffusion limitations. High selectivities were obtained for the hydrogenation of polyunsaturated triglycerides to produce mono-saturated products yet this also produced very high levels of TFA [20].

In an attempt to overcome the hydrogen supply limitations, an electrochemical process (Figure 5-2d) for the hydrogenation of vegetable oil has been devised [17, 21-23]. Oxygen and hydrogen are generated by splitting water electrochemically. The hydrogen is evolved at a cathode that also contacts the oil and acts as the hydrogenation catalyst. The oxygen is a byproduct. This approach produced very low TFA level. This approach essentially replaces the

hydrogen production via water gas shift reaction from natural gas with electrochemically produced hydrogen. Economics of the process compared to the traditional approach and our approach will be discussed below.

5.2.4 Approach employed here

We have devised an approach taking advantage of the high gas transport rates of integral-asymmetric polymeric membranes with essentially perfect non-porous ultrathin skins (about <1 micrometer effective skin thickness), but using the membrane "reversed" by applying hydrogen to the porous substructure of the membrane while liquid oil is present on the skin side (Figure 5-2e). Hydrogen molecules dissolve in the skin layer and diffuse towards the "oil" side under the partial pressure driving force created by essentially pure hydrogen on the substructure side and hydrogen consumption by hydrogenation on the oil side. The hydrogen transport rate can be adjusted through the partial pressure driving force that is applied. The hydrogen transport rate is self-regulating since the partial pressure of hydrogen in the oil phase increases if hydrogen is not consumed, which reduces the driving force for hydrogen transport. Hydrogen is essentially supplied to the catalyst “on demand” with the maximum rate of supply limited only by the hydrogen pressure and the membrane characteristics. In fact, the process is operated with a hydrostatic oil pressure exceeding the hydrostatic pressure of the hydrogen.

The ultrathin tight polymer membrane skin layer effectively excludes convective gas transport from the hydrogen side into the oil via bubbles. Gas transport in the skin is by solution-diffusion. Similarly, no oil can leak into the substructure of the membrane which would impede hydrogen transport and cause process upsets.

The membrane skin decouples the oil side hydraulically from the gas side allowing largely independent control of the hydrostatic pressure difference (and oil flow rate) from the hydrogen driving force and thereby hydrogen flux. A porous membrane on the other hand requires finely tuned control of hydrostatic pressure differences to avoid oil or gas intrusion and/or blow out for the membrane pores.

The smooth skin of integral asymmetric membranes provides a good support for uniform metal deposition with high surface-to-volume ratio. Any surface features might lead to uneven metal deposition and/or mass transfer obstacles.

5.3 Experimental

5.3.1 Materials

Soybean oil (Iodine Value IV = 129-131) was purchased from MP Biomedicals (Solon, OH). The composition of soybean oil as measured in our laboratory is (reported as weight percent): C16:0, 11.6-12.0; C18:0, 4.3-4.4; C18:1, 21.6-23.8; C18:2, 51.6-53.3; C18:3, 7.1-7.8; total trans fatty acids, 0.7-1.2; C18:1 trans, 0.0; C14:0-C24:0, 0.9-1.5. Polyetherimide (PEI, Ultem-1000) to cast the integral-asymmetric membranes was purchased from General Electric (Huntersville, NC). Acetic acid (HPLC grade), acetone (99.5%), p-xylene (99.9%), and dicholoromethane (99.9%), were from Fisher Scientific (Rochester, NY), 1,1,2,2-tetrachloroethane (98%) was from Sigma Aldrich (St. Louis, MO). The platinum (Pt) sputter target (99.95wt% Pt) was from Ted Pella Inc. (Redding, CA). Ultra high purity hydrogen (min. 99.999%) and nitrogen (min. 99.999%) were obtained from Linweld Inc. (Lincoln, NE).

5.3.2 Membrane preparation and testing

Integral asymmetric polyetherimide (PEI) membranes were fabricated using the phase inversion process as described elsewhere [24]. A 15.9 wt% solution of PEI was prepared in a mixture of solvents (dichloromethane 54.6wt%; 1,1,2,2-tetrachloroethane 4.8wt%) and pore forming agents (xylene 17.6wt%; acetic acid 7.1wt%). The polymer solution was cast on a cooled glass plate (11x8.5 inch, 16-18°C) using a Gardner knife set to a gap of about 350 micrometers (μm). The knife gap establishes the thickness of the polymer solution layer but the enormous success of asymmetric membranes is based on the about three orders of magnitude thinner (compared to the final total membrane thickness) selective skin layer formed during phase inversion. After 3 seconds of air drying the glass plate carrying the polymer solution layer was immersed in acetone (12-16°C, 30 minutes). The nascent membrane floats off the glass plate and is then air dried overnight. The membranes thus formed are integral-asymmetric membranes with a dense skin of thickness of about 0.1-0.5 μm and a porous substructure 100-160 μm thick. Figure 5-3 shows a scanning electron micrograph (SEM) and transmission electron micrograph (TEM) of a cross-section of an integral-asymmetric PEI membrane. The expected highly porous substructure and thin dense skin can be seen. It should be noted that we designate the membrane skin layers as ultrathin based on the fact that essentially perfect sub-micron effective skin layer thicknesses are obtained (as tested by comparison to thick film hydrogen/nitrogen selectivities).

This is an example of a perfect nano-scale material (thickness down to on the order of 100 nanometer) produced on a macroscopic scale.

Circular stamps 4.7 cm in diameter were cut from the membrane sheets and tested in a filter holder (model XX4404700, Millipore Corp., Billerica. MA) for their gas fluxes (hydrogen and nitrogen) using a constant-volume variable-pressure apparatus (similar to the one described elsewhere [25]) at 25°C and 50 psig. The normalized gas fluxes in GPU (Gas Permeation Unit, 1 GPU = 10^{-6} cm^3(STP) cm^{-2} s^{-1} cm Hg^{-1}) were measured and the ideal gas selectivity $\alpha_{H2/N2}$ was calculated as the ratio of the normalized single gas fluxes. Thick films of PEI have been measured and show an $\alpha_{H2/N2}$ of about 181 at 25°C [26, 27].

Pt was applied to the membrane skin by sputtering (using DESK II magnetron sputter, Denton Vacuum, Moorestown, NJ, 3-9 seconds at 45 mA, 100 mtorr) before using the membrane for hydrogenation run. Sputtered membranes were re-tested for their gas fluxes and ideal gas selectivities for quality control. In most cases the gas flux of the membranes was reduced after sputtering as can be expected due to the relatively nonpermeable nature of the metal. Hydrogen permeation through Pt is negligible when compared to the gas transport through PEI at temperatures below 80 °C [28].

The Pt loading on the membrane was estimated by sputtering Pt on a quartz crystal for 3, 6, and 9 seconds and measuring the weight change (Table 5-1) using a quartz crystal microbalance (QCM, model RQCM, Maxtek Inc., East Syracuse, New York). The Pt loading increased fairly linearly with sputtering time in this time range.

5.3.3 Hydrogenation system and experimental procedures

Hydrogen is supplied from the porous substructure (often termed permeate-) side of the membrane which is mounted skin side up in a stainless steel filter holder (47 mm, model XX4404700, Millipore Corp., Billerica. MA). The partial pressure of hydrogen is the driving force for diffusional mass transfer through the skin layer (see Figure 5-2e). The hydrostatic pressure on the oil side is held above the hydrostatic pressure of the hydrogen to prevent blow-out of the unsupported oil side of the membrane. No gaseous hydrogen will be able to enter the oil in form of bubbles even if membrane defects or pinholes are present since the hydrostatic oil pressure exceeds that of the hydrogen. On the other hand, hydrogen will permeate the membrane skin to be consumed by the hydrogenation reaction after emerging from the oil side surface of

the membrane skin. Hydrogen consumption by hydrogenation will maintain the partial pressure driving force across the skin for hydrogen permeation. If the reaction were to reach completion, the hydrogen partial pressure on the two faces of the membrane would eventually equilibrate and no further transport would occur.

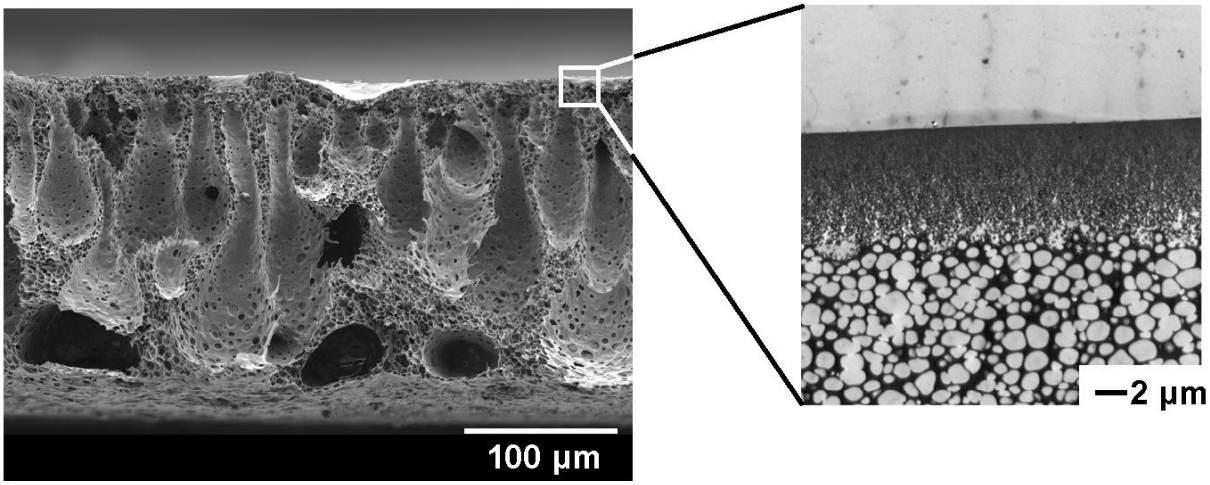

Figure 5-3: Cross-section of integral asymmetric PEI membrane showing the porous substructure and the dense skin. Left, SEM of the substructure with the skin at the top of the image. Right: TEM image of the skin of the membrane showing the transition from a highly porous substructure to an essentially defect-free, dense skin.

A gear pump circulates the hot oil and pressure gauges are present on the hydrogen and oil sides of the membrane. Before the start of the experiment the Pt catalyst on the membrane skin was reduced using hydrogen at 60ºC for 15 hours with the permeate side open to the atmosphere. After reduction about 13.7 g of soybean oil was added to the reactor system and the system was purged with nitrogen. The oil was then heated to the reaction temperature and circulated at about 25 grams/min across the Pt sputtered skin side of the membrane. Oil side pressure was always 60 psig using a blanket of ultra high purity (UHP) nitrogen on the oil reservoir. UHP hydrogen was supplied from the porous substructure side of the membrane at 50 psig, and the reaction temperature was maintained at 70°C. Soybean oil samples were taken at regular intervals and analyzed using gas chromatography. A small hydrogen bleed stream was established from the hydrogen (substructure) side of the membrane to prevent accumulation of nitrogen gas permeating from the oil side through the membrane.

5.3.4 Oil analysis

Oil samples (about 0.1-0.14 grams) were converted to their corresponding fatty acid methyl esters (FAMEs, alternate method in AOCS official method Ce 2-66 [29]). FAMEs thus obtained were analyzed by gas chromatography (GC, 100m CP-Sil 88 column, Hewlett-Packard 6890 series gas chromatograph). AOCS official method Ce 1h-05 was followed for the analysis of fatty acids(Injection port and column250ºC and 181ºC, respectively, He carrier gas 1 ml/min, split ratio 1:100).

The extent of hydrogenation of vegetable oil is customarily represented by its Iodine Value (IV) which is the mass of iodine in grams that is consumed under standard conditions by 100 grams of a lipid [30]. The iodine value of the oils was calculated from the compositional analysis (above) by [31]:

$$IV = (\%C16{:}1 \times 0.9502) + (\%C18{:}1 \times 0.8598) + (\%C18{:}2 \times 1.7315) + (\%C18{:}3 \times 2.6152) \quad \text{Equation 5-1}$$

5.4 Results and discussion

5.4.1 Membrane characterization

5.4.1.1 Physical characterization of the membrane surface

The morphology of the membrane surface after Pt sputter deposition was studied using atomic force microscopy (AFM). Figure 5-4 shows the AFM of the native polymer membrane skin and after Pt sputter deposition for 3, 6, and 9 s at 25°C, 100 mTorr air, and 45 mA (note the differences in Z-axis scale from 10 to 250 to 400 nm). Images were analyzed using SPIP software (Image Metrology, Denmark) to calculate the roughness and height of these features on the surface. The native polymer membrane surface is smooth with an average roughness of about 1 nm. Image analysis indicates crests and troughs with a height of up to 5 nanometers and lateral dimensions of about 30-40 nm. These features may be the result of the asymmetric membrane fabrication process. Manual casting can certainly not guarantee a constant speed of the casting knife over the polymer solution and this may well introduce thickness differences such as the "waves" in Figure 5-4.

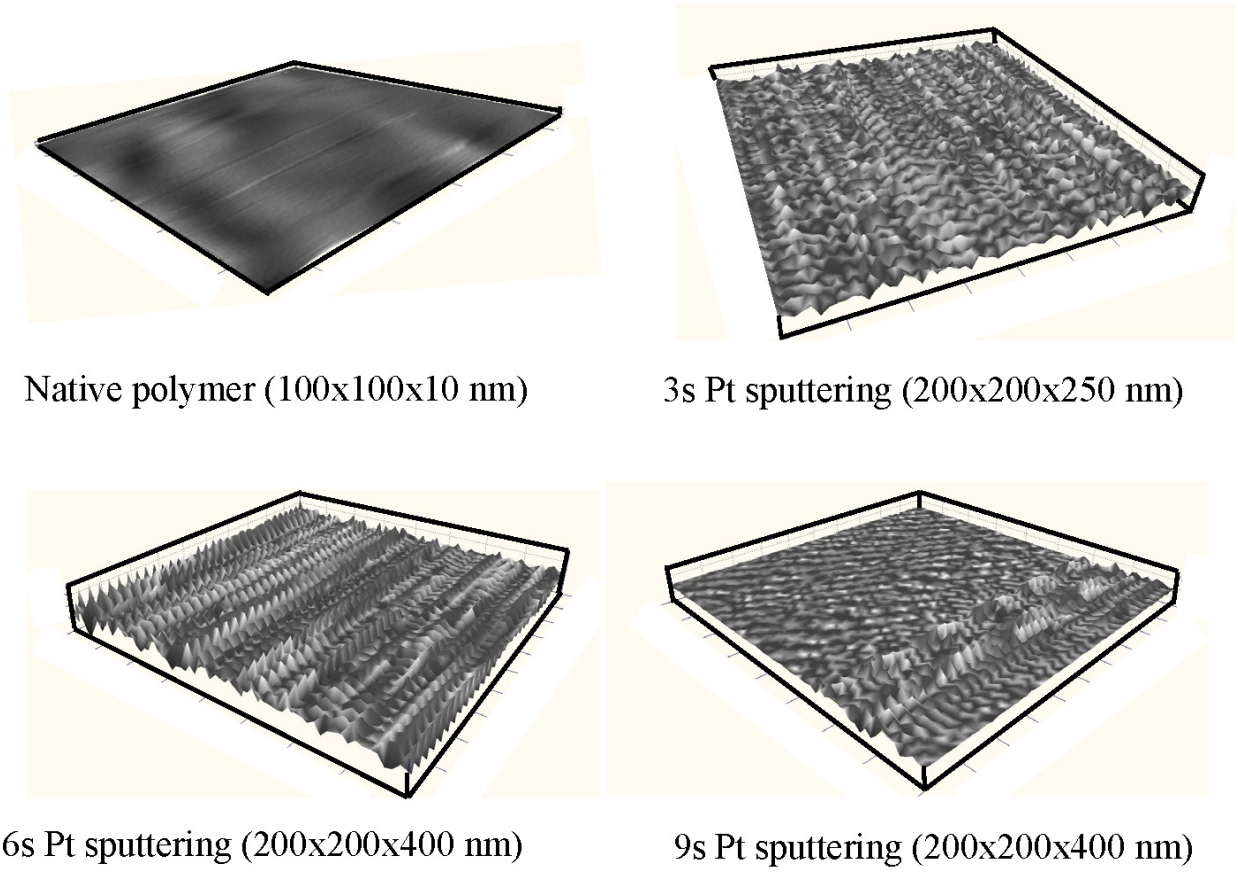

Figure 5-4: AFM of native polymer surface and after sputtering with Pt. The native membrane surface is flat. Uniformly sized features appear on the membrane surface after 3 s Pt sputtering. These features grow in height after 6 s sputtering and appear flattened after 9 s Pt sputtering, as the valleys between the peaks are gradually filled.

After Pt sputter deposition for 3 s uniformly sized features (likely Pt metal) are seen throughout the membrane surface. The features grow in height from 131 nm at 3 s to 340 nm at 6 s Pt sputtering time. Another prominent feature seen after 3 s and 6 s Pt sputtering is the presence of ripples with lateral dimensions of about 30 nm. A rippled topography after sputtering has been observed by others [32, 33]. These ripples may be caused by geometrical effects of atoms deposited on sloped surfaces (see wave-like surface features of the native polymer membrane) through intricate mechanisms [34]. After 9 s sputtering these features become less prominent and a smoother surface is seen. The average roughness decreases from 69 nm to 27 nm from 6 s to 9 s

sputtering. This change in topography may indicate the formation of a more continuous Pt film due to coalescence of small Pt islands (see below).

A thin layer (< 100 nm) of PEI was spin coated on a TEM grid (2000 mesh copper grid, Electron Microscopy Sciences, Hatfield, PA) followed by sputtering under the same conditions as used for the AFM images. This was done to approximate the surface sputtering of the membranes while allowing TEM's to be taken. Figure 5-5 shows the surface of the polymer film sputtered with Pt for 3, 6, and 9 s, respectively. The dark grey to black Pt islands appear to grow and coalesce with sputtering time. Table 5-1 gives the properties of the sputtered surface as calculated using the image analysis software ImageJ [35]. As the sputtering time is increased from 3 to 6 s the Pt loading increases from 0.9 to 1.7 μg cm^{-2}, the surface area covered by Pt increases from 24 area% to 30 area%, the size of the islands increases from about 4 to about 10 nm, and the island density decreases from 5 to 2 islands per 100 nm^2. At 9 s sputtering a network of large interconnected islands with little exposed membrane area is apparent. The Pt loading at this stage is 3.4 μg cm^{-2} with about 72 area% of the polymer surface covered with Pt.

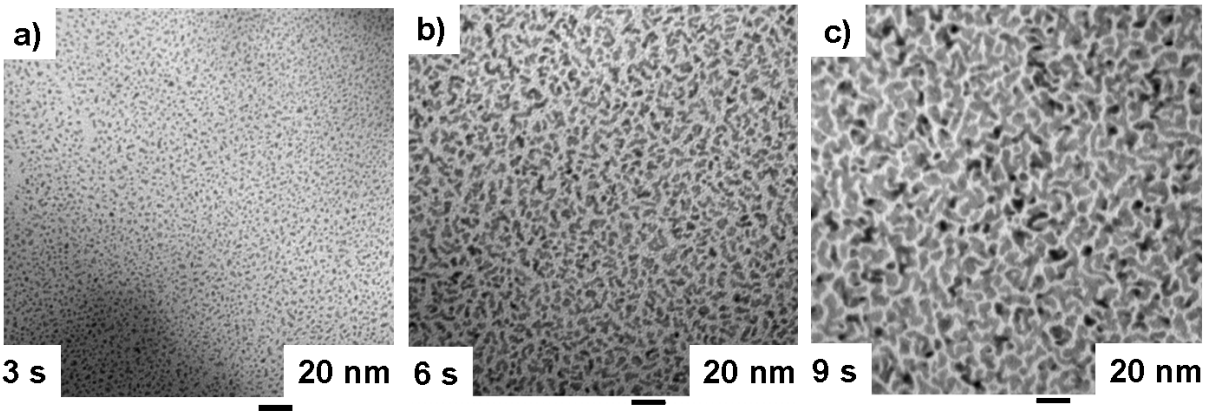

Figure 5-5: TEMs of the surface of PEI films sputtered with platinum. Isolated platinum metal islands formed after 3s sputtering increase in size after 6s sputtering and grow to an interconnected network of islands after 9s sputtering. Further sputtering leads to grain coarsening.

Figure 5-5 seems to indicate growth of Pt islands according to the Volmer-Weber mechanism [36]. In this mechanism during the first growth stage, metal nucleation occurs and metal clusters grow in diameter and there is an increase in the metal islands density. These features are consistent with the 3 s sputtering seen on Figure 5-5a. As growth proceeds, islands

coalesce and enlarge and there is a decrease in island density (Figure 5-5b). Finally the islands increase in size by branching with other meandering islands until a percolation network of Pt forms [36] as is seen for 9 s (Figure 5-5c).

The membranes used for hydrogenation experiments were sputtered with Pt under the same conditions and sputtering times as above. We attempt below to rationalize hydrogenation results by drawing on the morphological information presented here and the single gas permeation measurements to characterize membranes before and after sputtering.

Table 5-1: Metal deposition and membrane area coverage for platinum sputtering of the skin side of integral-asymmetric PEI gas separation membranes.

Sputtering time [s]	Platinum loading,[μg cm^{-2}]	Approx. average metal island diameter[nm]	Number of metal islands per area [#/100 nm^2]	Metal coverage [area %]
3	0.9	4	5	24
6	1.9	10	2	30
9	3.4	-	Interconnected network of islands	72

5.4.1.2 Degree of skin perfection

The asymmetric membranes evaluated in this study had a range of skin thicknesses and different degrees of skin perfection. The mainly size selective $\alpha_{H2/N2}$ determined by dividing single gas fluxes at 50 psig and room temperature was used as a stringent quality criterion. A perfect membrane skin would be indicated by an $\alpha_{H2/N2}$ of about 181 (as measured on a thick polymer film at 25 °C [26, 27]). The effective average skin thickness of perfect membrane skins can then be calculated from the known permeability coefficients of PEI films with known thickness. Defects in the polymer skin (transport not by solution-diffusion) will deteriorate $\alpha_{H2/N2}$ very rapidly. $\alpha_{H2/N2}$ between 181 (thick PEI film) and 3.7 (Knudsen selectivity of pores with a size below the mean free path of gas molecules) indicate that the gas is permeating through the membrane via some combination of solution-diffusion in the dense membrane skin and via permeation through defects with small pore sizes which still will likely prevent oil intrusion into

the substructure. $\alpha_{H2/N2}$ greater than 181 for sputtered membranes could indicate either that a fraction of the hydrogen is permeating through the metal layer (which has a low permeation rate at this temperature, but an infinite $\alpha_{H2/N2}$) or that the membrane skin polymer has been modified (perhaps densified) by the sputtering process, or a combination of the above.

While membrane skin perfection requirements are very important for gas separation membranes this is less so for the process presented here. Oil intrusion into the membrane and hydrogen bubbling into the oil can be prevented even if $\alpha_{H2/N2}$ is less than the intrinsic value since some Knudsen-diffusion level defects will not cause bubbling or oil intrusion while they will certainly reduce the high intrinsic $\alpha_{H2/N2}$ significantly.

The influence of the hydrogen delivery mode judged by $\alpha_{H2/N2}$ of the membranes on the reaction rates and catalytic selectivities was evaluated. While $\alpha_{H2/N2}$ was in the range of 4 to 220, in no case was oil permeation into the membrane support or through the membrane observed.

If polymeric membranes with minor skin layer defects could be successfully employed in this application, they would be cheaper and easier to manufacture than corresponding membranes with perfectly defect-free skins.

Detection of defects in the sub-micron thick skin of macroscopic areas (several cm^2) of integral-asymmetric membranes on the scale of Knudsen-diffusion type pores is very difficult by direct means. TEM, SEM, and AFM analyses can only scan very small areas. The defects may be few and the skin is inseparably connected to the porous sub-structure that contains the bulk of the polymer. Gas molecules however can serve as very sensitive skin morphology "probes" since the high selectivity $\alpha_{H2/N2}$ of glassy polymers like PEI is easily destroyed by even a few Knudsen diffusion-scale defects. Therefore, we will attempt below to rationalize the membrane morphology and impact of skin defects based on known physical properties of PEI and Pt, and the measured $\alpha_{H2/N2}$. It must be acknowledged that gas permeation measurements are certainly only circumstantial evidence of structure and morphology, but they are nonetheless quite sensitive and non-destructive, and are very useful in the absence of other methods to characterize the fine structure of ultrathin layers of a thin film "soft" material bonded to a bulky substructure of the same material.

5.4.1.3 Effect of plasma sputtering on polymeric membranes

The possible change in membrane properties (H_2 flux and $\alpha_{H2/N2}$) due to surface modification by ion bombardment in addition to the metal deposition complicates tracking the

effect of sputtering. Depending on the conditions employed (ion-energy, composition of ions, ion energy, polymer material, etc.), plasmas are reported to remove adsorbed surface materials/contaminants, etch the polymer, cross-link polymer chains, chemically modify the surface of the polymer, or even create new functional groups on the polymer surface [37-39]. The processes that lead to these modifications on the polymer surface are known to be highly complex and can not be exhaustively discussed here [39-43].

Sputtering only modifies the surface (up to about 2 nm depth) without significantly affecting the bulk properties of the material [40]. Therefore, we do not expect additional defects to result from the sputtering process.

Integral asymmetric PEI membranes were processed in the sputtering setup without a metal target to isolate effects on the polymer skin. Figure 5-6 shows the change in H_2 flux and $\alpha_{H2/N2}$ after processing the membrane in the sputterer without any target at 25°C, 100 mTorr air, and 45 mA. The pre-processing $\alpha_{H2/N2}$ values indicate that all samples had defects but likely on the order of Knudsen-diffusion type pores. Most of the membranes showed a decrease in selectivity as high as 60% with perhaps a minor increase or no change in hydrogen flux. Ion bombardment can lead to chemical modification, densification of the polymer surface and ablation of the polymer. The chemical modification and densification of the surface layer can lead to a decrease in $\alpha_{H2/N2}$ since the leak flux (not impacted by the sputtering plasma) becomes more prominent versus the "selective" flux through the defect-free and now densified areas of the polymer skin. This may also lead to the observed minor overall decrease in hydrogen flux. However, etching of the polymer surface may result in an increase in the membrane flux.

Probing the membranes by gas permeation does not deliver first-hand evidence but one may surmise that the impact of the plasma in the sputtering process (no metal deposited) seems consistent with effects reported in the literature (densification causing increased ideal gas selectivity but lower flux, ablation increasing the flux through decreasing the skin thickness, unchanged flux though small defects). The sputtering process itself certainly does not cause major changes in the gas transport properties as far as impacting the hydrogenation process is concerned.

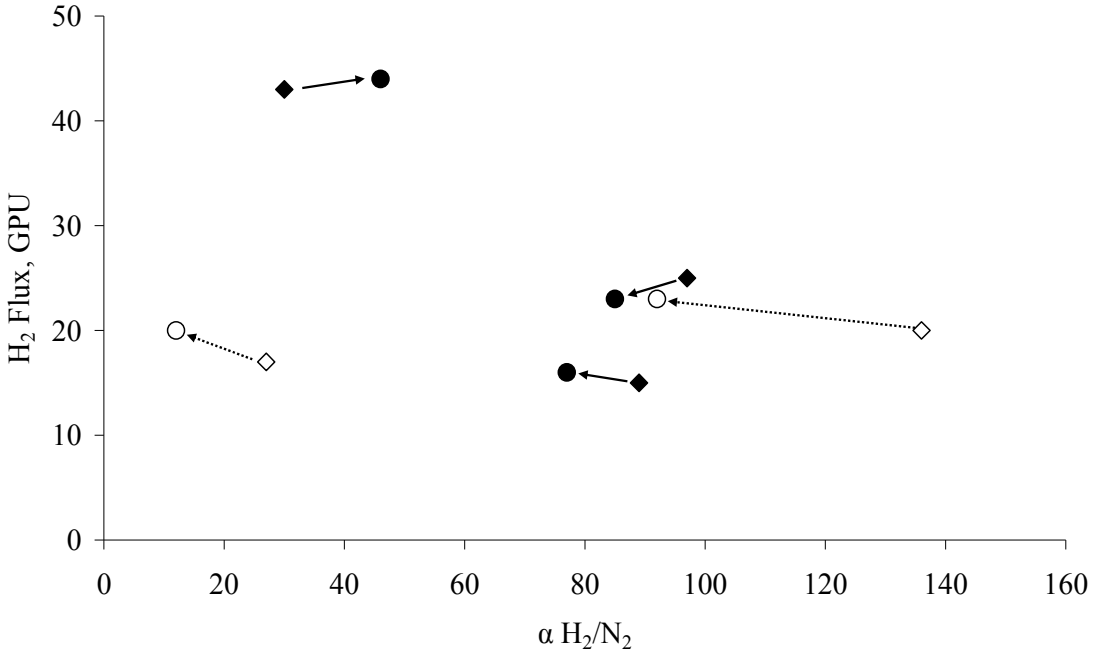

Figure 5-6: Effect of the sputter process in the absence of a metal target on the properties of integral asymmetric PEI membranes (100 mTorr air, 25°C, 45 mA). A decrease in selectivity is observed for most membranes with a moderate increase in hydrogen flux. From the limited data presented, no distinguishing patterns can be observed for the treatment at 3 s versus 9 s.

5.4.1.4 Effect of metal sputtering on polymeric membranes

For the hydrogenation experiments integral-asymmetric PEI membranes were sputter deposited with Pt. Figure 5-7 shows the percentage reduction in hydrogen flux as a function of virgin membrane $\alpha_{H2/N2}$ after Pt sputtering for 3, 6, and 9 s at 25°C, 100 mTorr air pressure, and 45 mA.

A wide variation in the reduction of hydrogen flux after sputtering is evident (0 to 90% flux reduction) even for membranes sputtered for the same amount of time and having similar virgin membrane $\alpha_{H2/N2}$. The factors impacting the gas transport property changes of membranes by metal sputtering can be grouped as follows:

- Flux increase, no selectivity change: plasma ablation of polymer from the non-metal coated areas of the skin

• Flux decrease, selectivity increase: plugging of defects by metal deposition, coverage of polymer with low-permeability/high H_2 selectivity metal, densification/cross linking of polymer via plasma.

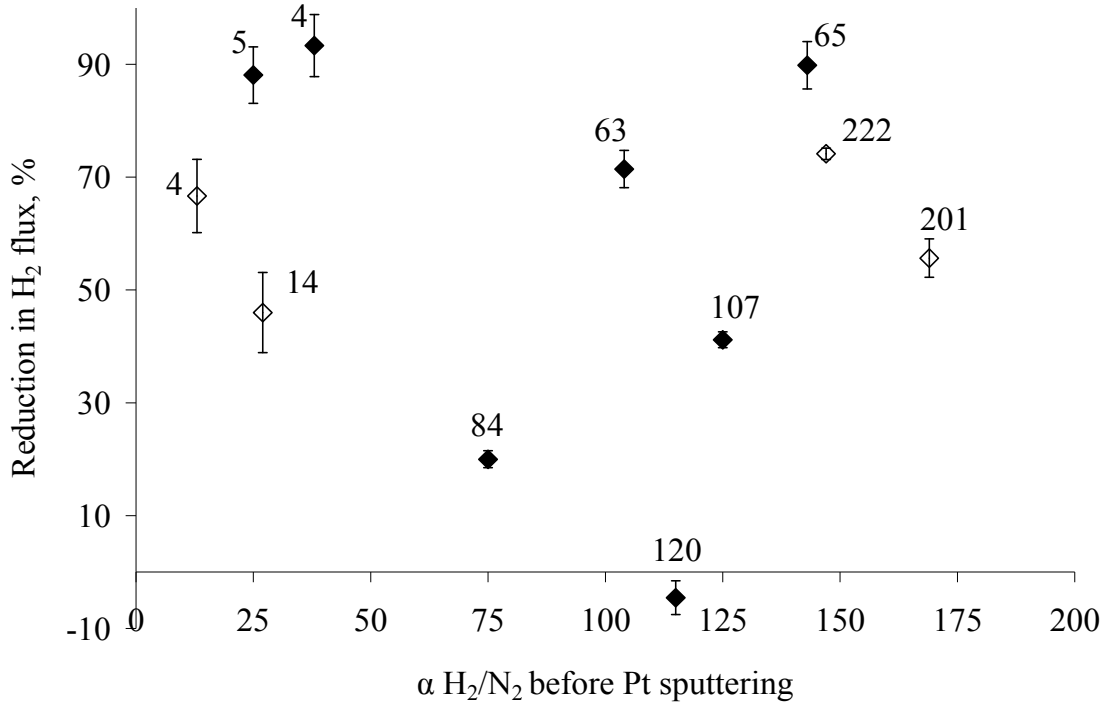

Figure 5-7: Effect of Pt metal sputtering on hydrogen flux and selectivity for 3 s (◊), and 9 s (♦) Pt sputtering. Labels indicate $\alpha_{H2/N2}$after sputtering. The figure shows a wide variation in the reduction of hydrogen flux through sputtering with Pt. (error bars represent the standard deviation of multiple analyses).

5.4.2 Hydrogenation results

Table 5-2 gives the properties of the integral-asymmetric PEI membranes before and after Pt sputtering that were used for hydrogenation experiments. These membranes were selected to evaluate the effect of membrane properties (H_2 flux, and the form of hydrogen supplied) and catalyst loading on the hydrogenation rate, the cis-trans isomerization, and the hydrogenated product composition.

It is important to keep in mind that the single gas hydrogen flux measurements of membranes do not represent the hydrogen flux under hydrogenation conditions. The driving force for single gas measurements of membranes is well defined and constant. However, the

driving force during a hydrogenation experiment can change significantly due to perhaps even local buildup of dissolved hydrogen in the oil if hydrogen consumption via hydrogenation cannot keep pace with the hydrogen supplied. The single gas flux measurements nonetheless indicate a "ceiling" for hydrogen transport and can be used to compare membranes with each other, especially in regard to defects.

Table 5-2: Properties of integral-asymmetric PEI membranes used in the experiment, before and after sputtering with platinum. (25 °C, 50 psig feed pressure)

H_2 flux [GPU]	Ideal gas selectivity $\alpha_{H2/N2}$	H_2 flux [GPU]	Ideal gas selectivity $\alpha_{H2/N2}$
Before sputtering		After sputtering	
	3 seconds sputtering		
35	169	15	201
29	147	7.5	222
40	27	22	14
38	13	12.5	4
	6 seconds sputtering		
24	136	15	196
21	125	6	183
11	120	4	140
17	20	14	19
77	17	19	5
	9 seconds sputtering		
59	143	6	65
17	125	10	107
22	115	23	120
7	104	2	63
1*	75	0.8*	84
60	38	4	4
84	25	10	5

* Membrane with 4 GPU flux operated at 10 psig hydrogen pressure (equivalent flux=0.8 GPU).

5.4.2.1 Effect of membrane flux and selectivity

The hydrogen flux of the membrane controls the maximum rate at which hydrogen can permeate through the membrane during a hydrogenation run. Using membranes with higher hydrogen flux is expected to increase the hydrogenation rate until the catalytic process becomes limiting. The ideal gas selectivity $\alpha_{H2/N2}$ of a membrane indicates how hydrogen is supplied to the membrane surface. A high selectivity membrane will result in a more uniform supply of

hydrogen across the membrane surface by solution-diffusion through the skin layer while a low selectivity membrane may indicate a portion of hydrogen being supplied through defects and concentrated at relatively few locations on the membrane surface. This hydrogen may or may not contribute effectively towards hydrogenation depending on the distribution of catalyst in the vicinity of the hydrogen source. It should be kept in mind, however, that no hydrogen bubbling can occur since the hydrostatic pressure of the oil exceeds that of the gaseous hydrogen.

In general, hydrogenation rates increase with hydrogen flux of the membrane and then level off. Figure 5-8 shows the hydrogenation rate (represented as iodine value IV hr^{-1}) with membranes having different hydrogen flux and $\alpha_{H2/N2}$. In an attempt to try to understand the factors influencing the variability in hydrogenation rate within the data set, we will explore the behavior of a few subsets of the data.

5.4.2.1.1 High catalyst loading

For membranes with high catalyst loading (3.4 μg Pt cm^{-2}), there is an increase in hydrogenation rate with increasing membrane flux and the selectivity of the membrane appears to have only a minor influence on the hydrogenation rate. The hydrogenation rate increased from 1.2 IV hr^{-1} for a membrane with a hydrogen flux of 0.8 GPU ($\alpha_{H2/N2}$=84) to 7.4 IV hr^{-1} for a membrane with hydrogen flux of 10 GPU ($\alpha_{H2/N2}$=5). This increase in the hydrogenation rate with increasing membrane flux indicates that the hydrogenation rate is limited by the supply of hydrogen through the membrane. Despite this apparent possible hydrogen "starvation" of the catalyst, lower TFA formation as compared to slurry reactors was observed [5].

For a catalyst loading of 3.4 μg cm^{-2}, about 70 % of the membrane area is covered with Pt. Thus, the reduction in hydrogen flux is expected to be close to 70% for an essentially defect-free membrane and assuming no significant effect of plasma ion-bombardment on the exposed polymer surface. However, the presence of defects complicates the impact of metal sputtering on gas transport rates beyond the simple relation to the metal-covered area. A hydrogen flux reduction lower than 70% despite 70% metal area coverage is possible if the distribution of Pt on the membrane surface is such that defects are unaffected by Pt sputtering. This also means that for these cases relatively more of the gas transport after sputtering is through the defects. This can also affect the hydrogenation rate as is seen in Figure 5-8. Some membranes show lower hydrogenation rates than expected. The membrane with a hydrogen flux of 10 GPU ($\alpha_{H2/N2}$=107) and the membrane with a hydrogen flux of 23 GPU ($\alpha_{H2/N2}$=120) both produced hydrogenation

rates of about 4.8 IV hr^{-1}, less than might have been expected from the trend of the other data. The membranes that produced unexpectedly low hydrogenation rates also exhibited lower reduction in hydrogen flux after sputtering (refer to Figure 5-8) which may indicate gas transport through defects. Only a 40% reduction in hydrogen flux after Pt sputtering is observed for the membrane with a final hydrogen flux of 10 GPU ($\alpha_{H2/N2}$=107), and almost no reduction in hydrogen flux by sputtering is observed for the membrane with a final hydrogen flux of 23 GPU ($\alpha_{H2/N2}$=120), as compared to close to 90% reduction in hydrogen flux for some other membranes (refer to Figure 5-7). High hydrogen availability in only certain regions where defects are present can not increase the overall hydrogenation rate proportionally since the process becomes limited by the available catalyst, rather than the hydrogen availability. If all hydrogen was for the sake of argument available in only one location on the membrane surface then most of the catalyst would be likely starved and a low hydrogenation rate would result.

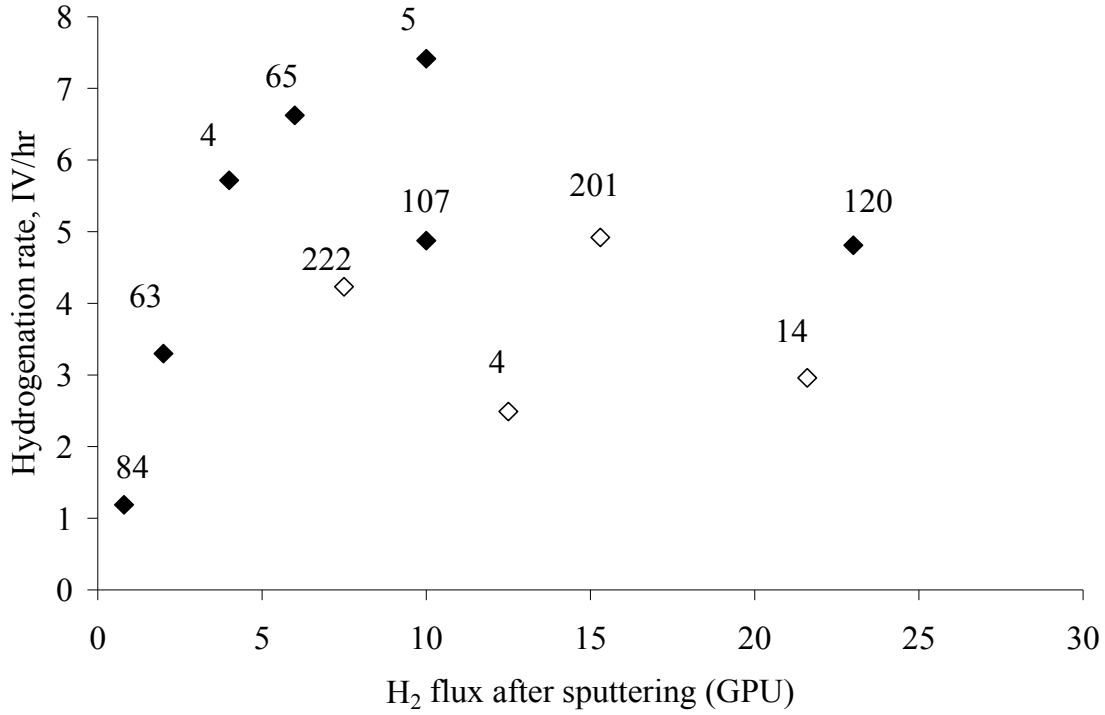

Figure 5-8: Effect of hydrogen flux and $\alpha_{H2/N2}$ (both measured after sputtering) on the hydrogenation rate, Pt sputtering for 3 seconds (◊), and 9 seconds (♦). The labels indicate $\alpha_{H2/N2}$ after sputtering. Reaction conditions: 70 °C, hydrogen pressure 50 psig.

5.4.2.1.2 Low catalyst loading

For membranes with low catalyst loading (0.9 μg cm^{-2}), a moderate increase in hydrogenation rate was obtained by using defect-free membranes having higher hydrogen fluxes. The hydrogenation rate increased from 4.2 IV hr^{-1} for membrane with a flux of 8 GPU ($\alpha_{H2/N2}$=222) to 4.9 IV hr^{-1} for a membrane with a hydrogen flux of 15 GPU ($\alpha_{H2/N2}$=201). However, the membranes sputtered for 3 s with Pt showed a significant decrease in hydrogenation rates when using membranes with low $\alpha_{H2/N2}$. The hydrogenation rate decreased from 4.2 IV hr^{-1} to 2.5 IV hr^{-1} when using a membrane with higher hydrogen flux but a much lower selectivity (12.5 GPU and $\alpha_{H2/N2}$=4 as compared to 7.5 GPU and $\alpha_{H2/N2}$=222). Even the membrane with a hydrogen flux of 22 GPU and $\alpha_{H2/N2}$=14 had a lower hydrogenation rate as compared to membrane with a hydrogen flux of 12.5 GPU and an essentially defect-free membrane skin. This significant drop in hydrogenation rate for low selectivity membranes can be explained by comparing the distribution of catalyst on the membrane surface for 3 s sputtering with the distribution obtained after sputtering for 9 s. Sputtering the membrane for 3 s results in small Pt islands (4 nm) with large distances between them and lower surface coverage (24%) while sputtering for 9 s results in an interconnected network of large Pt islands and higher surface coverage (72%) of the membrane with Pt (refer to Figure 5-5 and Table 5-1). A defective membrane sputtered with Pt for 3 s would likely result in a significant amount of hydrogen being supplied through these defects on average farther away from most catalytic sites, due to the distribution of catalyst as obtained after sputtering for 3 s. This would result in reduced hydrogen availability at catalytic sites and lead to lower hydrogenation rates as is seen in Figure 5-8.

In the range studied, the hydrogen flux of the membrane as determined by single gas permeation measurements appeared to have a minor influence on the formation of TFA. Figure 5-9 compares the TFA formed at an IV of 95 for membranes with different flux and catalyst loadings. For membranes sputtered for 3 s, TFA formation at an IV of 95 was 3.5 wt% for membrane with a hydrogen flux of 15 GPU ($\alpha_{H2/N2}$=201) and 4.3 wt% for a membrane with a hydrogen flux of 8 GPU ($\alpha_{H2/N2}$=222). For membranes sputtered for 9 s, TFA formation at an IV of 95 was in the range of 2.6-2.8 wt% irrespective of the flux of the membrane.

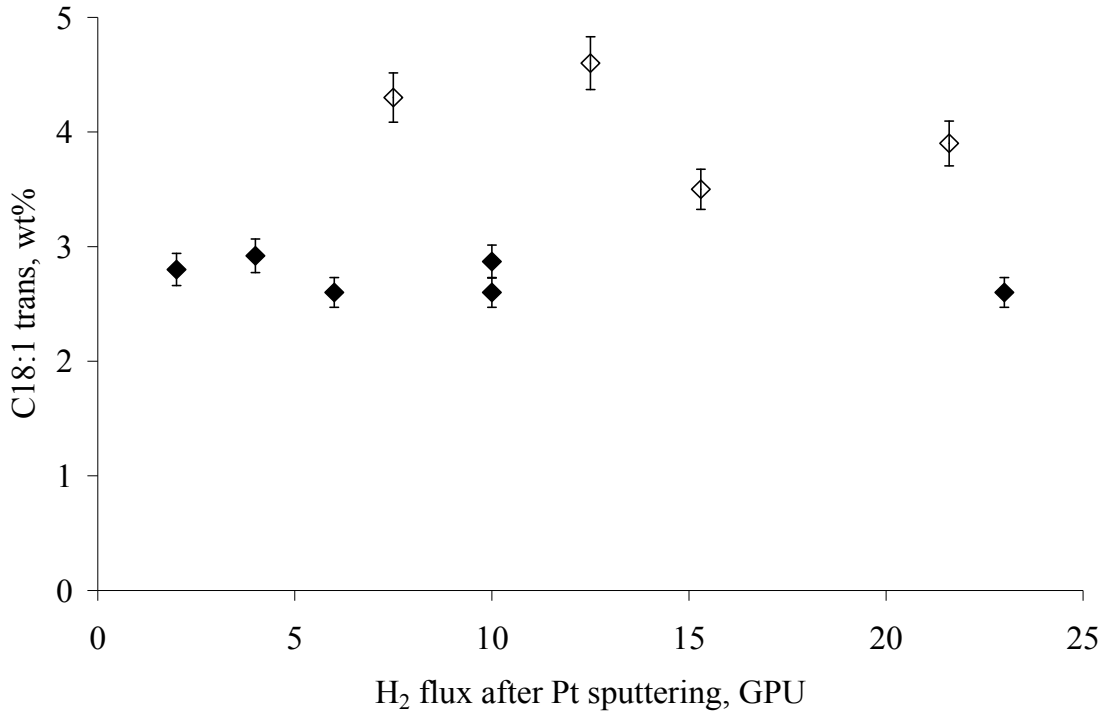

Figure 5-9: Effect of hydrogen flux of the membrane (measured after sputtering) on TFA formation (at IV 95), Pt sputtering for 3 seconds (◊), and 9 seconds (♦). Reaction conditions 70°C, hydrogen pressure 50 psig (error bars represent the standard deviation of multiple analyses).

5.4.2.2 Effect of catalyst loading for membranes with similar transport properties

For membranes with similar hydrogen flux after sputtering, a lower catalyst loading resulted in increased TFA formation at similar hydrogenation levels (refer to Figure 5-9). A membrane with a hydrogen flux of 8 GPU and catalyst loading 0.9 μg cm^{-2} produced 4.3 wt% TFA as compared to 2.6 wt% TFA produced by a membrane with a hydrogen flux of 6 GPU and catalyst loading of 3.4 μg cm^{-2} (sputtering time 9 s).This trend of decreased TFA formation with increased catalyst loading is opposed to what is observed in slurry systems where an increase in applied catalyst produces higher TFAs as it results in hydrogen starvation at the surface of the catalyst [4]. However, for catalytic membranes studied here, an increase in catalyst loading from 0.9 μg cm^{-2} to 3.4 μg cm-2, results in a significantly different physical catalyst morphology on the surface of the membrane. Small discrete Pt metal clusters are obtained at 0.9 μg cm^{-2}, while 3.4 μg cm-2 results in large interconnected network of islands. When membranes having similar

hydrogen flux are used, the catalyst distribution obtained at higher catalyst loadings (3.4 µg cm^{-2}) result in higher probability that the hydrogen will be usable by the catalyst thereby producing lower TFAs.

A decrease in TFA formation due to high concentration of hydrogen at the catalyst surface is also generally accompanied by an increase in the amount of fully saturated oil produced [4]. Figure 5-10 shows the amount of TFA and saturates formed at an IV of 95 for membranes having different catalyst loading. With the increase in catalyst loading from 0.9 µg cm^{-2} to 3.4 µg cm^{-2}, the amount of TFA decreased from 4.6wt% to 2.6 wt%, with an increase in C18:0 saturates from 13 wt% to 19 wt%. The high amount of saturates obtained with membranes having high catalyst loadings suggests a trade-off between low TFA formation and higher amount of saturates during hydrogenation by having higher hydrogen concentrations at the catalyst surface, as reported in other studies [44, 4].

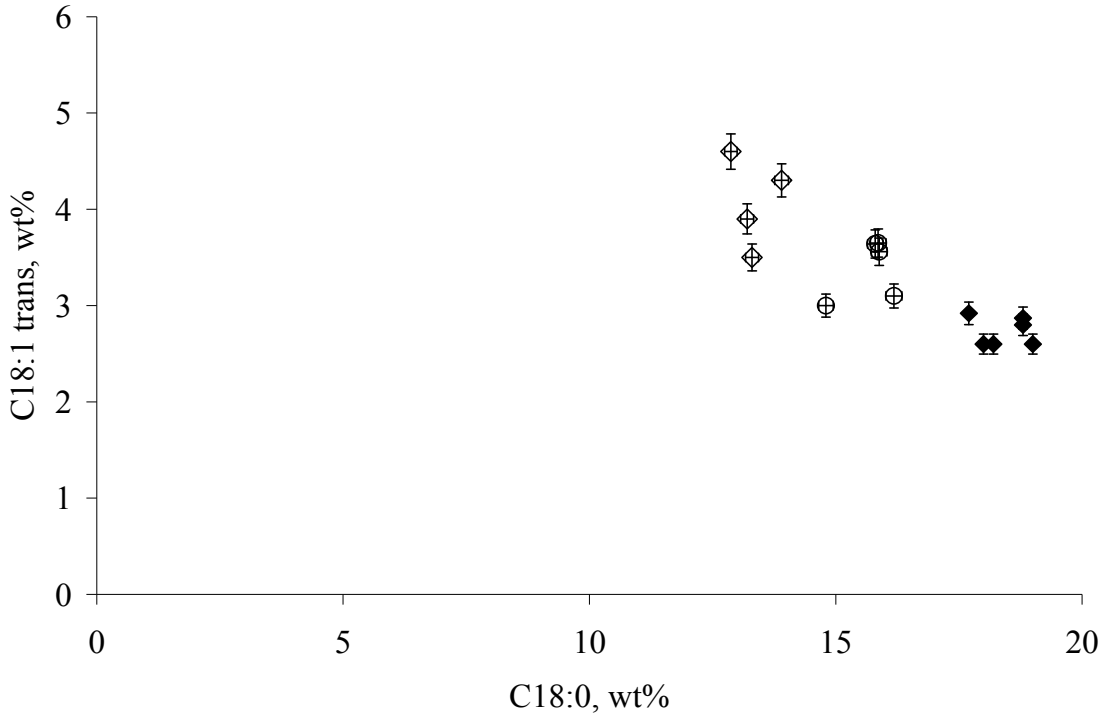

Figure 5-10: Effect of sputtering time on TFA and saturates (at IV 95) for 3 seconds (◊), 6 seconds (○), and 9 seconds (♦) Pt sputtering. Reaction conditions 70°C, hydrogen pressure 50 psig. A decrease in TFA formation and increase in C18:0 saturates is seen with increase in catalyst loading. (error bars represent the standard deviation of multiple analyses).

5.4.2.3 Effect of membrane properties and catalyst loading on product composition

For the same catalyst and process conditions, the product composition at similar hydrogenation levels will vary depending on the concentration of hydrogen at the surface of the catalyst. The hydrogenation reaction is more selective if the concentration of hydrogen at the surface of the catalyst is low [45]. Figure 5-11 shows how catalyst loadings can have an effect on the composition of the hydrogenated product. Linolenic acid (C18:3) hydrogenates at the same rate for both the cases. However, the composition profile for all other components varies. Higher amounts of saturates (C18:0), and linoleic acid (C18:2), and lower amounts of oleic acid (C18:1) at similar hydrogenation levels, are produced by using membranes with higher catalyst loadings and a slightly higher hydrogen flux. This may be due to high hydrogen concentration obtained at higher catalyst loading (3.4 μg cm^{-2}) as discussed above.

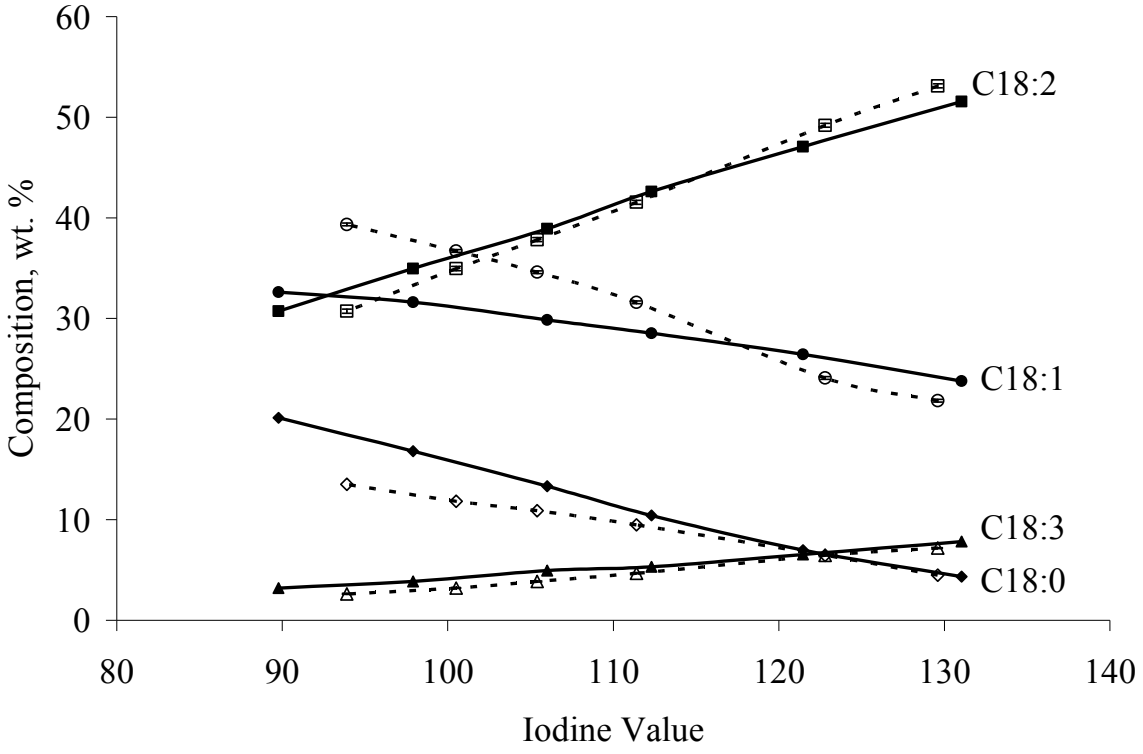

Figure 5-11: Effect of membrane properties on the composition of soybean oil during hydrogenation:

solid lines: catalyst loading 0.9 μg cm^{-2}, hydrogen flux = 8 GPU

dashed lines: catalyst loading 3.4 μg cm^{-2}, hydrogen flux = 10 GPU

(Reaction conditions 70 °C, hydrogen pressure 50 psig)

5.5 Process comparison and outlook

A base case of 100 metric tons of soybean oil to be hydrogenated per day from IV 130 to IV 90 will be assumed. This will stoichiometrically require about 3.7 mol of hydrogen atoms per second. The approach using electrochemical generation of hydrogen [21] will be compared to our approach since both can be performed under conditions compatible with existing facilities and both approaches significantly reduce TFA.

The electrochemical process will require about 270 m^2 of electrochemical reactor area configured as plate and frame cells as suggested in the publication (based on 90% current efficiency and 135 mA/cm^2). About 6.7 kg catalyst will be needed. This can perhaps be reduced by about 10% by using one anode per two cathodes in a cathode-anode-cathode stack design. The electrochemical process will consume electricity worth about 0.2 cents per kg of soybean oil hydrogenated (0.0678 $/kWh, per U.S. EIA, April 09) which compared to the raw oil cost is not significant. An electrochemical process will require auxiliary equipment such as rectifiers and control systems to supply over 360,000 A DC current at low voltage.

The metal-decorated membrane approach will require about 2,700 m^2 membrane area with a total of about 0.09 kg of Pt (~$3,600). This is based on the 9 s Pt sputtered membranes and about 5 hours to hydrogenate about 13.8 g of oil from IV 130 to 90, using 17.3 cm^2 of membrane area. A preferred configuration would be outside-skin hollow fibers spun from a glassy polymer like PEI or polysulfone. Metal deposition on various fibers is well established on the industrial scale for optical fibers and many other applications. Gas permeation hollow fibers and modules have been industrially used for many years for processes such as hydrogen separation from gas mixtures or nitrogen production from air. With the relatively high packing density of hollow fiber modules one can envision a module bank of perhaps a hundred to a few hundred 40 inch by 8 inch hollow fiber modules as sufficient to satisfy the above base case. Existing facilities could also gain incremental capacity by adding membrane modules in a bypass to their hydrogenation systems since pressures and temperatures are compatible. No auxiliary equipment besides oil pumping, gas manifolding, and pressure control is needed. Existing facilities are already familiar with these requirements.

The operating costs for both systems seem reasonable considering a much superior product will be made, and since existing hydrogen is assumed to be used. The catalyst costs appear to be lower for the metal-decorated phase inversion membrane system proposed here.

The electrochemical system will require significant numbers of relatively costly and complex plate-and-frame systems while the metal-decorated membranes rely on existing hollow fiber spinning, and module technology, augmented by metal vapor deposition or sputtering on the outside of the fibers. The simplicity of operating the hollow fiber modules compared to introducing an electrochemical system to the soybean oil industry may be an issue to consider. Module replacement also seems perhaps simplified and less expensive with hollow fiber modules compared to electrochemical fuel cells.

5.6 Conclusion

This study investigated the use of metal decorated integral-asymmetric polymer membranes for partial hydrogenation of soybean oil as an alternative to traditional slurry reactor systems and with the goal to significantly lower the undesirable trans fat content of the traditional hydrogenated product. Hydrogen was supplied directly at or near the skin surface of a Pt-sputtered integral-asymmetric polymeric membrane by pressurizing the porous substructure of the membrane with hydrogen. The oil flows past the Pt sputtered side of the membrane. Dissolved hydrogen and the liquid phase (soybean oil) come in direct contact with each other at the catalyst surface. This approach minimizes the gas-liquid mass-transfer limitations that are often experienced in three phase systems when using traditional slurry reactors. The level of TFA produced in the membrane reactor was very low (2.6-4.6 wt% at Iodine Value of 95). The system is compatible with existing hydrogenation facilities as far as temperature and pressures are concerned. Since the catalyst is immobilized on the membrane, no catalyst recovery is required, and a small amount of catalyst is sufficient. Membranes having different hydrogen flux, H_2/N_2 selectivity and catalyst loadings were tested for hydrogenation runs to evaluate the properties that have a significant impact on the process. The results show that hydrogen flux and H_2/N_2 selectivity of the composite membrane have only a minor influence on TFA formation. In the range studied, TFA formation decreased with an increase in the catalyst loading.

5.6 Reference

1. U.S. Census. Bureau, Current industrial reports. M311K, Fats and oils production, consumption, and stocks. in: U.S. Census Bureau, (Ed.), 2007.

2. Dejonge, A., J.W.E. Coenen, and C. Okkerse, Selective Hydrogenation of Linolenate Groups in Soya-Bean Oil. Nature 206 (1965) 573-574.

3. Musavi, A., M. Cizmeci, A. Tekin, and M. Kayahan, Effects of hydrogenation parameters on trans isomer formation, selectivity and melting properties of fat. European Journal of Lipid Science and Technology 110 (2008) 254-260.

4. Dijkstra, A.J., Revisiting the formation of trans isomers during partial hydrogenation of triacylglycerol oils. European Journal of Lipid Science and Technology 108 (2006) 249-264.

5. Singh, D., P.H. Pfromm, and M.E. Rezac, Partial Hydrogenation of Soybean Oil with Minimal Trans Fat Production Using a Pt-Decorated Polymeric Membrane Reactor. Journal of American Oil Chemists' Society 86 (2009) 93-101.

6. Mateos, R., M. Trujillo, M.C. Perez-Camino, W. Moreda, and A. Cert, Relationships between oxidative stability, triacylglycerol composition, and antioxidant content in olive oil matrices. Journal of Agricultural and Food Chemistry 53 (2005) 5766-5771.

7. Hunter, J.E., Dietary levels of trans-fatty acids: basis for health concerns and industry efforts to limit use. Nutrition Research 22 (2005) 499-513.

8. Oomen, C.M. , M.C. Ocke, E.J.M. Feskens, M.A.J. van Erp-Baart, F.J. Kok, and D. Kromhout, Association between trans fatty acid intake and 10-year risk of coronary heart disease in the Zutphen Elderly Study: a prospective population-based study. Lancet 357 (2001) 746-751.

9. Veldsink, J.W.B., Martin J.; Schoon, Nils-H.; Beenackers, Antonie A. C. M., Heterogeneous hydrogenation of vegetable oils: a literature review. Catalysis Reviews - Science and Engineering 39 (1997) 253-318.

10. Grau, R.J., A.E. Cassano, and M.A. Baltanas, Catalysts and Network Modeling in Vegetable Oil Hydrogenation Processes. Catalysis Reviews-Science and Engineering 30 (1988) 1-48.

11. Farr, W.E., Hydrogenation: processing technologies. in: F. Shahidi, (Ed.), Bailey's Industrial Oil and Fat Products, John Wiley & Sons, 2005.

12. Horiuti, I., and M. Polanyi, Exchange reactions of hydrogen on metallic catalysts. Trans. Faraday Soc. 30 (1934) 1164 - 1172.

13. Fillion, B., B.I. Morsi, K.R. Heier, and R.M. Machado, Kinetics, gas-liquid mass transfer, and modeling of the soybean oil hydrogenation process. Industrial & Engineering Chemistry Research 41 (2002) 697-709.

14. Grau, R.J., A.E. Cassano, and M.A. Baltanas, Solution of a Complex-Reaction Network - the Methyl-Linoleate Catalytic-Hydrogenation. Chemical Engineering Communications 58 (1987) 17-36.

15. Plourde, M., K. Belkacemi, and J. Arul, Hydrogenation of sunflower oil with novel Pd catalysts supported on structured silica. Industrial & Engineering Chemistry Research 43 (2004) 2382-2390.

16. List, G.R., W.E. Neff, R.L. Holliday, J.W. King, and R. Holser, Hydrogenation of soybean oil triglycerides: Effect of pressure on selectivity. Journal of the American Oil Chemists Society 77 (2000) 311-314.

17. Pintauro, P.N., Synthesis of a low-trans content edible oil, non-edible oil, or fatty acid in a solid polymer electrolyte reactor, US Patent No. 6,218,556 B1, 2001.

18. Piqueras, C.M., I.O. Costilla, P.G. Belelli, N.J. Castellani, and D.E. Damiani, Pd-gamma Al2O3 applied to triglycerides hydrogenation with supercritical propane Experimental and theoretical catalysts characterization. Applied Catalysis a-General 347 (2008) 1-10.

19. Schmidt, A., and R. Schomacker, Partial hydrogenation of sunflower oil in a membrane reactor. Journal of Molecular Catalysis a-Chemical 271 (2007) 192-199.

20. Veldsink, J.W., Selective hydrogenation of sunflower seed oil in a three-phase catalytic membrane reactor. Journal of the American Oil Chemists Society 78 (2001) 443-446.

21. Pintauro, P.N., M.P. Gil, K. Warner, G. List, and W. Neff, Electrochemical hydrogenation of soybean oil with hydrogen gas. Industrial & Engineering Chemistry Research 44 (2005) 6188-6195.

22. An, W.D., J.K. Hong, P.N. Pintauro, K. Warner, and W. Neff, The electrochemical hydrogenation of edible oils in a solid polymer electrolyte reactor. II. Hydrogenation selectivity studies. Journal of the American Oil Chemists Society 76 (1999) 215-222.

23. Mondal, K., and S.B. Lalvani, Electrochemical hydrogenation of canola oil using a hydrogen transfer agent. Journal of the American Oil Chemists Society 80 (2003) 1135-1141.

24. Peinemann, K.V., K. Fink, and P. Witt, Asymmetric Polyetherimide Membrane for Helium Separation. Journal of Membrane Science 27 (1986) 215-216.

25. Obrien, K.C., W.J. Koros, T.A. Barbari, and E.S. Sanders, A New Technique for the Measurement of Multicomponent Gas-Transport through Polymeric Films. Journal of Membrane Science 29 (1986) 229-238.

26. Barbari, T.A., W.J. Koros, and D.R. Paul, Polymeric Membranes Based on Bisphenol-a for Gas Separations. Journal of Membrane Science 42 (1989) 69-86.

27. Rezac, M.E., and B. Schoberl, Transport and thermal properties of poly(ether imide) acetylene-terminated monomer blends. Journal of Membrane Science 156 (1999) 211-222.

28. Steward, S.A., Review of hydrogen isotope permeability through materials, Lawrence Livermore National Laboratory, 1983.

29. AOCS, Preparation of methyl esters of fatty acids, Official methods and recommended practices of the AOCS, American Oil Chemists' Society, Champaign, Ill., 1998, pp. Ce 2-66.

30. Nawar, W.W. Chemistry. in: Y.H. Hui, (Ed.), Bailey's Industrial Oil & Fat Products John Wiley & Sons, Inc., 1996.

31. Petursson, S., Clarification and expansion of formulas in AOCS recommended practice Cd 1c-85 for the calculation of iodine value from FA composition. Journal of the American Oil Chemists Society 79 (2002) 737-738.

32. Balaji, S., P.V. Satyam, V. Lakshminarayanan, and S. Mohan, Influence of secondary ion bombardment on the composition, structure and surface properties of platinum thin films. Nuclear Instruments & Methods in Physics Research Section B-Beam Interactions with Materials and Atoms 217 (2004) 423-428.

33. Scott, E.R., H.S. White, and D.J. Mcclure, Scanning Tunneling Microscopy of Platinum Films on Mica - Evolution of Topography and Crystallinity during Film Growth. Journal of Physical Chemistry 93 (1989) 5249-5253.

34. Cahill, D.G. Morphological instabilities in thin-film growth and etching. Journal of Vacuum Science & Technology A 21 (2003) S110-S116.

35. Collins, T.J., ImageJ for microscopy. Biotechniques 43 (2007) 25-30.

36. Andreazza, P., C. Andreazza-Vignolle, J.P. Rozenbaum, A.L. Thomann, and P. Brault, Nucleation and initial growth of platinum islands by plasma sputter deposition. Surface & Coatings Technology 151 (2002) 122-127.

37. Coates, D.M., and S.L. Kaplan, Modification of polymeric surfaces with plasmas. Mrs Bulletin 21 (1996) 43-45.

38. Foerch, R. and D.H. Hunter, Remote Nitrogen Plasma Treatment of Polymers - Polyethylene, Nylon 6,6, Poly(Ethylene Vinyl Alcohol), and Poly(Ethylene-Terephthalate). Journal of Polymer Science Part a-Polymer Chemistry 30 (1992) 279-286.

39. Vegh, J.J., D. Nest, D.B. Graves, R. Bruce, S. Engelmann, T. Kwon, R.J. Phaneuf, G.S. Oehrlein, B.K. Long, and C.G. Willson, Molecular dynamics simulations of near-surface modification of polystyrene: Bombardment with Ar+ and Ar+/radical chemistries. Journal of Applied Physics 104 (2008) 034308.

40. Coen, M.C., R. Lehmann, P. Groening, and L. Schlapbach, Modification of the micro- and nanotopography of several polymers by plasma treatments. Applied Surface Science 207 (2003) 276-286.

41. Delcorte, A., P. Bertrand, and B.J. Garrison, Collision cascade and sputtering process in a polymer. Journal of Physical Chemistry B 105 (2001) 9474-9486.

42. Delcorte, A., and B.J. Garrison, Kiloelectronvolt argon-induced molecular desorption from a bulk polystyrene solid. Journal of Physical Chemistry B 108 (2004) 15652-15661.

43. Maya, P.N., U. von Toussaint, and C. Hopf, Synergistic erosion process of hydrocarbon films: a molecular dynamics study. New Journal of Physics 10 (2008) Article # 023002.

44. Piqueras, C.A., G. Tonetto, S. Bottini, and D.E. Damiani, Sunflower oil hydrogenation on Pt catalysts: Comparison between conventional process and homogeneous phase operation using supercritical propane. Catalysis Today 133 (2008) 836-841.

45. Patterson, H.B.W., Hydrogenation of fats and oils, Applied Science Publishers Ltd., 1983.

CHAPTER 6 - Overcoming mass-transfer limitations in the partial hydrogenation of soybean oil using metal decorated polymeric membrane reactors: impact of temperature and pressure on performance

6.1 Introduction

Multiphase reactions are widely used in the chemical, petrochemical, biotechnology, and food processing industries. Multiphase reactions are often constrained by mass transfer limitations which in many cases lead to low reaction rates and undesirable product distribution[1,2].

The partial hydrogenation of vegetable oil is an important reaction in the food industry, used to improve the oxidative stability and increase the solid fat content in vegetable oil. In the U.S. alone, the annual production of margarines and shortenings was around 8 billion pounds in 2007[3]. Partial hydrogenation is a three phase (gas-liquid-solid) reaction with hydrogen as a gas, oil as a liquid and the catalyst as a solid. The conventional hydrogenation of vegetable oil is carried out in a batch autoclave (Figure 1a) over nickel based catalyst in slurry at around 110-190ºC, 30-70 psi hydrogen pressure, with 0.01-0.15wt% Ni catalyst [2] generally supported on kieselguhr or silica-alumina [4]. The traditional slurry approach to vegetable oil hydrogenation relies on the dissolution of hydrogen in the oil to supply required hydrogen to the catalytic sites. A batch autoclave (typically capable of handling 30,000-90,000 pound batch sizes [5]) equipped with a hydrogen gas distributor, agitator (common agitators provide approximately 100 rpm, and radial flow impellers are used [5]), and heating/cooling coils is generally used.

The vegetable oil hydrogenation process can be described by the Horiuti-Polanyi Mechanism[6, 7]. The hydrogen dissolves in liquid oil, diffuses through the oil and is adsorbed on the catalyst surface where it dissociates into two adsorbed hydrogen atoms. The adsorbed hydrogen atom reacts with the adsorbed fatty acid molecule to form an unstable half hydrogenated intermediate complex. If the concentration of hydrogen at the catalyst surface is high the addition of second H atom to the half hydrogenated intermediate dominates over isomerization reactions. When the hydrogen coverage of the surface is low, abstraction of

hydrogen may be more likely than insertion[2], thus promoting isomerization and formation of undesirable TFA at the expense of hydrogenation.

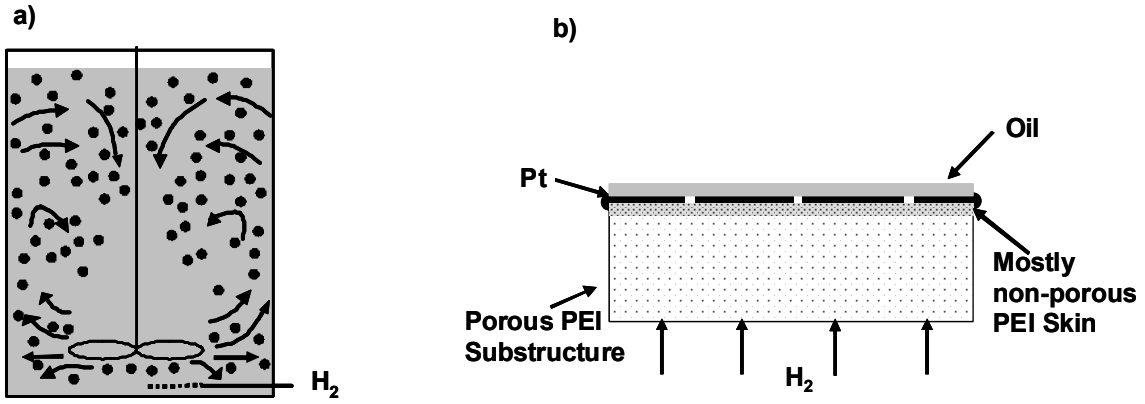

Figure 6-1: Schematic of slurry reactor and metal polymer composite membrane reactor for hydrogenation of soybean oil.

In the conventional slurry reactor design, low solubility of hydrogen in oil leads to increased mass transfer limitations and a scarcity of hydrogen at the catalyst surface. This promotes the isomerization reaction at the expense of hydrogenation and results in significant amounts of TFAs.

Interfacial mass transfer effects has been recognized as the major limiting step in the hydrogenation process[2] and many modifications on conventional agitated autoclaves, novel reactor designs [8-10] and processes[11, 12] have been evaluated to reduce interfacial mass transfer resistance. A more recent type of reactor for three phase reactions is a membrane contactor. In this type of reactor the gas and liquid reactants are allowed to come in direct contact with each other without the need for the dispersion of one phase into the other as is practiced traditionally.

In a recent paper [13], we demonstrated the hydrogenation of soybean oil using a metal decorated polymeric membrane. The metal decorated polymeric membrane produced significantly lower TFAs as compared to the traditional approach. Other advantages of the proposed reactor include: the process is compatible with existing hydrogenation facilities as far as temperature and pressure are concerned, is simpler than some of the alternatives[11, 14] being studied and no catalyst recovery from the oil is needed since the catalyst is immobilized on the membrane.

Temperature and pressure are important parameters in reactor design. Operation at higher temperatures is often desired due to higher reaction rates. For the case of hydrogenation of

vegetable oil in traditional slurry reactor, an increase in temperature increases the rate of formation of TFA due to (1) a lower hydrogen solubility in oil and (2) an increased hydrogenation rate. These factors both lead to reduced hydrogen availability at the catalyst surface. Higher pressures can be used to increase the solubility of hydrogen in oil and reduce the formation of TFAs.

If metal decorated polymeric membranes are able to maintain a high concentration of hydrogen at catalyst surface even at higher temperatures, we could obtain higher reaction rates without the usual increase in TFA. Furthermore, because the membrane reactor supplies hydrogen directly to the catalyst, modest system pressures should be sufficient. This work studies the behavior of metal decorated polymeric membranes for partial hydrogenation of soybean oil, with specific focus on the influence of system temperature and pressure. The behavior is also compared with that of traditional slurry reactors for partial hydrogenation of soybean oil.

6.1.1 Metal decorated polymeric membrane

Figure 6-1b shows the schematic of a metal decorated polymeric membrane studied in this work. It consists of an integral asymmetric polymeric membrane with high flux and selectivity for hydrogen and negligible permeability to vegetable oil. The polymeric membrane consists of a highly porous substructure with a thin (approximately 0.1-0.3 μm), dense and nearly defect-free layer known as the membrane skin. Subsequently the membrane skin was decorated with palladium or platinum catalyst using magnetron sputtering. The distribution of the metal catalyst on the membrane surface is shown in Figure 6-2. The metal was deposited as a network of large interconnected islands with some exposed membrane area. One of our previous studies showed that the catalyst distribution as obtained (Figure 6-2) gave high hydrogenation rates with minimum formation of TFA[15].

6.2 Experimental

6.2.1 Materials

Soybean oil (Iodine Value IV = 129-131) was obtained from MP Biomedicals (Solon, OH). The composition of soybean oil as measured in our laboratory is (reported as weight percent): C16:0, 11.6-12.0; C18:0, 4.3-4.4; C18:1, 21.6-23.8; C18:2, 51.6-53.3; C18:3, 7.1-7.8;

total trans fatty acids, 0.7-1.2; C18:1 trans, 0.0; C14:0-C24:0, 0.9-1.5. Acetic acid (HPLC grade), acetone (99.5%), p-xylene (99.9%), and dicholoromethane (99.9%), used in membrane casting were obtained from Fisher Scientific (Rochester, NY). 1,1,2,2-tetrachloroethane (98%) was obtained from Sigma Aldrich (St. Louis, MO). PEI to cast asymmetric membranes was obtained from General Electric (Huntersville, NC, Ultem-1000). Platinum (99.95wt% platinum) and palladium (99.95 wt% palladium) targets for sputtering were obtained from Ted Pella Inc. (Redding, CA).

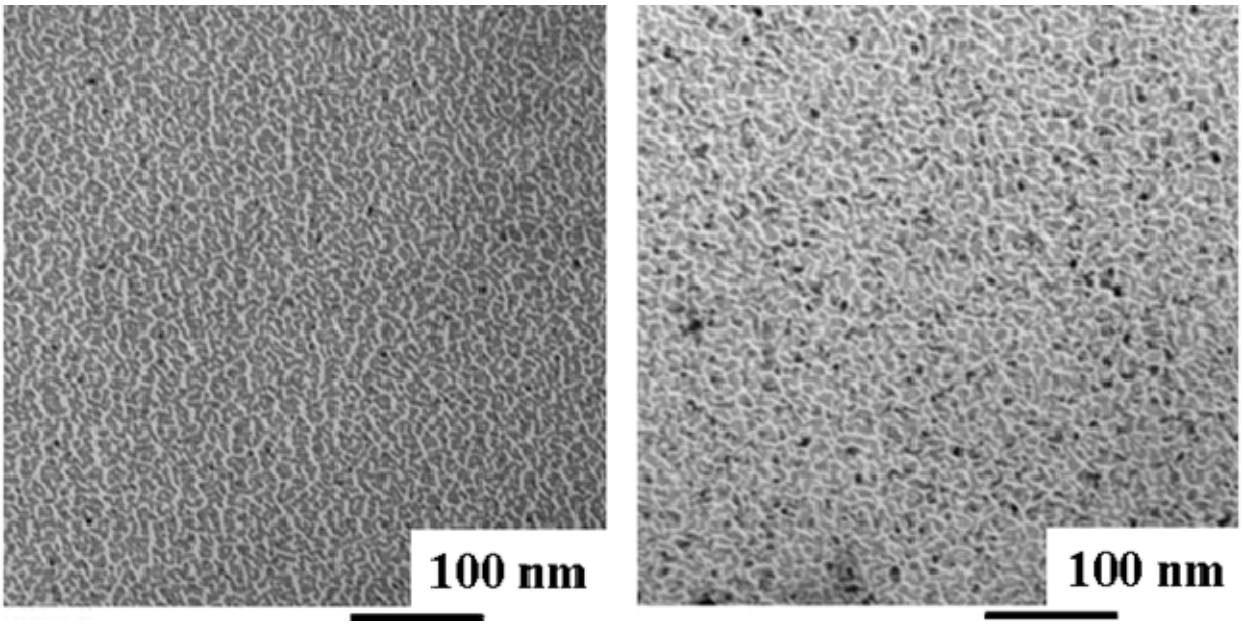

Figure 6-2: TEMs of the surface of PEI films sputtered with palladium/platinum for 9 seconds. The images show an interconnected network of Pd/Pt islands formed at the surface of PEI film.

6.2.2 Membrane preparation

The integral asymmetric PEI membranes used in this study were fabricated in our lab using the phase inversion process as described by Peinemann[16]. Circular stamps (4.6 cm diameter) were cut from membrane sheets and tested for their gas flux using a constant-volume variable-pressure apparatus similar to the one described elsewhere[17]. All evaluations were completed at 25 °C with a feed pressure of 50 psig. The normalized gas flux and the ideal gas selectivity (H_2/N_2) are calculated as a quality control. The ideal gas selectivity $\alpha H_2/N_2$ is the ratio of the normalized gas fluxes for gas H_2 and N_2 at a given temperature and feed pressure. The hydrogen flux of these membranes can be as high as 100 GPU (one gas permeation unit or GPU equals 10^{-6} cm^3(STP) $cm^{-2}s^{-1}cmHg^{-1}$) and ideal gas selectivities measured by single gas

permeation of $\alpha H_2/N_2$ up to 181 at 25 °C(ideal $\alpha H_2/N_2$ for PEI) [18, 19]. Any defects in the membrane skin result in ideal gas selectivities that are lower than the ideal value of 181.

Before use in hydrogenation experiments the membranes were sputtered on the skin side with palladium or platinum metal catalyst using a DESK II magnetron sputter (Denton Vacuum, Moorestown, NJ, for 9 seconds at 45 mA, 100 mtorr) and were re-tested for their gas transport properties. The gas flux of the membranes is reduced after sputtering as can be expected from coverage of the membrane with a resistive metal layer. Gas selectivities after sputtering also change and the change depends on factors such as initial $\alpha H_2/N_2$, partial coverage of the membrane surface with metal, and the modification of the membrane skin due to plasma sputtering process [20, 21].

The loading of the metal catalyst on the membrane was determined by sputtering the metal on a quartz crystal under the same sputtering conditions as used for hydrogenation runs and measuring the weight of the deposited ($\mu g\ cm^{-2}$) platinum using a quartz crystal microbalance.

The morphology of the membrane surface and catalyst distribution after sputter deposition was studied using transmission electron microscopy (TEM). For this purpose, a thin layer (< 100 nm) of PEI was spin coated on a TEM grid (2000 mesh copper grid, Electron Microscopy Sciences, Hatfield, PA) followed by palladium/platinum sputtering under the same conditions (25 °C, 100 mTorr air, 45 mA for 9 seconds) as used for the hydrogenation runs. The TEM grids with a thin layer of PEI sputtered with the metal catalyst were analyzed using TEM.

6.2.3 Experimental setup and procedures

The platinum sputtered membrane was installed in a stainless steel 47 mm filter holder (model XX4404700, Millipore Corp., Billerica. MA). The filter holder was installed in an experimental set up equipped with gear pump for soybean oil circulation, heating tapes, temperature controller and pressure gauge on both sides of the membrane. Before the start of the hydrogenation reaction the catalyst on the membrane was reduced by flowing hydrogen at 60 ºC for 15 hours on the skin side of the membrane with the permeate side open to the atmosphere. After reduction soybean oil was added to the system. To avoid oxidation of oil, air was removed from the system with a nitrogen purge before heating the oil. The oil was circulated with a flow rate of about 25 grams/min across the skin side of the membrane using a gear pump (series GA,

Micropump Inc., Vancouver, WA). UHP hydrogen was supplied from the porous substructure side of the membrane at the required pressure after the desired reaction temperature was attained. The oil side pressure was always maintained at a pressure 10 psi higher than the hydrogen side pressure (to prevent damage to the unsupported membrane) using ultra high purity (UHP) nitrogen applied to the headspace of the reactor. Oil samples were taken at regular intervals and analyzed using methods as discussed below.

6.2.4 Analysis

Oil samples were converted to their corresponding fatty acid methyl esters (FAMEs) following the alternate method in AOCS official method Ce 2-66. FAMEs thus obtained were analyzed by gas chromatography (GC) using a 100 m CP-Sil 88 column in a Hewlett-Packard 6890 series gas chromatograph. AOCS official method Ce 1h-05 was followed for the analysis of fatty acids. Injection port and column were maintained at 250 ºC and 181 ºC, respectively, helium carrier gas at 1 ml/min and split injection (split ratio 1:100) was used. The IV of hydrogenated oil was calculated from the composition obtained by GC analysis using Equation 5-2[21].

$$\mathrm{IV} = (\%\mathrm{C16:1}\times 0.9502)+(\%\mathrm{C18:1}\times 0.8598)+(\%\mathrm{C18:2}\times 1.7315)+(\%\mathrm{C18:3}\times 2.6152) \quad \text{Equation 6-1}$$

6.2.5 Hydrogenation selectivity

If the hydrogenation of soybean oil is represented by the first-order irreversible reaction scheme as shown in Equation 6-2 then it is possible to calculate hydrogenation selectivities using the experimental composition data from our experiments[22].

$$C18:3(Ln)\xrightarrow{k_1}C18:2(L)\xrightarrow{k_2}C18:1(O)\xrightarrow{k_3}C18:0(S) \quad \text{Equation 6-2}$$

Where k_1, k_2, k_3 are pseudo-first-order rate constants. The linolenate (S_{Ln}), Linoleate (S_L), and, isomerization selectivity (S_i) selectivities are defined as

$$S_{Ln}=\frac{k_1}{k_2} \quad \text{Equation 6-3}$$

$$S_{L}=\frac{k_2}{k_3} \quad \text{Equation 6-4}$$

$$S_i = \frac{\Delta trans}{\Delta IV}$$ Equation 6-5

Integrating the appropriate rate equations based on Equation 5-2 for the mol% of linolenate [Ln], linoleate [L], and oleate [O] fatty acids and rearranging yields[22]:

$$[Ln]_t = [Ln]_{t=0} e^{-k_1 t}$$ Equation 6-6

$$[L]_t = [Ln]_{t=0}\left(\frac{k_1}{k_2 - k_1}\right)\left(e^{-k_1 t} - e^{-k_2 t}\right) + [L]_{t=0} e^{-k_2 t}$$ Equation 6-7

$$[O]_t = [Ln]_{t=0}\left(\frac{k_1}{k_2 - k_1}\right)\left(\frac{k_2}{k_3 - k_1}\right)\left(e^{-k_1 t} - e^{-k_3 t}\right) \quad - \quad [Ln]_{t=0}\left(\frac{k_1}{k_2 - k_1}\right)\left(\frac{k_2}{k_3 - k_2}\right)\left(e^{-k_2 t} - e^{-k_3 t}\right) +$$

$$[L]_{t=0}\left(\frac{k_2}{k_3 - k_2}\right)\left(e^{-k_2 t} - e^{-k_3 t}\right) + [O]_{t=0} e^{-k_3 t}$$ Equation 6-8

The selectivities reported here were calculated using our experimentally determined oil composition and then solving Equation 5-7, Equation 5-8, and Equation 5-9 to obtain k_1, k_2, and k_3 using a computer code as described in AOCS official method Tz 1b-79 . The code was rewritten in Java with a convergence criterion of 0.01%.

6.3 Results and discussion

Hydrogenation runs were performed at different temperatures (50-90 °C) and pressures (50-200 psig), using palladium and platinum polymer composite membranes, to determine their behavior for partial hydrogenation of soybean oil. Table 6-1 gives the properties of the membranes used in the hydrogenation run and the corresponding pressure and temperature.

The membranes studied here have a range of hydrogen flux and H_2/N_2 selectivities depending on the skin thickness of produced membranes and presence/absence of defects on the membrane skin. Due to the range of properties of membranes used in this study, a brief discussion on the effect of membrane properties on hydrogenation rate and TFA formation is provided below.

6.3.1 Effect of membrane properties

The hydrogen flux of a composite membrane controls the maximum rate at which hydrogen can permeate through the membrane during a hydrogenation run. Using membranes

with higher hydrogen flux will increase the hydrogenation rate until the catalyst surface becomes saturated with hydrogen. The H_2/N_2 selectivity of a membrane is an indirect indicator of the defects in the membrane skin. It provides insight into the dominant hydrogen transport mechanisms. A high selectivity membrane will result in a more uniform supply of hydrogen to the membrane surface while a low selectivity membrane may result in a part of hydrogen being supplied through defects and concentrated at a few locations on the membrane surface. This hydrogen may or may not contribute effectively towards hydrogenation reaction depending on the distribution of catalyst in the vicinity of the defect.

Table 6-1: Properties of membranes and hydrogenation conditions used in the study.

H_2 flux [GPU]	Ideal gas selectivity $\alpha_{H2/N2}$	Temperature	Pressure, psig
Catalyst: Palladium,1.4 μg cm^{-2}			
12	164	50	50
81	6	70	50
59	145	90	50
7	100	70	50-200
Catalyst: Platinum, 3.4 μg cm^{-2}			
4	18	60	50
10	5	70	50
46	64	90	50
7	14	70	50-200

An earlier study in our lab evaluated platinum polymer composite membranes having a range of hydrogen fluxes, skin defects, and catalyst loadings. It was observed that hydrogenation rates increase with hydrogen flux and then level off. For Pt sputtering of 9 seconds (also the sputtering time used here), for majority of the cases low H_2/N_2 selectivity of the membrane had no influence on hydrogenation rate. The hydrogen flux and membrane selectivity showed little influence on TFA formation[15].

For this work, based on the observation of earlier studies in our lab, for each hydrogenation run we chose a membrane with properties such that it could supply sufficient hydrogen for the temperature.

6.3.2 Effect of temperature

It is desirable to operate at high temperatures due to higher reaction rates; however, higher temperatures conventionally also lead to increased formation of TFAs. This section

discusses the influence of temperature on hydrogenation rate, cis-trans isomerization and hydrogenation selectivities. The results are compared with those of slurry based systems under similar conditions.

6.3.2.1 Hydrogenation rate

Figure 6-3 shows the effect of temperature on hydrogenation rate using Pd decorated polymeric membrane reactor at 50 psig hydrogen pressure. The hydrogenation rate was 3.4 IV hr-1 at 50 °C, increased to 10.4 IV hr-1 at 70 °C, and to 22.4 IV hr-1 at 90 °C. The Pt decorated polymeric membrane reactor , however, showed little activity at 50 °C, so hydrogenation runs were performed at 60, 70, and 90 °C. The hydrogenation rate for Pt polymer membrane was 3.6 IV hr-1 at 60 °C and increased to 17.2 IV hr-1 at 90 °C. The conventional slurry reactors show considerably higher rates than those reported here for metal polymer membranes. The hydrogenation rate for palladium slurry reactor was 5-15 times higher[24] as compared to palladium catalytic membranes due to higher catalyst surface area in the slurry reactor system.

The apparent activation energy (E_a) for hydrogenation for Pd catalyst was 11.2 kcal mol^{-1} and that for Pt was 11.7 kcal mol^{-1}. The slightly higher activation energy for platinum is due to the lower activity of platinum as compared to palladium[2]. Hsu et al.[23] observed activation energy of 7.7 kcal mol^{-1} for palladium catalyst in a slurry reactor. Although activation energy is independent of the type of reactor, it is significantly affected by the presence of mass transfer limitations. Lower apparent activation energies are obtained in conditions influenced by mass transfer limitations, which may be the case for the slurry reactor system.

6.3.2.2 Trans fatty acid formation

In a traditional three phase slurry reactor an increase in temperature increases the rate of hydrogen consumption, with minor change in the supply rate of hydrogen. This increases the hydrogen starvation of the catalyst and leads to higher TFA formation. In the metal decorated polymeric membranes, hydrogen is supplied to the catalyst “on demand” with the maximum rate of supply at a given hydrogen pressure limited by the membrane characteristics. Additionally, permeability of hydrogen through PEI increases with temperature with an activation energy of about 3.2 kcal mol^{-1} [18]. So if membranes with appropriate characteristics (low skin defects) and sufficient hydrogen flux are used, an increase in temperature will lead to minimum starvation of the catalyst and thus minimum increase in TFA.

This can also be seen in Figure 6-4 which compares TFA formed during hydrogenation as the temperature was increased, for the palladium decorated polymeric membrane reactor and conventional slurry reactor using Pd/alumina catalyst [24].

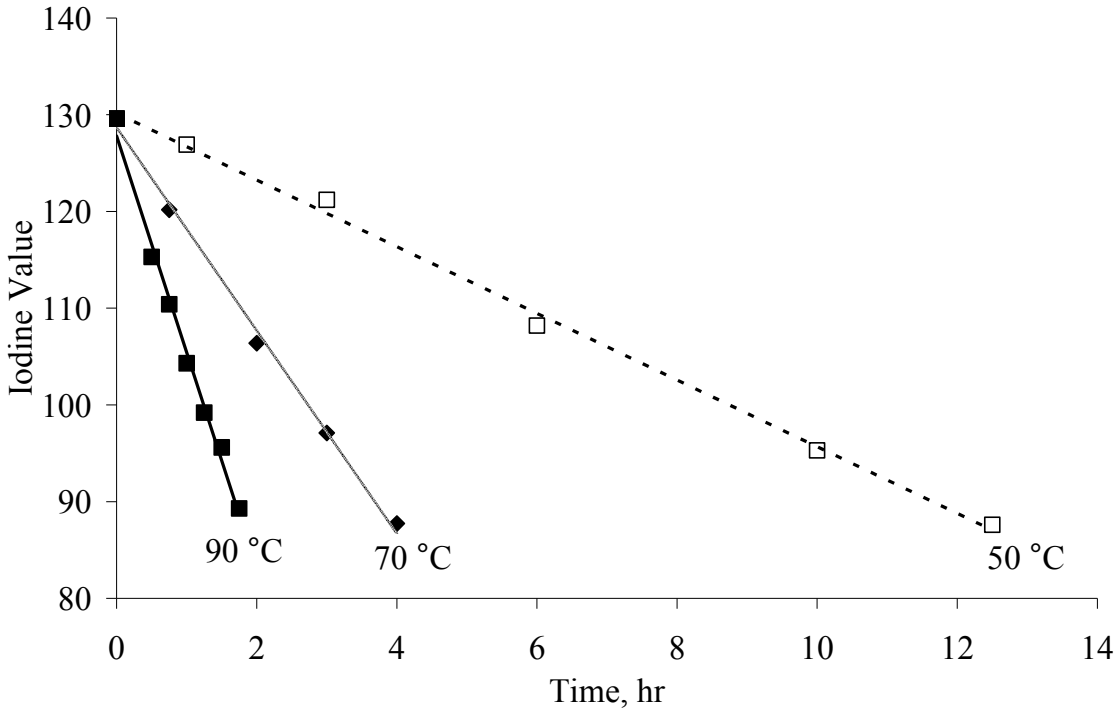

Figure 6-3: Effect of temperature on the hydrogenation of soybean oil using a palladium polymer composite reactor.

Figure 6-4 shows a minor increase in TFA formation with temperature for the case of Pd decorated polymeric membrane reactor and a large increase in TFA with temperature in conventional Pd/C slurry reactor. In palladium decorated polymeric membrane reactor, at an IV of 90, 11 wt% TFA were formed at 50 °C, which increased slightly to 13 wt% at 70 °C and remained at that level at 90 °C. However, for the case of slurry reactor around 11 wt% TFA were formed at 50 °C, increasing to 21 wt% at 70 °C, and to 31 wt% at 90 °C. A similar trend is seen while using platinum decorated polymeric membrane reactor (Figure 6-5). The amount of TFA formed at an IV of 90 increases only slightly from 2.2 wt% at 60 °C, to 3.0 wt% at 70 °C, and 3.6 wt% at 90 °C. However Pt/C slurry reactor produced about 8.4 wt% TFA at 70 °C and an IV of 94. The minor influence of temperature on TFA, for the case of palladium and platinum decorated polymeric membrane reactors can be attributed to similar hydrogen concentrations at

the catalyst surface even at different temperatures. Table 6-2 lists the specific isomerization index for all the cases. The specific isomerization index for the membrane reactors remained nearly constant in the temperature range of 50-90 °C.

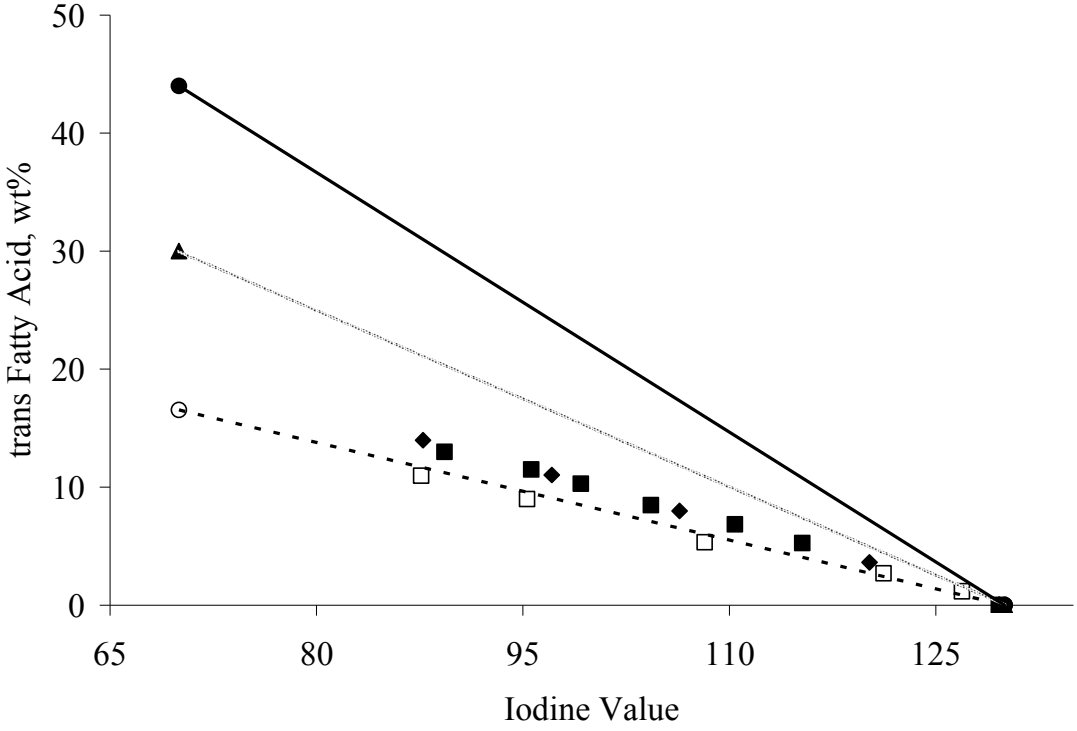

Figure 6-4: Trans fatty acid content as a function of Iodine Value during hydrogenation of soybean oil at different temperature using palladium polymer composite membrane and Pd/alumina slurry reactor[24]. Palladium polymer composite membrane at 50 °C (□), 70 °C (♦), and 90 °C (■) , Pd/alumina slurry reactor[24] at 50 °C (○), 70 °C (▲), and 90 °C (●).

6.3.2.3 Hydrogenation selectivity

The hydrogenation selectivity describes the preference of hydrogenation of polyenes over monoenes. If hydrogenation selectivity is very high no saturated acid is formed until almost all polyene has been hydrogenated [25]. Hydrogenation selectivity operates very much according to conditions obtained at the catalyst surface[26]. If the degree of adsorbed hydrogen on the catalyst surface is low, polyenes are preferentially adsorbed and mutibonded on the catalyst surface. They are bonded much more strongly thereby monopolizing the surface and excluding monoenes[27]. Thus polyenes are preferentially hydrogenated. However, when the degree of

adsorbed hydrogen on the catalyst surface is high, a significant portion of polyenes may never reach the polybonded state and thus will have an initial state similar to monoenes. So there will be an equal chance of reaction for both polyenes and monoenes[27], thus decreasing hydrogenation selectivity. For conventional slurry systems, increase in temperature leads to a decrease in surface coverage of adsorbed hydrogen and ultimately increases the hydrogenation selectivity. The hydrogenation selectivity results for metal decorated polymeric membranes are shown in Table 6-2. The trend is opposite to what is observed in slurry systems. The linoleic selectivity decreased almost 60 percent, from 4.2 to 1.6, with an increase in temperature from 50 °C to 90 °C. The decrease in linoleic selectivity with increase in temperature can be attributed to higher hydrogen coverage of the catalyst surface at higher temperature due to the high flux membranes used.

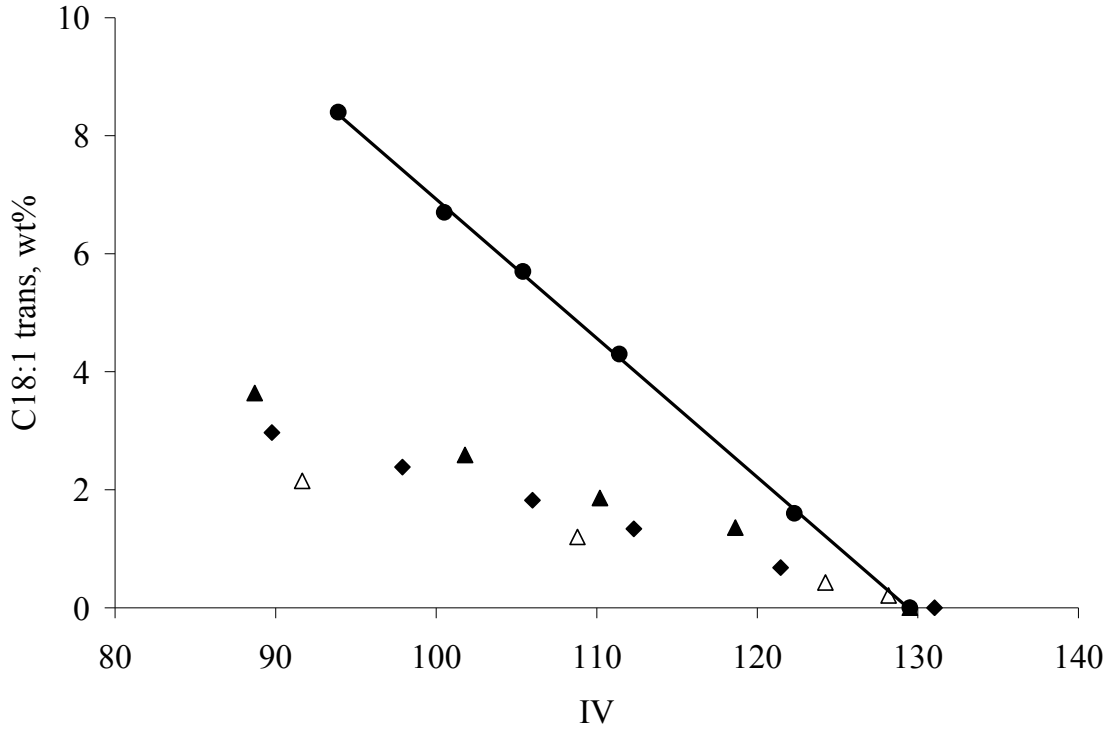

Figure 6-5: Trans fatty acid content as a function of Iodine Value during hydrogenation of soybean oil at different temperature using platinum polymer composite membrane and Pt/C slurry reactor13. Platinum polymer composite membrane at 60 °C (Δ), 70 °C (♦), and 90 °C (▲) , Pt/C slurry reactor at 70 °C (●).

Table 6-2: Effect of temperature and pressure on hydrogenation selectivities for palladium and platinum composite membranes.

Temperature, °C	Pressure, psig	Linolenic Selectivity, S_{Ln}	Linoleic Selectivity, S_{Lo}	Specific Isomerization Index, S_i
		Catalyst: Palladium		
50	50	1.7	4.2	0.28
70	50	1.7	3.0	0.33
90	50	1.2	1.6	0.32
70	200	1.2	3.2	0.28
		Catalyst: Platinum		
60	50	1.6	1.0	0.05
70	50	1.4	1.1	0.06
90	50	1.3	0.9	0.09
70	200	1.4	1.1	0.04

This is also illustrated by Figure 6-6 which shows the change in composition with IV for palladium membrane reactor at 50 and 90 °C. At an IV of 90, hydrogenation at 90 °C resulted in 25 percent more saturates and 20 percent less monoenes, as compared to hydrogenation at 50 °C.

The apparent activation energy for the individual rate constants as described in Equation 5-3 was calculated from the plot of rate constants as obtained by solving Equation 5-7 to Equation 5-9 with the inverse of temperature and are reported in Table 6-3. For the case of palladium, the activation energy for linolenate, linoleate, oleate rate constants were 7.8, 10.0, and 15.6 kcal mol^{-1}, respectively. The lower linolenate activation energy as compared to linoleate and lower linoleate activation energy as compared to oleate also explains the decrease in hydrogenation selectivity with increase in temperature. For the case of platinum, the activation energy for linolenate, linoleate, oleate rate constants were 10.5, 12.3, and 13.5 kcal mol^{-1}, respectively.

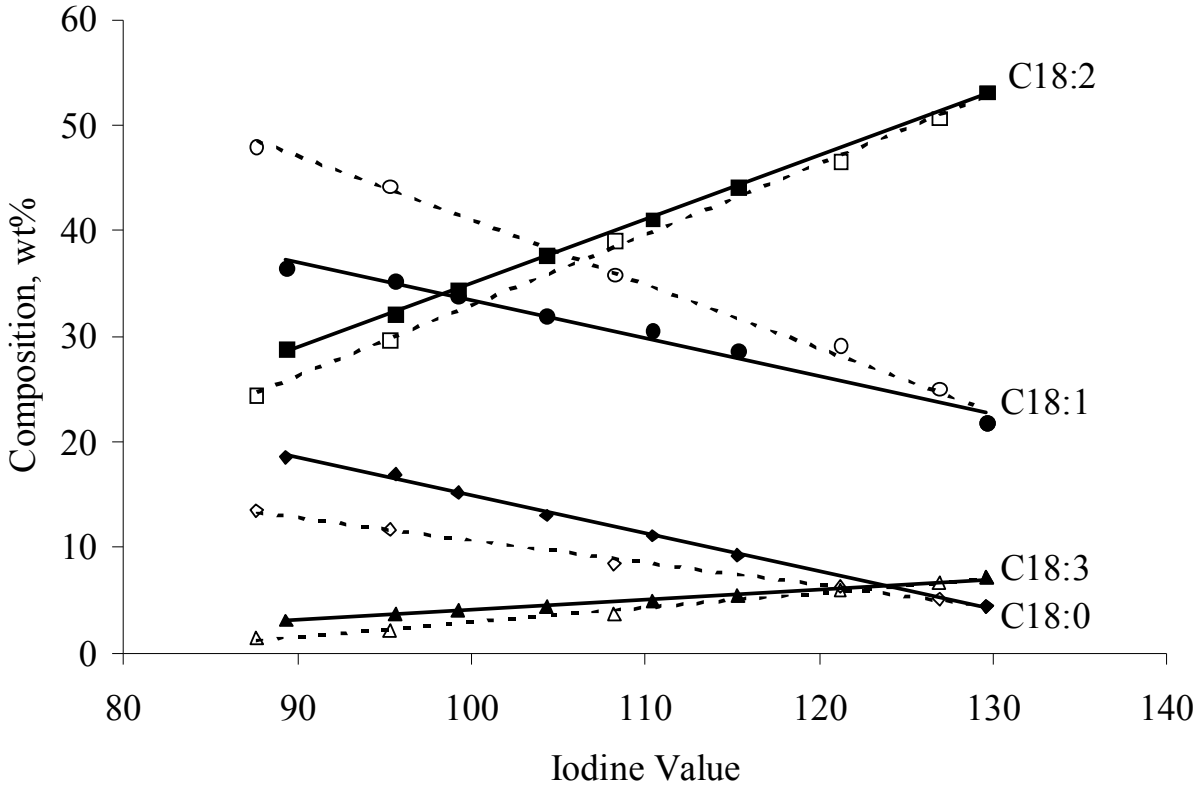

Figure 6-6: Composition profiles for hydrogenation of soybean oil using palladium composite membranes at 50 °C(---------) and 90 °C (_____).

6.3.3 Effect of pressure

In traditional slurry reactors the rate of hydrogenation depends upon the concentration of hydrogen in the bulk oil[7] which control the catalyst's surface coverage of hydrogen. Increase in hydrogen pressure increases the solubility of hydrogen in oil thus increasing the hydrogenation rate and decreasing TFA formation. For hydrogenation of soybean oil using Pd-Al_2O_3 catalyst, Hsu et al. observed a reaction order of 0.6, with respect to hydrogen[23]. Other authors have observed reaction orders in the range of 0.2-1.6, for palladium slurry reactors. The pressure dependencies substantially lower than unity [28] have been attributed to the presence of intraparticle hydrogen diffusion limitations[2]. Boyes et al.[29] reported a reaction order higher than unity with Pd/C catalyst which was attributed to simultaneous reaction involving more than one hydrogen molecule.

Table 6-3: Activation energy

E_{a1}, kcal mol^{-1}	E_{a2}, kcal mol^{-1}	E_{a3}, kcal mol^{-1}
Catalyst: Palladium		
7.8 (R^2=0.896)	10.0 (R^2=0.985)	15.6 (R^2=1.000)
Catalyst: Platinum		
10.5 (R^2=0.985)	12.3 (R^2=0.972)	13.5 (R^2=0.997)

For the case of metal polymer composite membranes, an increase in hydrogen pressure increases the hydrogen flux of the membrane linearly according to the following equation:

$$J_{Hydrogen} = P_{Hydrogen} \frac{\Delta p}{l} \qquad \text{Equation 6-9}$$

where $J_{Hydrogen}$ is the hydrogen flux through the membrane, $P_{Hydrogen}$ is the permeability coefficient, Δp is the pressure difference across the membrane, l is the thickness of the membrane. So for a given membrane during a hydrogenation run, the hydrogen flux depends not only on the pressure but also on the rate of hydrogen consumption during a reaction. If hydrogen builds up in the oil side then the driving force for hydrogen permeation will diminish which represents a type of self-limiting mechanism for hydrogen transport. The solubility of hydrogen in oil does not play a significant role for soybean oil hydrogenation when using metal decorated polymeric membranes.

To study the effect of pressure on hydrogenation using palladium polymer composite membrane, hydrogenation run was started at 50 psig and 70 °C, the pressure was increased to 100 psig when the IV was 115, and then increased to 200 psig when the IV was around 100. The hydrogenation was continued until an IV of 90. The palladium membrane used for hydrogenation run had a hydrogen flux of 7 GPU and H_2/N_2 selectivity of 100. A similar procedure was followed using platinum polymer composite membrane. The platinum decorated polymeric membrane used for hydrogenation run had a hydrogen flux of 7 GPU and a lower H_2/N_2 selectivity of 14. It should also be noted here that the membranes used for these runs had relatively low hydrogen fluxes.

6.3.3.1 Hydrogenation rate

For palladium polymer composite membrane, an increase in hydrogen pressure from 50 psig to 200 psig resulted in a minor increase in hydrogenation rate (Figure 6-7). The hydrogenation rate

increased from 9.3 IV hr^{-1} at 50 psig to 10.6 IV hr^{-1} at 200 psig. The order of reaction with respect to hydrogen pressure was 0.2 (Figure 6-8). The modest dependence of rate on hydrogen pressure may be attributed to the insensitivity of hydrogen to system pressure. Clearly, any increase in pressure will thus not have as large an effect as observed in traditional slurry reactors.

The platinum decorated polymeric membrane run, however, showed a slightly greater dependence of rate on hydrogen pressure. An increase in hydrogen pressure from 50 psig to 200 psig resulted in an increase in hydrogenation rate from 5.2 IV hr^{-1} to 7.8 IV hr^{-1}. The order of reaction with respect to hydrogen pressure was 0.5. The higher dependence of rate on hydrogen pressure for platinum decorated polymeric membrane is attributed to the use of membrane having the same hydrogen flux as in the case of palladium polymer composite membrane but a much lower H_2/N_2 selectivity. The lower H_2/N_2 selectivity indicates that the membrane had more defects which may result in significant portion of hydrogen being supplied through defects and concentrated at a few locations on the membrane surface. This may result in lower overall surface coverage of catalyst by hydrogen.

6.3.3.2 Isomerization and hydrogenation selectivity

For palladium polymer membranes, the isomerization index decreased slightly from 0.35 to 0.28 with the increase in pressure from 50 to 100 psig. There was no change in isomerization index with the increase in pressure from 100 to 200 psig. Due to already high concentration of hydrogen at 50 psig, obtained by using membranes, a further increase in hydrogen pressure had little influence on isomerization selectivity. For the case of platinum polymer membranes, the isomerization index remained in the range of 0.04-0.07 with increase in pressure from 50 to 200 psig (Table 6-2). The Linoleic acid selectivities showed no change (at 70 °C) for both palladium and platinum membrane reactors with increase in pressure from 50 psig to 200 psig.

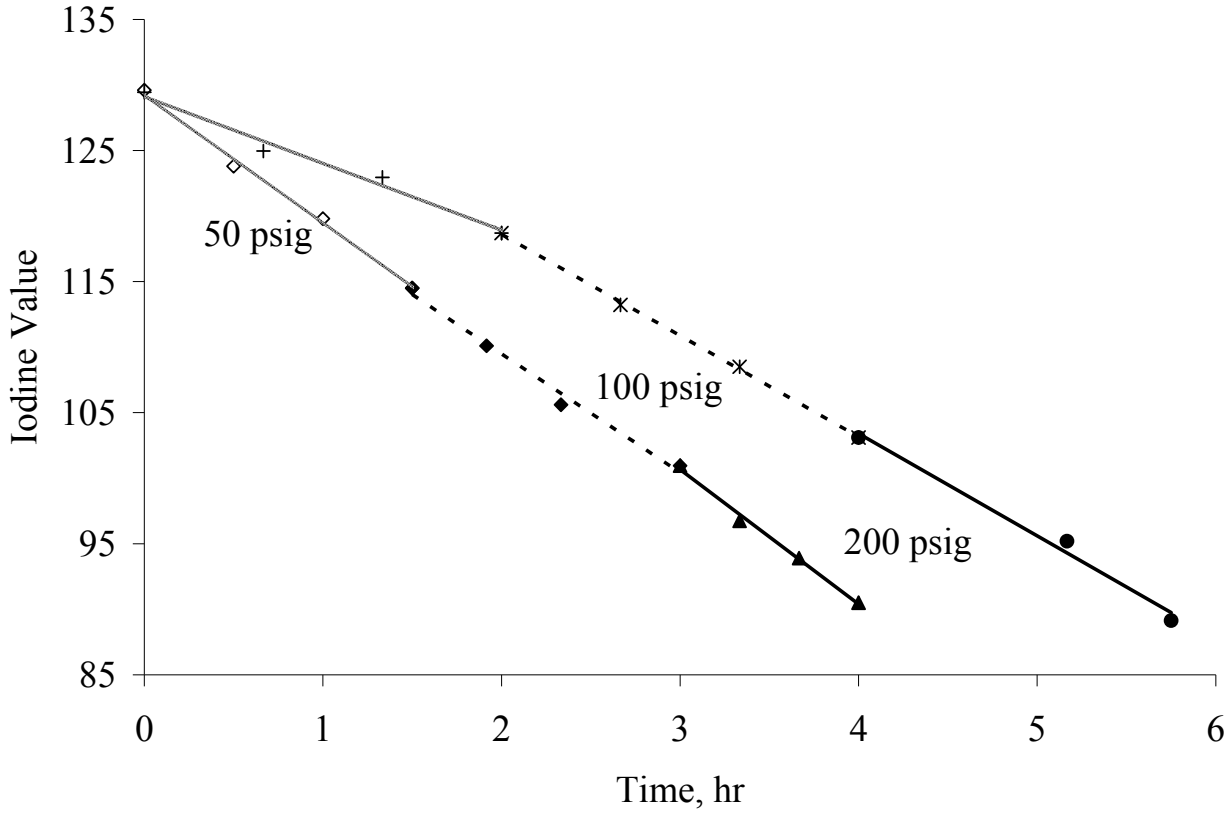

Figure 6-7: Effect of pressure on hydrogenation rate for palladium and platinum composite membranes at 70 °C. Pd membrane reactor at 50 psig (◊), Pd membrane reactor at 100 psig (♦), Pd membrane reactor at 200 psig (▲), Pt membrane reactor at 50 psig (+), Pt membrane reactor at 100 psig (x), Pt membrane reactor at 200 psig (●).

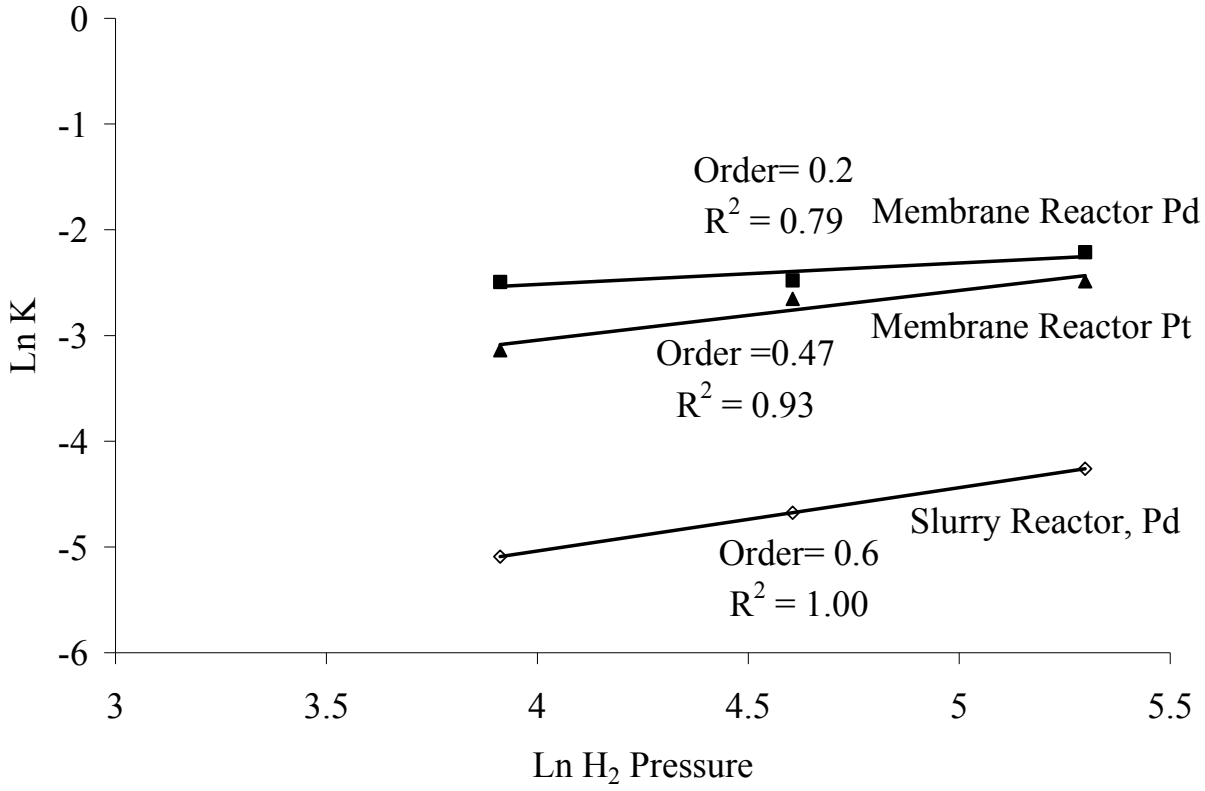

Figure 6-8: Effect of pressure on the hydrogenation rate of palladium composite membrane, platinum composite membrane, and Pd/alumina slurry reactor[23] at 70 °C.

6.4 Conclusion

Metal polymer composite membranes were used to allow the soybean oil and hydrogen to come in direct contact with each other at the catalyst surface, without the dispersion of one phase into other as is practiced in traditional slurry reactors. In the range studied, metal polymer composite membrane showed little influence of temperature and pressure on TFA formation. This may be attributed to the ability of the composite membranes to maintain a high concentration of hydrogen at the surface of the catalyst. Moreover scale-up of slurry reactor will lead to a further decrease in mass transfer efficiency; a membrane reactor can be scaled-up without any decrease in mass transfer efficiency.

6.5 Reference

1. Guettel, R.; Kunz, U.; Turek, T., Reactors for Fischer-Tropsch synthesis. Chemical Engineering & Technology 2008, 31, (5), 746-754.

2. Veldsink, J. W. B., M.J.; Schoon, N.H.; Beenackers, Antonie A. C. M., Heterogeneous hydrogenation of vegetable oils: a literature review. Catalysis Reviews - Science and Engineering 1997, 39, (3), 253-318.

3. Census., U. S. B. o. t., Current industrial reports. M311K, Fats and oils production, consumption, and stocks. In Bureau, U. S. C., Ed. 2007.

4. Grau, R. J.; Cassano, A. E.; Baltanas, M. A., Catalysts and Network Modeling in Vegetable Oil Hydrogenation Processes. Catalysis Reviews-Science and Engineering 1988, 30, (1), 1-48.

5. Farr, W. E., Hydrogenation: processing technologies. In Bailey's Industrial Oil and Fat Products, Shahidi, F., Ed. John Wiley & Sons: 2005; Vol. 5.

6. Horiuti, I.; Polanyi, M., Exchange reactions of hydrogen on metallic catalysts. Trans. Faraday Soc. 1934, 30, 1164 - 1172.

7. Dijkstra, A. J., Revisiting the formation of trans isomers during partial hydrogenation of triacylglycerol oils. European Journal of Lipid Science and Technology 2006, 108, (3), 249-264.

8. Pintauro, P. N.; Gil, M. P.; Warner, K.; List, G.; Neff, W., Electrochemical hydrogenation of soybean oil with hydrogen gas. Industrial & Engineering Chemistry Research 2005, 44, (16), 6188-6195.

9. Veldsink, J. W., Selective hydrogenation of sunflower seed oil in a three-phase catalytic membrane reactor. Journal of the American Oil Chemists Society 2001, 78, (5), 443-446.

10. Boger, T.; Zieverink, M. M. P.; Kreutzer, M. T.; Kapteijn, F.; Moulijn, J. A.; Addiego, W. P., Monolithic catalysts as an alternative to slurry systems: Hydrogenation of edible oil. Industrial & Engineering Chemistry Research 2004, 43, (10), 2337-2344.

11. Piqueras, C. A.; Tonetto, G.; Bottini, S.; Damiani, D. E., Sunflower oil hydrogenation on Pt catalysts: Comparison between conventional process and homogeneous phase operation using supercritical propane. Catalysis Today 2008, 133, 836-841.

12. King, J. W.; Holliday, R. L.; List, G. R.; Snyder, J. M., Hydrogenation of vegetable oils using mixtures of supercritical carbon dioxide and hydrogen. Journal of the American Oil Chemists Society 2001, 78, (2), 107-113.

13. Singh, D.; Pfromm, P. H.; Rezac, M. E., Partial Hydrogenation of Soybean Oil with Minimal Trans Fat Production Using a Pt-Decorated Polymeric Membrane Reactor. Journal of American Oil Chemists' Society 2009, 86, (1), 93-101.

14. Pintauro, P. N. Synthesis of a low-trans content edible oil, non-edible oil, or fatty acid in a solid polymer electrolyte reactor. 6218556 B1, 2001.

15. Peinemann, K. V. Method for producing an integral, asymmetric membrane and the resultant membrane. 4,673,418, 1987.

16. Obrien, K. C.; Koros, W. J.; Barbari, T. A.; Sanders, E. S., A New Technique for the Measurement of Multicomponent Gas-Transport through Polymeric Films. Journal of Membrane Science 1986, 29, (3), 229-238.

17. Barbari, T. A.; Koros, W. J.; Paul, D. R., Polymeric Membranes Based on Bisphenol-a for Gas Separations. Journal of Membrane Science 1989, 42, (1-2), 69-86.

18. Rezac, M. E.; Schoberl, B., Transport and thermal properties of poly(ether imide) acetylene-terminated monomer blends. Journal of Membrane Science 1999, 156, (2), 211-222.

19. Coates, D. M.; Kaplan, S. L., Modification of polymeric surfaces with plasmas. Mrs Bulletin 1996, 21, (8), 43-45.

20. Delcorte, A.; Bertrand, P.; Garrison, B. J., Collision cascade and sputtering process in a polymer. Journal of Physical Chemistry B 2001, 105, (39), 9474-9486.

21. Petursson, S., Clarification and expansion of formulas in AOCS recommended practice Cd 1c-85 for the calculation of iodine value from FA composition. Journal of the American Oil Chemists Society 2002, 79, (7), 737-738.

22. Albright, L. F., Quantitative Measure of Selectivity of Hydrogenation of Triglycerides. Journal of the American Oil Chemists Society 1965, 42, (3), 250-253.

23. Hsu, N.; Diosady, L. L.; Rubin, L. J., Catalytic Behavior of Palladium in the Hydrogenation of Edible Oils. Journal of the American Oil Chemists Society 1988, 65, (3), 349-356.

24. Hsu, N.; Diosady, L. L.; Rubin, L. J., Catalytic Behavior of Palladium in the Hydrogenation of Edible Oils .2. Geometrical and Positional Isomerization Characteristics. Journal of the American Oil Chemists Society 1989, 66, (2), 232-236.

25. Coenen, J. W. E., Hydrogenation of Edible Oils. Journal of the American Oil Chemists Society 1976, 53, (6), 382-389.

26. Patterson, H. B. W., Hydrogenation of fats and oils. 1983 ed.; Applied science publishers ltd.: 1983.

27. Hsu, N. Catalytic hydrogenation of canola and soybean oils using transition metal complexes and supported/unsupported palladium. University of Toronto, Toronto, 1987.

28. Bern, L.; Hell, M.; Schoon, N. H., Kinetics of Hydrogenation of Rapeseed Oil .2. Rate Equations of Chemical-Reactions. Journal of the American Oil Chemists Society 1975, 52, (10), 391-394.

29. Boyes, A. P.; Chugtai, A.; Khan, Z.; Raymahasay, S.; Sulidis, A. T.; Winterbottom, J. M., The Cocurrent Downflow Contactor (Cdc) as a Fixed-Bed and Slurry Reactor for Catalytic-Hydrogenation. Journal of Chemical Technology and Biotechnology 1995, 64, (1), 55-65.

CHAPTER 7 - Stability of metal decorated polymeric membranes for partial hydrogenation of soybean oil

7.1 Introduction

Partial hydrogenation of vegetable oil using metal polymer composite membranes offer several advantages: they produce significantly lower trans fatty acids (TFAs) as compared to traditional slurry reactors[1]; the process is compatible with existing hydrogenation facilities as far as temperature and pressure are concerned; is simpler than some of the alternatives being studied[2, 3]; and no catalyst recovery from the oil is needed since the catalyst is immobilized on the membrane. However, the economics of the process will in part be influenced by the stability of metal polymer composite membranes. This chapter focuses on determining the stability of the composite membranes as a function of time in use.

7.2 Experimental procedure

7.2.1 Hydrogenation runs

The platinum sputtered membrane (sputtered using a DESK II magnetron sputter for 9 seconds at 45 mA, 100 mtorr) was installed in a stainless steel 47 mm filter holder (model XX4404700, Millipore Corp., Billerica. MA). Table 7-1 gives the properties of the membrane used for hydrogenation experiments in this work. The hydrogenation run using soybean oil was carried at 90 °C and 50 psig hydrogen pressure using the same apparatus and procedures as outlined in section 3.2. For each hydrogenation run, after taking the last sample, hydrogen was turned off. The oil side was purged using nitrogen to remove all the hydrogenated oil while the temperature was still close to 90 °C. The reactor was allowed to cool overnight to room temperature under an atmosphere of nitrogen. After cooling the system was washed with hexane twice (at around 40 °C) by circulating it through the system for about 5 minutes. After washing with hexane the system was purged with nitrogen for about 2 minutes. For the first repeat run, the platinum catalyst was reduced with hydrogen at 60 °C for 15 hrs. However subsequent repeat runs were performed without any reduction. About 13.8 g of virgin soybean oil was added to the

reactor. The same hydrogenation procedure was followed hereafter. A total of four runs were performed with the same membrane using the procedure as explained above.

Table 7-1: Properties of catalytic membrane used in soybean oil hydrogenation experiment

	Before Pt sputtering	After Pt sputtering
H_2 flux, GPU	71	46
H_2/N_2 selectivity	18	64
Catalyst loading, μg cm^{-2}	-	3.4

Samples were taken periodically and analyzed following standard procedures for composition determination, iodine value, and hydrogenation selectivity calculations as discussed in section 3.2.4.

7.2.2 ICP-MS analysis

ICP-MS analysis was performed to determine if platinum deposited on the membrane leaches into the oil. For this purpose a fresh platinum sputtered membrane (sputtered for 9 seconds at 45 mA, 100 mtorr) was installed in the filter holder. The filter holder was installed in the experimental setup. The platinum on the membrane skin was reduced as explained in section 3.2 of the thesis. About 13.8 g of oil was added to the reactor and circulated over the membrane while temperature was maintained at 90 °C. The oil side pressure was maintained at 60 psig using UHP nitrogen and the gas side pressure was maintained at 50 psig using UHP nitrogen. After 2 hours the oil was taken out and analyzed using ICP-MS. The system was cooled overnight under an atmosphere of nitrogen. The system was then washed with hexane. Another batch of oil was again added and circulated under the same conditions as explained above. After 9 hours the oil was taken out and analyzed using ICP-MS.

In another experiment the platinum sputtered membrane was put in a shaker flask with 6.5 g of soybean oil and stirred at 300 rpm for 1300 hours with temperature varying from room temperature to 50 °C. After the experiment the oil was tested for platinum using ICP-MS.

7.3 Results and discussion

The results for repeat hydrogenation runs performed at 90 °C and 50 psig hydrogen pressure using platinum sputtered membrane are shown in Figure 7-1. The hydrogenation rate for the first run was 17.4 IV hr^{-1} which decreased to around 14.5 IV hr^{-1} for the second run using the

same membrane and to 10.7 IV hr^{-1} during the fourth run. The average decrease in hydrogenation activity was around 10 percent after each run. The reduction of the catalyst performed between the first and the second run appear to have no influence on the activity.

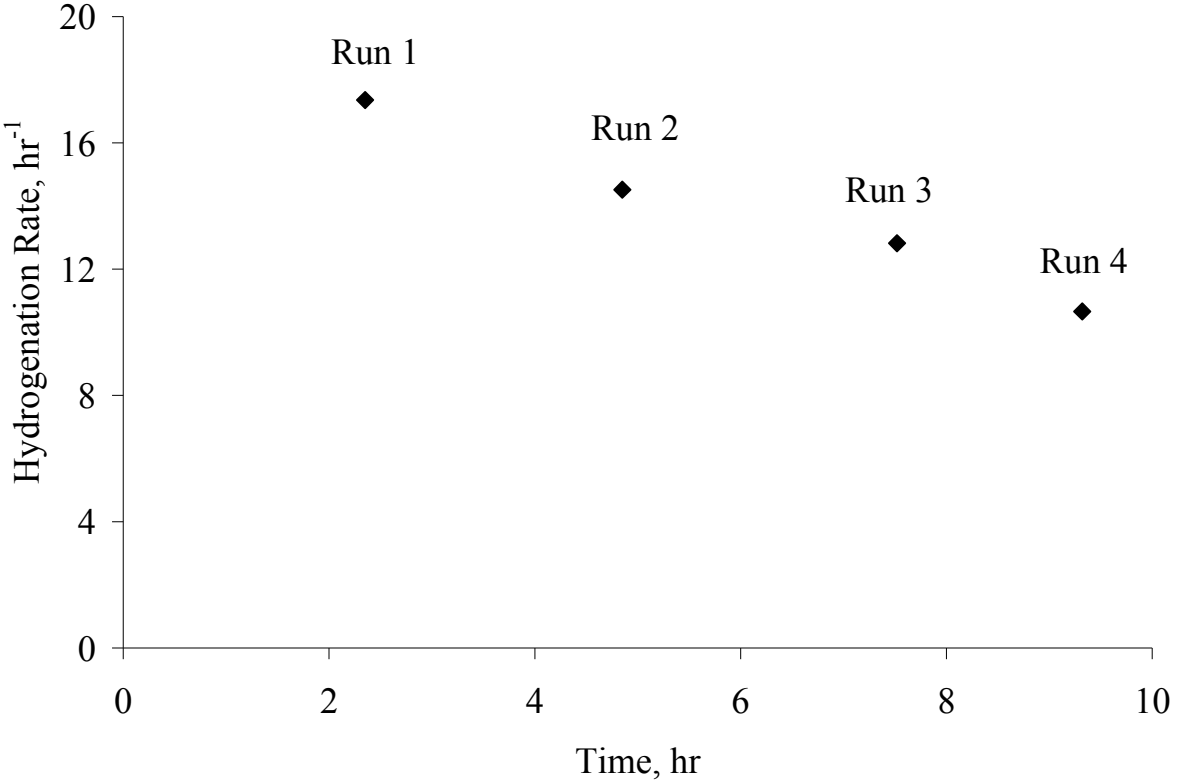

Figure 7-1: Repeat hydrogenation runs performed using same platinum sputtered membrane at 90 °C and 50 psig.

The ICP-MS analysis performed to determine the loss of catalyst from the membrane indicated negligible leaching of the catalyst for the duration of the runs. Only 0.4% of the platinum was lost when soybean oil was circulated across the platinum sputtered side of the membrane for 2 hrs. Washing of the system with hexane and circulating soybean oil for 9 additional hours resulted in negligible loss of the catalyst. Rigorous shaking of the membrane for 1300 hours led to a 7% loss of the catalyst from the membrane. Due to negligible loss of platinum for the duration of the run, it can be eliminated as the possible cause of decreased reaction rates.

The decrease in hydrogenation activity with subsequent runs may be attributed to the deactivation of the catalyst due to poisons present in the oil[4-7] or deactivation by coke deposition

which results in blocking of the active sites[8, 9]. The poisons present in the oil that have a deleterious effect on edible oil hydrogenation catalyst include sulfur compounds, phosphorous compounds, free fatty acids, soaps, and oxidation products of the oil. Of all the poisons present in oil sulfur has the most deleterious effect on hydrogenation rate followed by phosphorous[7]. The poisoning of nickel catalysts by sulfur is also accompanied by an increase in the amount of trans isomers[6] as triglycerides adsorb on the sulfur-poisoned site and may be released in the trans isomer form. Figure 7-1 shows the change in composition of soybean oil as hydrogenation proceeds for both fresh platinum polymer membrane (Run 1) and deactivated platinum polymer membrane (Run 4). No change in the hydrogenation selectivity was observed between these runs. The linolenic selectivity was in the range of 1.3-1.6 with linoleic selectivity at 0.9 and specific isomerization index 0.08-0.09 (Table 7-2).

Table 7-2: Hydrogenation selectivities and isomerization indices for repeat hydrogenation runs performed using the same membrane at 90 °C and 50 psig hydrogen pressure.

Hydrogenation run	Linolenic Selectivity, S_{Ln}	Linoleic Selectivity, S_{Lo}	Specific Isomerization Index, S_i
1	1.3	0.9	0.09
2	1.5	0.9	0.08
3	1.6	0.9	0.08
4	1.6	0.9	0.08

Deactivation by coke deposition has also been observed by various authors during partial hydrogenation of vegetable oil. Edvardsson et al.[8] studied the deactivation of palladium and platinum catalysts due to coke formation during hydrogenation of methyl esters of sunflower oil. Pd-γ-Al_2O_3 lost more than 50% of its initial activity after four batch experiments, while Pd-α-Al_2O_3 and Pt-γ-Al_2O_3 did not deactivate. Marki-Arvela et al.[9] also observed progressive deactivation of Pd/C catalyst (almost 75% loss of activity after 3 runs) during hydrogenation of linoleic acid. Such deactivation by coke deposition may also be the case for the platinum sputtered polymeric membranes. However a detailed study identifying the causes of deactivation of Pt on polymeric membranes and its possible mechanisms will provide more insight.

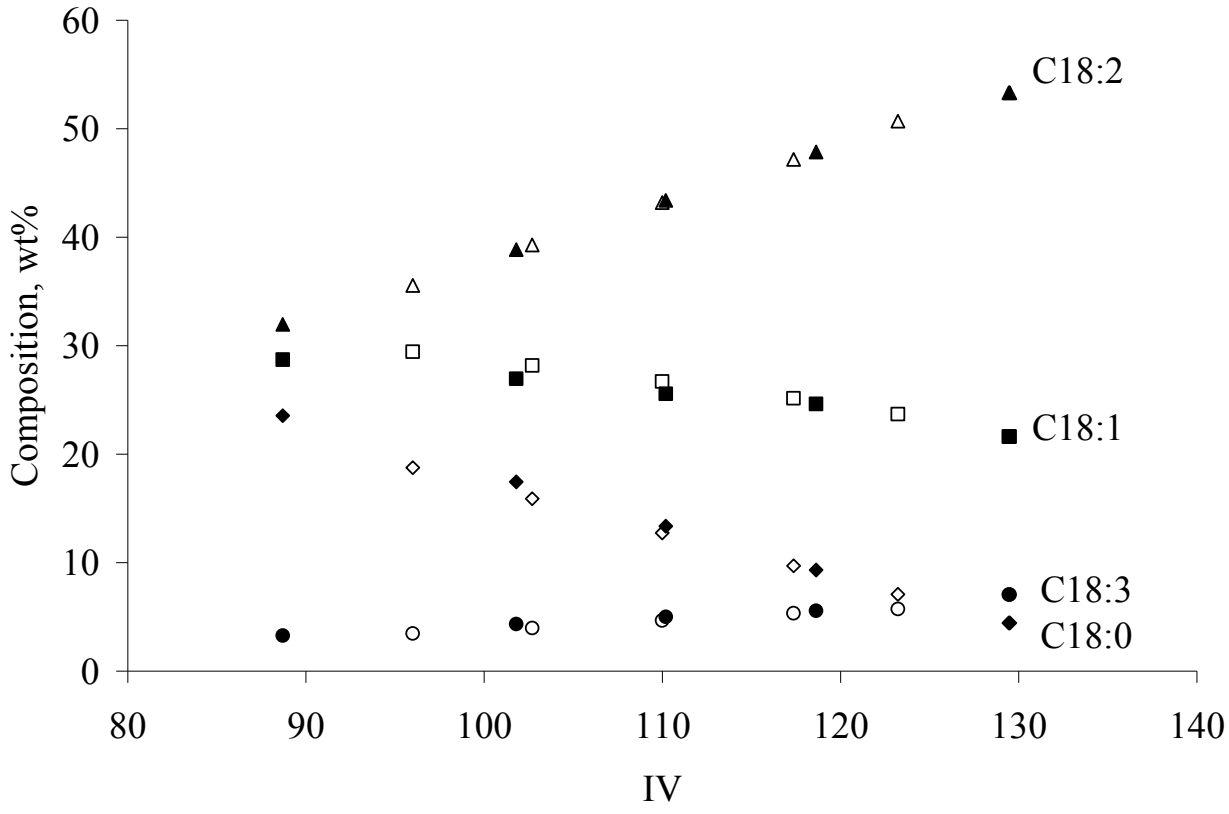

Figure 7-2: Comparison of product composition during hydrogenation using fresh (solid symbols) and deactivated platinum sputtered membrane (open symbols). Reaction conditions: Temperature= 90 °C, Pressure= 50 psig.

7.4 Conclusion

A decrease in hydrogenation activity was observed with time as with precious metal catalyst in slurry systems on conventional supports studied in the literature. The platinum metal polymer composite membrane lost around 40 percent of its initial activity after four experiments with no change in hydrogenation or isomerization selectivity. Coke deposition as the possible cause of deactivation should be investigated and possible regeneration procedures should be studied.

7.5 Reference

1. Singh, D.; Pfromm, P. H.; Rezac, M. E., Partial Hydrogenation of Soybean Oil with Minimal Trans Fat Production Using a Pt-Decorated Polymeric Membrane Reactor. Journal of American Oil Chemists' Society 2009, 86, (1), 93-101.

2. Pintauro, P. N.; Gil, M. P.; Warner, K.; List, G.; Neff, W., Electrochemical hydrogenation of soybean oil with hydrogen gas. Industrial & Engineering Chemistry Research 2005, 44, (16), 6188-6195.

3. Piqueras, C. A.; Tonetto, G.; Bottini, S.; Damiani, D. E., Sunflower oil hydrogenation on Pt catalysts: Comparison between conventional process and homogeneous phase operation using supercritical propane. Catalysis Today 2008, 133, 836-841.

4. Chu, Y. H.; Lin, L. H., Effects of Minor Compounds on Hydrogenation Rate of Soybean Oil. Journal of the American Oil Chemists Society 1992, 69, (9), 880-883.

5. Drozdowski, B.; Zajac, M., Effect of Concentration of Some Nickel-Catalyst Poisons in Oils on Course of Hydrogenation. Journal of the American Oil Chemists Society 1977, 54, (12), 595-599.

6. Abraham, V.; Deman, J. M., Effect of Some Isothiocyanates on the Hydrogenation of Canola Oil. Journal of the American Oil Chemists Society 1987, 64, (6), 855-858.

7. Klimmek, H., Influence of Various Catalyst Poisons and Other Impurities on Fatty-Acid Hydrogenation. Journal of the American Oil Chemists Society 1984, 61, (2), 200-204.

8. Edvardsson, J.; Rautanen, P.; Littorin, A.; Larsson, M., Deactivation and coke formation on palladium and platinum catalysts in vegetable oil hydrogenation. Journal of the American Oil Chemists Society 2001, 78, (3), 319-327.

9. Maki-Arvela, P.; Kuusisto, J.; Sevilla, E. M.; Simakova, I.; Mikkola, J. P.; Myllyoja, J.; Salmi, T.; Murzin, D. Y., Catalytic hydrogenation of linoleic acid to stearic acid over different Pd- and Ru-supported catalysts. Applied Catalysis a-General 2008, 345, (2), 201-212.

CHAPTER 8 - Conclusion and Recommendations

8.1 Conclusion

The dissertation focused on developing metal decorated polymeric membranes which were used for the partial hydrogenation of vegetable oil. Using metal decorated polymeric membranes, hydrogen was supplied directly at/near the catalyst surface thus reducing mass-transfer limitations and minimizing trans fatty acid formation.

Due to the low solubility of hydrogen in vegetable oil, its hydrogenation using traditional slurry reactors leads to significant mass-transfer limitations and thus produces high amounts of trans fatty acids (TFAs). The partial hydrogenation of soybean oil using the proposed metal decorated polymeric membranes produced significantly lower TFAs as compared to traditional slurry reactors. At an Iodine Value of 95 only 3.5 wt% TFA were formed using metal decorated polymeric membranes as compared to 8 wt% in slurry reactor. This may be due to reduced hydrogen starvation of the catalyst surface by rapid hydrogen permeation through a high performance asymmetric membrane.

Due to the defective nature of the metal layer on the membrane skin and the low temperatures at which hydrogenation was performed hydrogen permeability through metals had a minor influence on hydrogenation. This means that a range of metal catalysts could be used. Polymeric membranes decorated with platinum, palladium, and palladium-lead alloy were used for hydrogenation of soybean oil. All the metal decorated polymeric membranes tested showed activity for hydrogenation of soybean oil. The order of activity was Pd>Pt>>Pd-Pb alloy. Adding lead to palladium decreased the isomerization selectivity and also increased linolenic selectivity. Platinum showed minimum selectivity towards formation of TFA but also resulted in lower hydrogenation selectivities.

Metal polymer membranes having a range of hydrogen fluxes, skin defects, and catalyst loadings were characterized and evaluated. Sputtering of the metal on polymeric membranes changed the hydrogen flux and selectivity significantly due to the combined effects of modification of the membrane skin by ion bombardment, coverage of membrane surface with metal, and varying coverage of defects of the membrane skin with metal. As far as catalyst distribution on the membrane surface is concerned, an increase in platinum catalyst loading from

0.9 μg cm^{-2} to 3.4 μg cm^{-2} resulted in a change in catalyst distribution from isolated small metal islands at 0.9 μg cm^{-2} platinum catalyst loading to a large interconnected network of island at 3.4 μg cm^{-2} platinum catalyst loading. For hydrogenation experiments, all the membranes evaluated produced low level of TFAs (2.6-4.6 wt% at Iodine Value of 95). Membranes with high hydrogen fluxes resulted in higher hydrogenation rates but had little influence on TFA. However, the catalyst loading influenced TFA formation more strongly. For membranes with similar hydrogen flux (measured after metal sputtering), an increase in catalyst loading on membrane surface resulted in higher hydrogenation rate and saturate formation, and a decrease in TFA formation.

The behavior of metal decorated polymeric membranes to changes in temperature (50-90°C) and pressure (50-200 psig) was evaluated and compared with that of traditional slurry reactors. An increase in temperature increased the hydrogenation rate but showed little increase in the amount of TFA produced (11-13 wt% at IV of 90), however, traditional slurry reactor resulted in a significant increase of TFA with temperature (11-30 wt% at IV of 90).Metal decorated polymeric membranes showed a lower reaction order in hydrogen as compared to traditional slurry reactors. These differences may be attributed to the ability of metal decorated polymeric membranes to maintain a high concentration of hydrogen at the catalyst surface even at higher temperatures. Due to the already high hydrogen concentration at a given temperature, an increase in pressure showed little influence on hydrogenation rate and cis-trans isomerization.

The stability of metal decorated polymeric membranes was studied by using the same membrane for repeated hydrogenation runs. After four batches, about 40% loss in activity was observed without any change in hydrogenation or isomerization selectivities. Separate experiments indicate no leaching of metal from the membrane during the course of run. Initial data suggest that the sulfur poisoning or loss of catalyst from membrane surface may not be the cause of deactivation.

8.2 Recommendations

Metal decorated polymeric membranes were successfully applied for the three phase reaction of hydrogenation of soybean oil. They were able to minimize mass-transfer limitations and produced low TFA as compared to slurry reactor systems. Economics is an important part of any process, which will in part be influenced by the stability of metal decorated polymeric

membranes. Since decrease in activity was observed with repeated use, the deactivation mechanism should be identified. The catalyst is supported on an unconventional support (polyetherimide), so various methods like X-ray photoelectron spectroscopy (XPS) or temperature programmed oxidation (TPO) may be evaluated to determine which technique works best for the identification of the cause of deactivation. After identification of the cause of deactivation appropriate regeneration procedures may be studied. Additionally other metals and alloys may be evaluated for minimizing the affect of poisoning. All this information will be useful in extending the life of metal decorated polymeric membranes for partial hydrogenation of soybean oil.

A recent report suggests that the isomerization of trans olefins to their cis counterparts is promoted by (111) facet of platinum [1]. So an interesting area to explore will be if the sputtering conditions/process could be modified to obtain platinum surfaces that promote cis fatty acids.

The application of metal decorated polymeric membranes may also be extended to other multiphase reactions where the scarcity of desired reactants on the catalyst surface has a detrimental effect on product composition. Some examples of such reactions include aqueous-phase reforming of sorbitol for the production of heavier alkanes[2,3]; Fisher-Tropsch synthesis where pore diffusion and mass-transfer limitations lead to unfavorable product distribution[4].

8.3 References

I. Lee, F. Delbecq, R. Morales, M.A. Albiter, and F. Zaera, Tuning selectivity in catalysis by controlling particle shape. Nature Materials 8 (2009) 132-138.

2. Huber JW, Chheda JN, Barrett CJ, Dumesic JA. Production of liquid alkanes by aqueous-phase processing of biomass-derived carbohydrates. Science. 2005;308(5727):1446-1450.

3. Huber JW, Cortright RD, Dumesic JA. Renewable alkanes by aqueous-phase reforming of biomass-derived oxygenates. Angewandte Chemie-International Edition. 2004;43(12):1549-1551.

4. Guettel R, Kunz U, Turek T. Reactors for Fischer-Tropsch synthesis. Chemical Engineering & Technology. May 2008;31(5):746-754.

Appendix A - Growth of metals on PEI films

Appendix A lists TEM images. Some of them were not used in the text but may be useful for the reader.

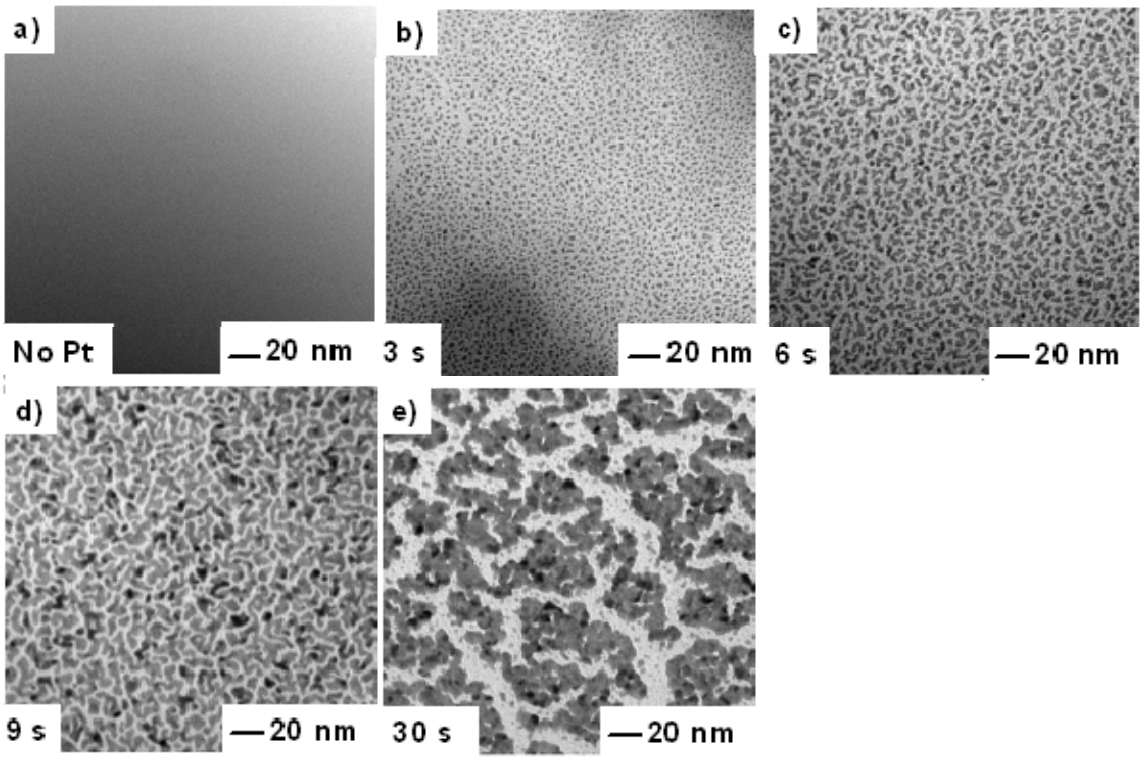

Figure A-1: TEMs of the surface of PEI films sputtered with platinum. Isolated platinum metal islands formed after 3s sputtering increase in size after 6s sputtering and grow to an interconnected network of islands after 9s sputtering. Sputtering for 30s leads to grain coarsening.

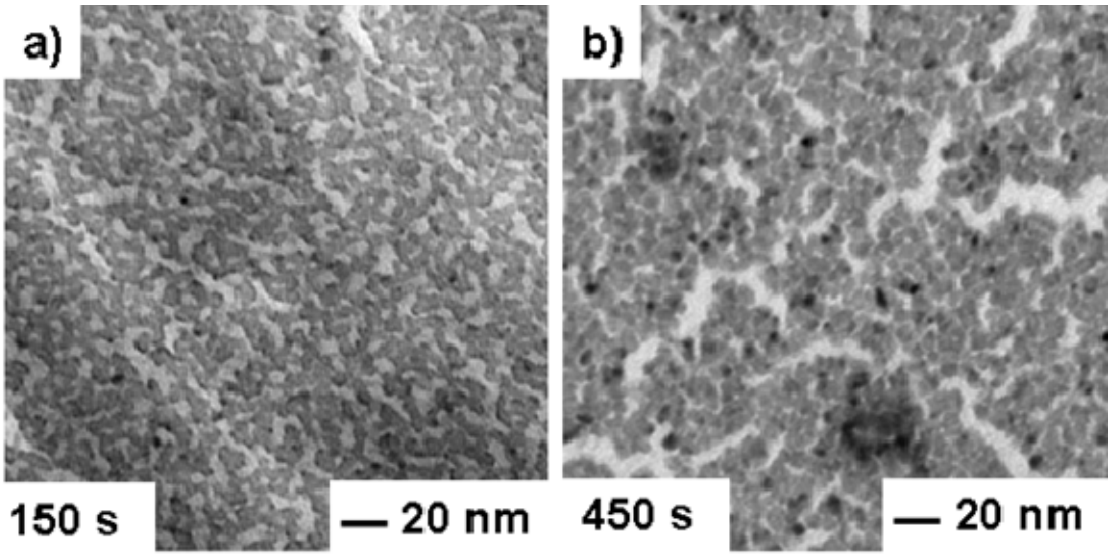

Figure A-2: TEMs of the surface of PEI films sputtered with nickel.

Appendix B - Hydrogenation runs with platinum decorated polymeric membranes

Appendix B lists the data from all the runs made with platinum decorated polymeric membranes. Some of them may not be used in the text but may still be useful for the reader.

Table B-1: Properties of membrane used for hydrogenation run.

H_2 flux [GPU]	Ideal gas selectivity $\alpha_{H2/N2}$	H_2 flux [GPU]	Ideal gas selectivity $\alpha_{H2/N2}$	Catalyst (Sputtering time , s)
Before sputtering		*After sputtering*		
60	39	4	4	Pt (9)

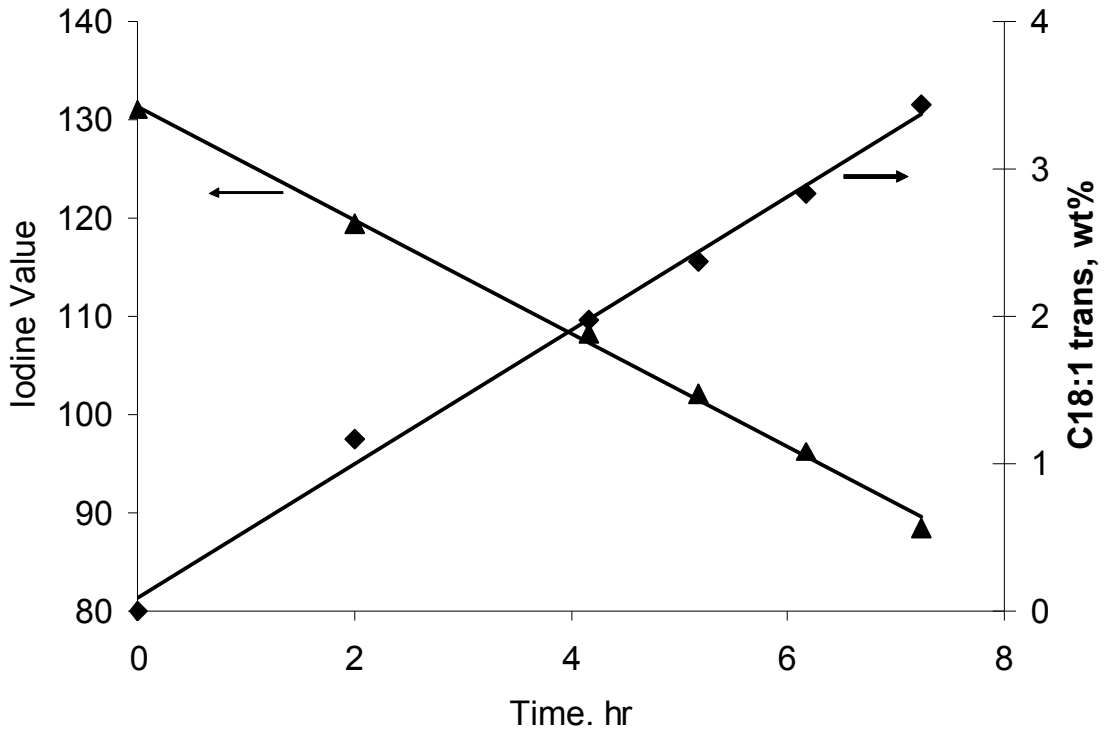

Figure B-1: TFA formation during hydrogenation of soybean oil using platinum decorated polymeric membrane. Reaction conditions: 70 °C, 50 psig hydrogen pressure.

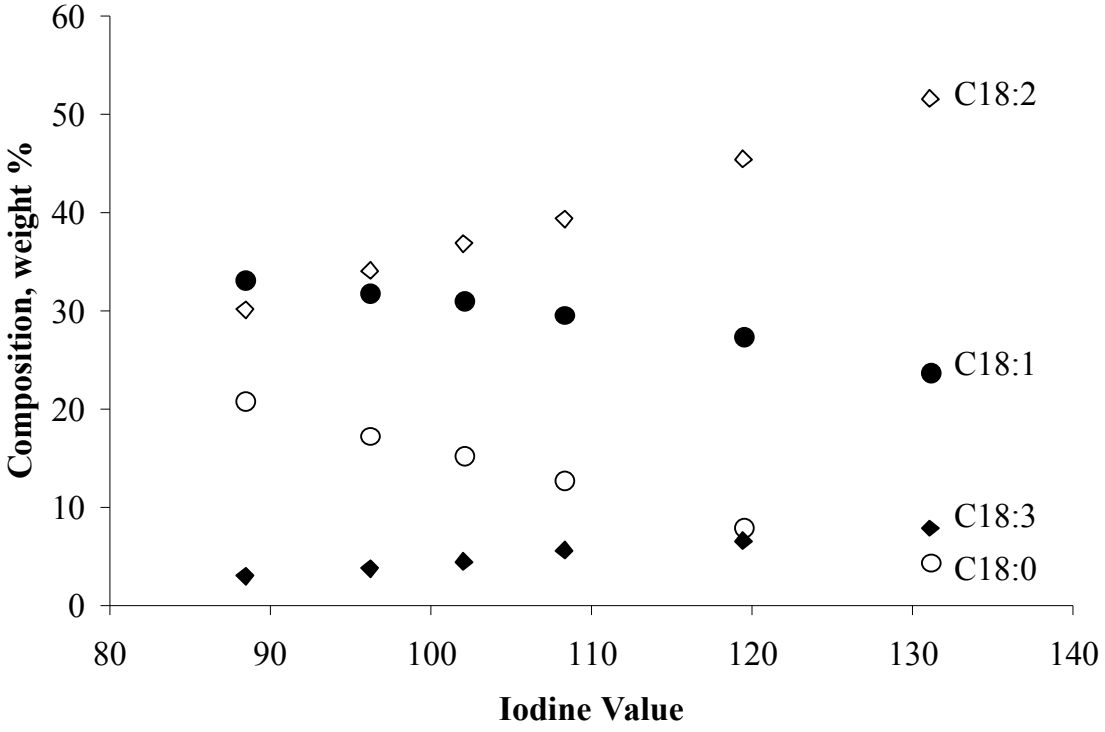

Figure B-2: Composition of soybean oil using platinum decorated polymeric membrane. Reaction conditions: 70 °C, 50 psig hydrogen pressure.

Table B-2: Properties of membrane used for hydrogenation run.

H_2 flux [GPU]	Ideal gas selectivity $\alpha_{H2/N2}$	H_2 flux [GPU]	Ideal gas selectivity $\alpha_{H2/N2}$	Catalyst (Sputtering time , s)
Before sputtering		*After sputtering*		Pt (9)
59	144	6	65	

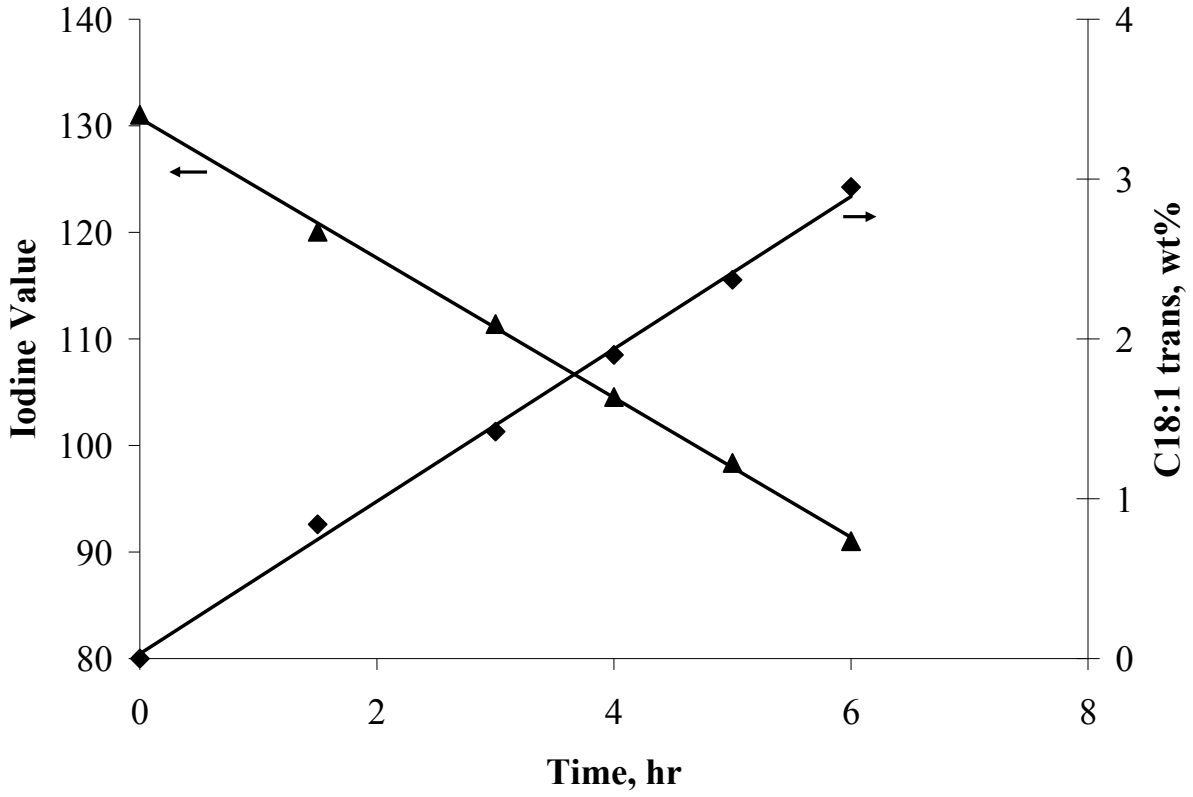

Figure B-3: TFA formation during hydrogenation of soybean oil using platinum decorated polymeric membrane. Reaction conditions: 70 °C, 50 psig hydrogen pressure.

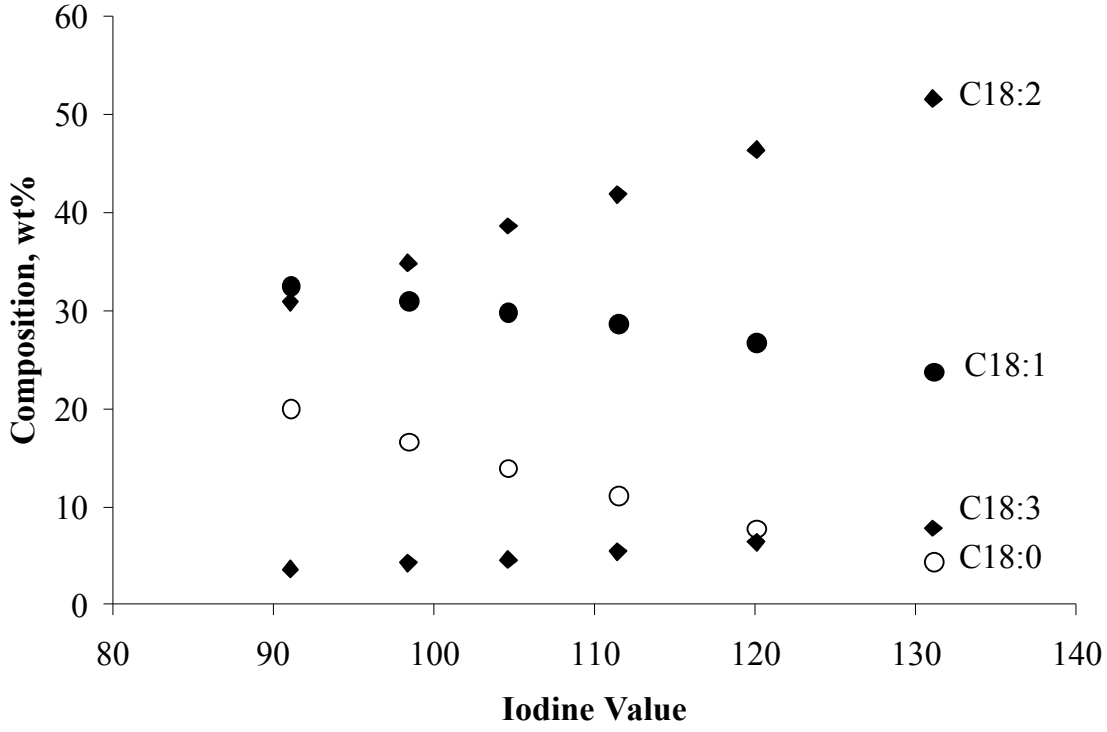

Figure B-4: Composition of soybean oil using platinum decorated polymeric membrane. Reaction conditions: 70 °C, 50 psig hydrogen pressure.

Table B-3: Properties of membrane used for hydrogenation run.

H_2 flux [GPU]	Ideal gas selectivity $\alpha_{H2/N2}$	H_2 flux [GPU]	Ideal gas selectivity $\alpha_{H2/N2}$	Catalyst (Sputtering time , s)
Before sputtering		*After sputtering*		Pt (9)
84	25	10	5	

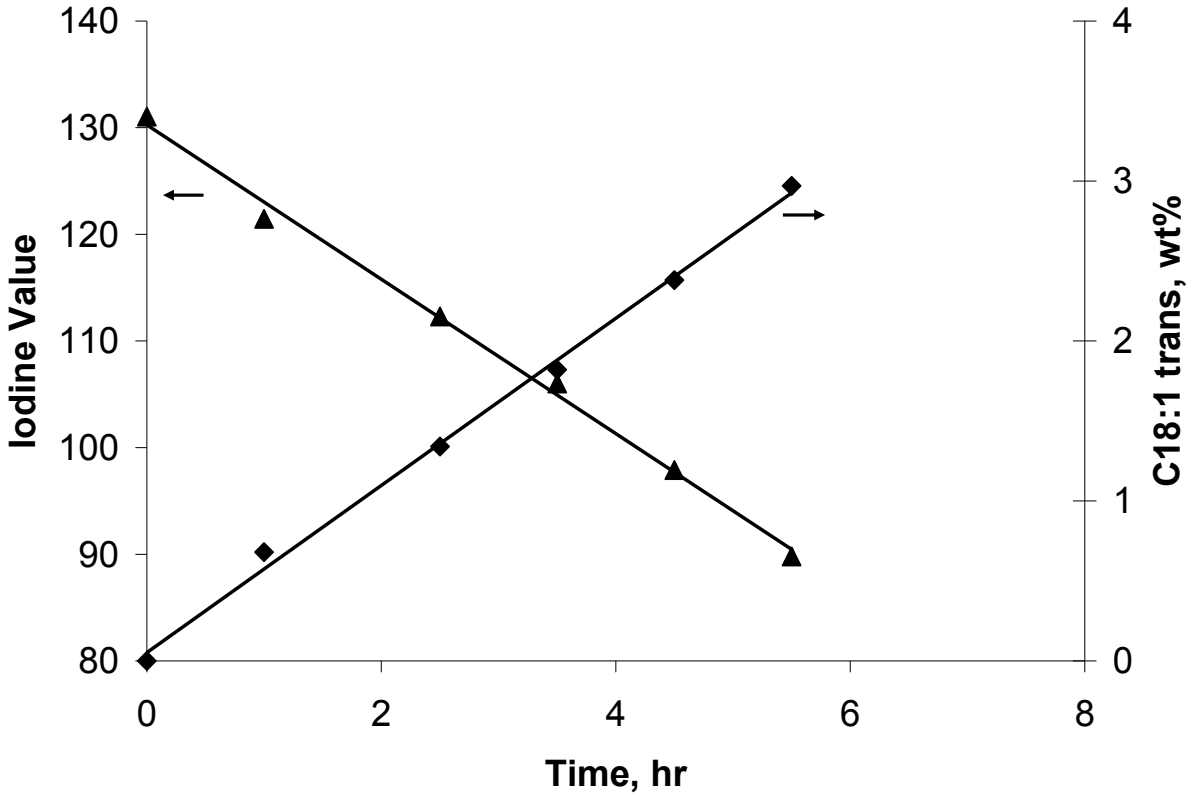

Figure B-5: TFA formation during hydrogenation of soybean oil using platinum decorated polymeric membrane. Reaction conditions: 70 °C, 50 psig hydrogen pressure.

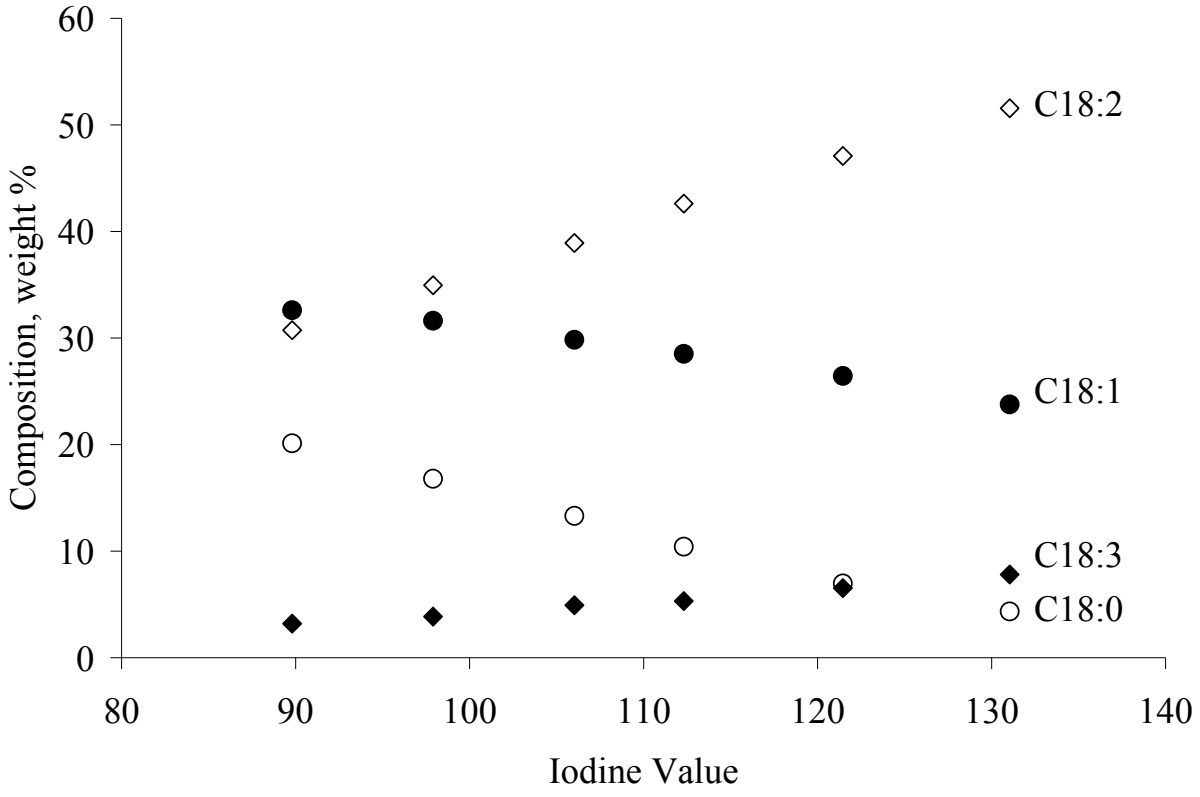

Figure B-6: Composition of soybean oil using platinum decorated polymeric membrane. Reaction conditions: 70 °C, 50 psig hydrogen pressure.

Table B-4: Properties of membrane used for hydrogenation run.

H_2 flux [GPU]	Ideal gas selectivity $\alpha_{H2/N2}$	H_2 flux [GPU]	Ideal gas selectivity $\alpha_{H2/N2}$	Catalyst (Sputtering time , s)
Before sputtering		*After sputtering*		Pt (9)
17	125	10	107	

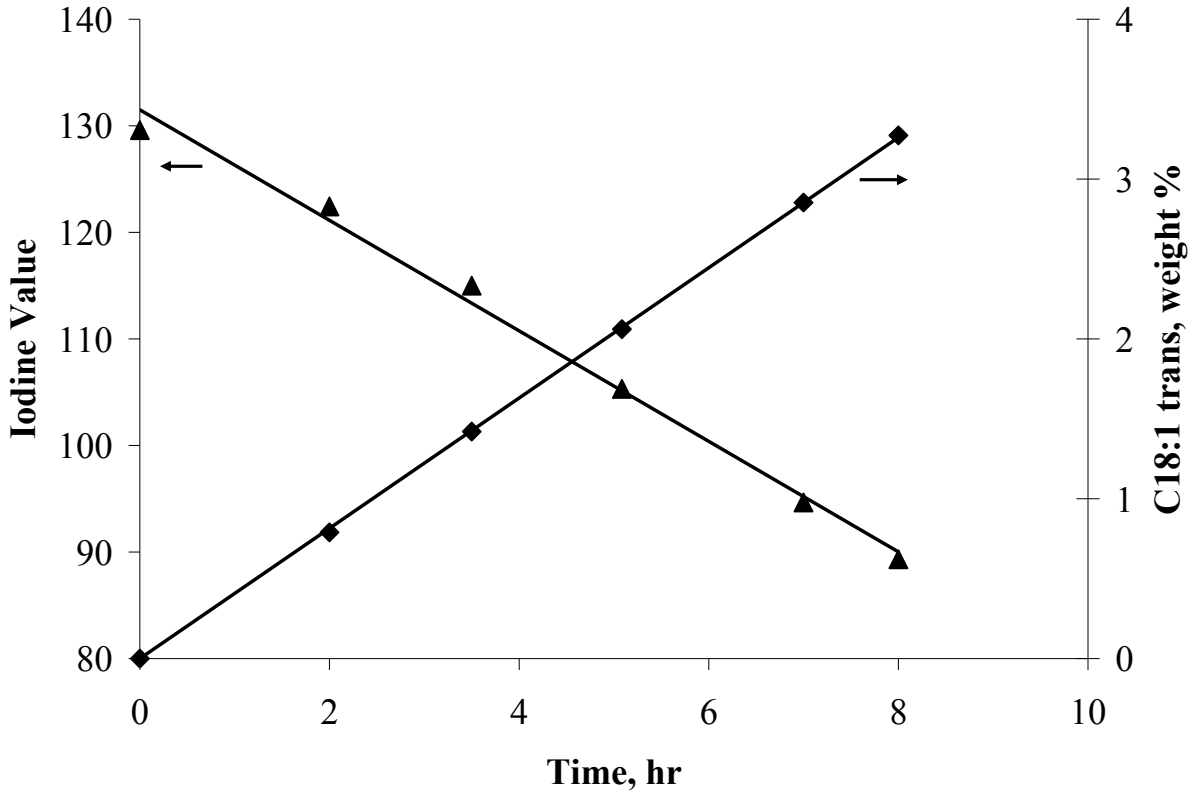

Figure B-7: TFA formation during hydrogenation of soybean oil using platinum decorated polymeric membrane. Reaction conditions: 70 °C, 50 psig hydrogen pressure.

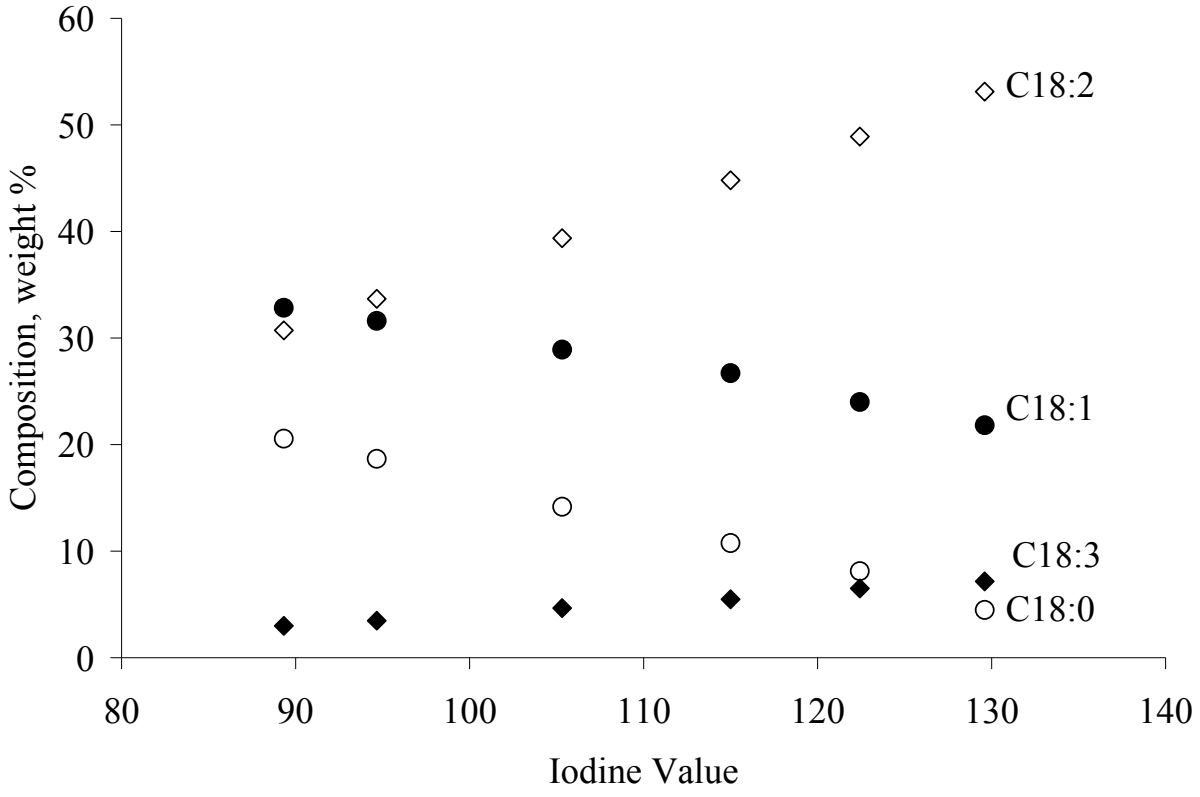

Figure B-8: Composition of soybean oil using platinum decorated polymeric membrane. Reaction conditions: 70 °C, 50 psig hydrogen pressure.

Table B-5: Properties of membrane used for hydrogenation run.

H_2 flux [GPU]	Ideal gas selectivity $\alpha_{H2/N2}$	H_2 flux [GPU]	Ideal gas selectivity $\alpha_{H2/N2}$	Catalyst (Sputtering time , s)
Before sputtering		*After sputtering*		Pt (9)
7	104	2	63	

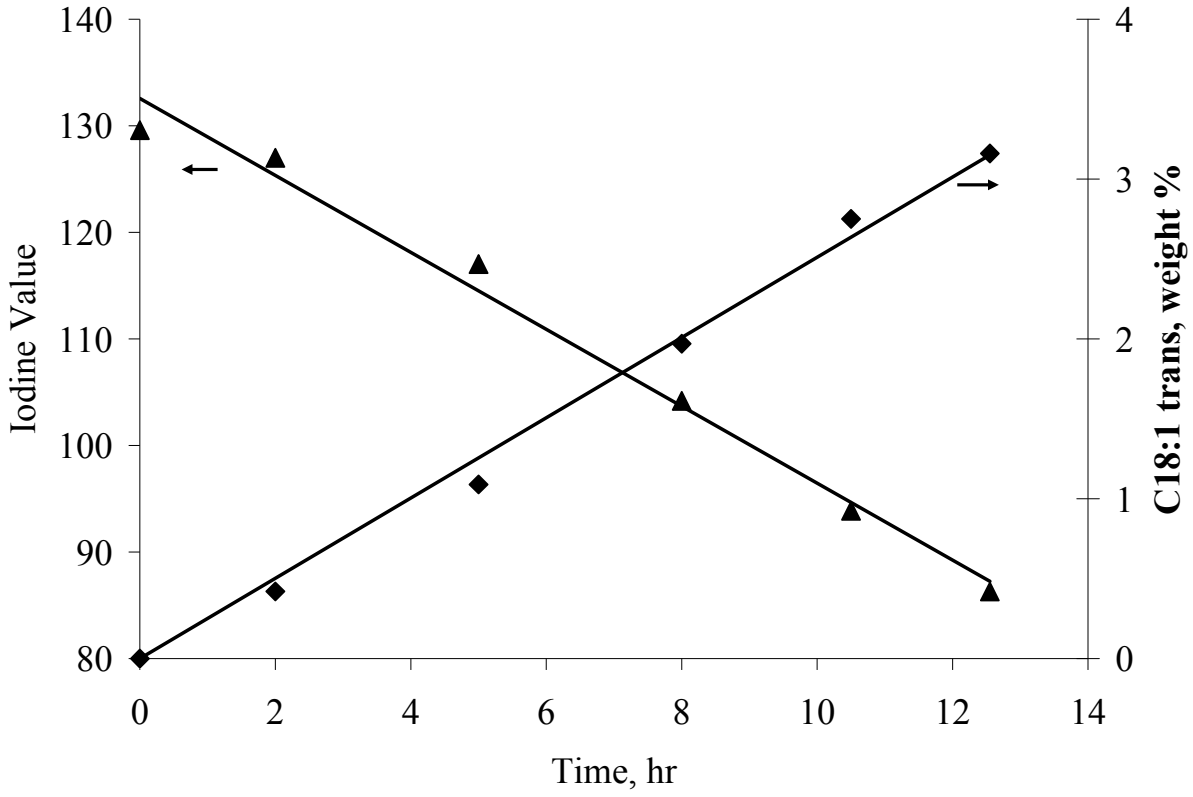

Figure B-9: TFA formation during hydrogenation of soybean oil using platinum decorated polymeric membrane. Reaction conditions: 70 °C, 50 psig hydrogen pressure.

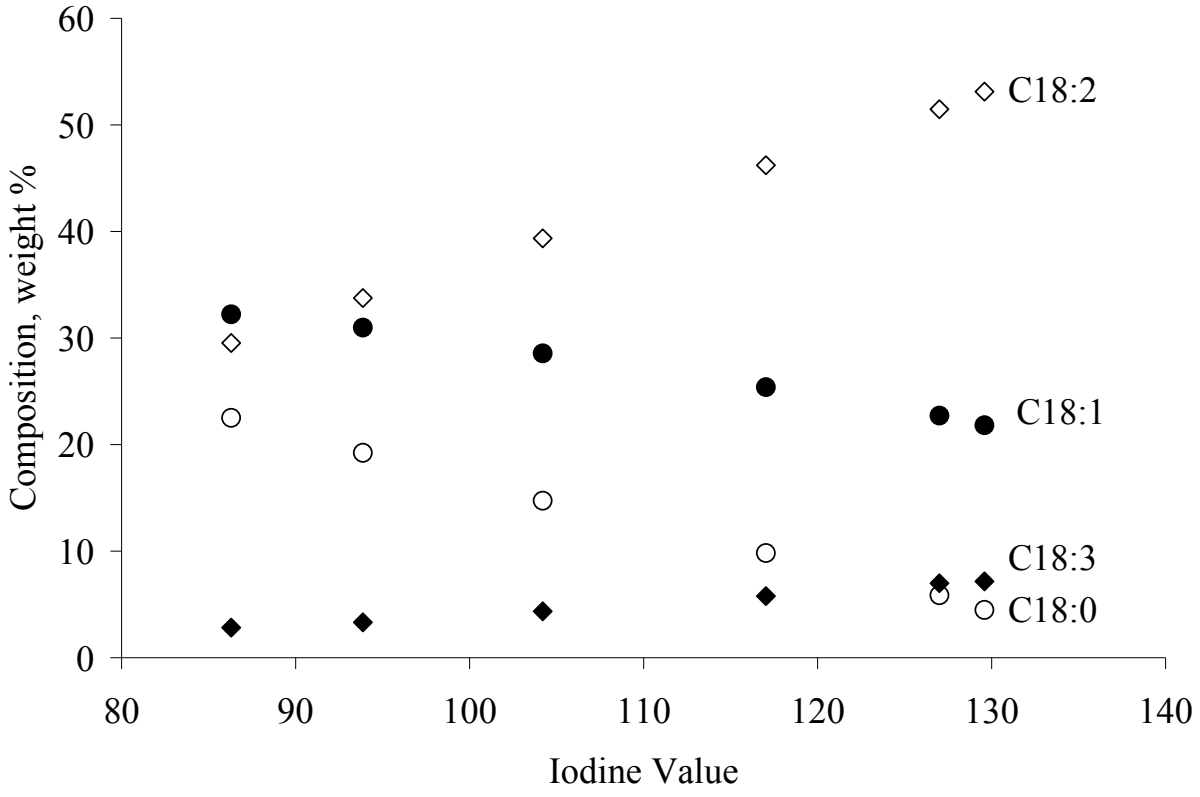

Figure B-10: Composition of soybean oil using platinum decorated polymeric membrane. Reaction conditions: 70 °C, 50 psig hydrogen pressure.

Table B-6: Properties of membrane used for hydrogenation run.

H_2 flux [GPU]	Ideal gas selectivity $\alpha_{H2/N2}$	H_2 flux [GPU]	Ideal gas selectivity $\alpha_{H2/N2}$	Catalyst (Sputtering time , s)
Before sputtering		*After sputtering*		Pt (9)
22	115	23	120	

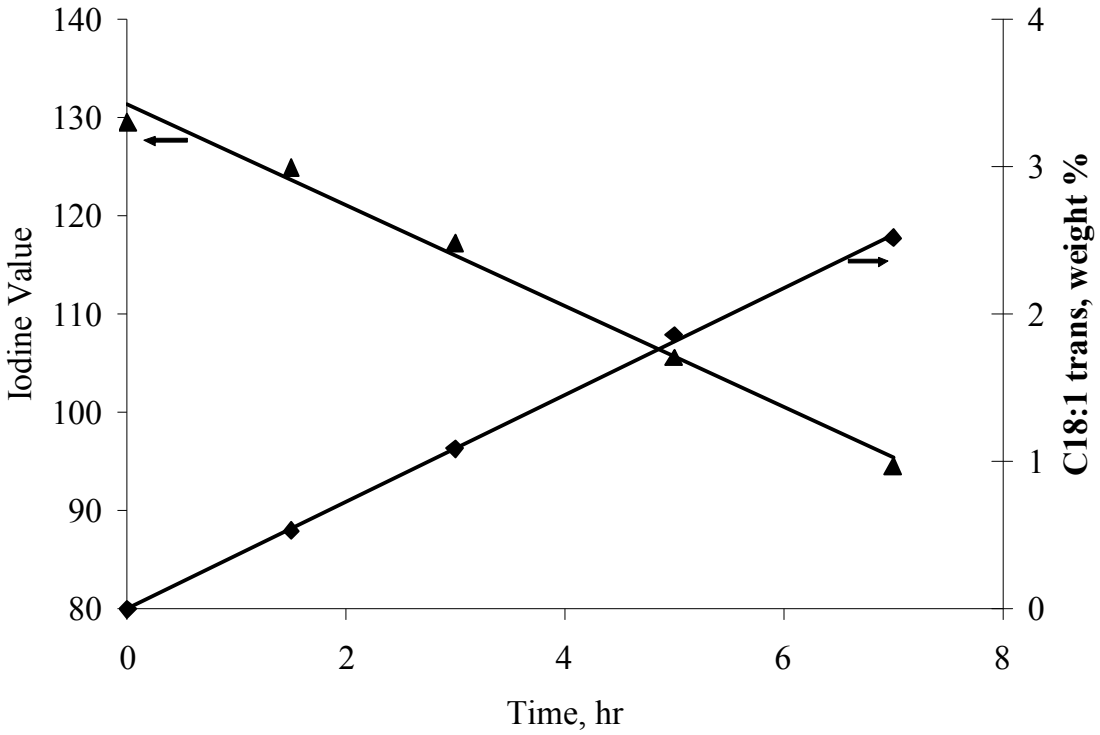

Figure B-11: TFA formation during hydrogenation of soybean oil using platinum decorated polymeric membrane. Reaction conditions: 70 °C, 50 psig hydrogen pressure.

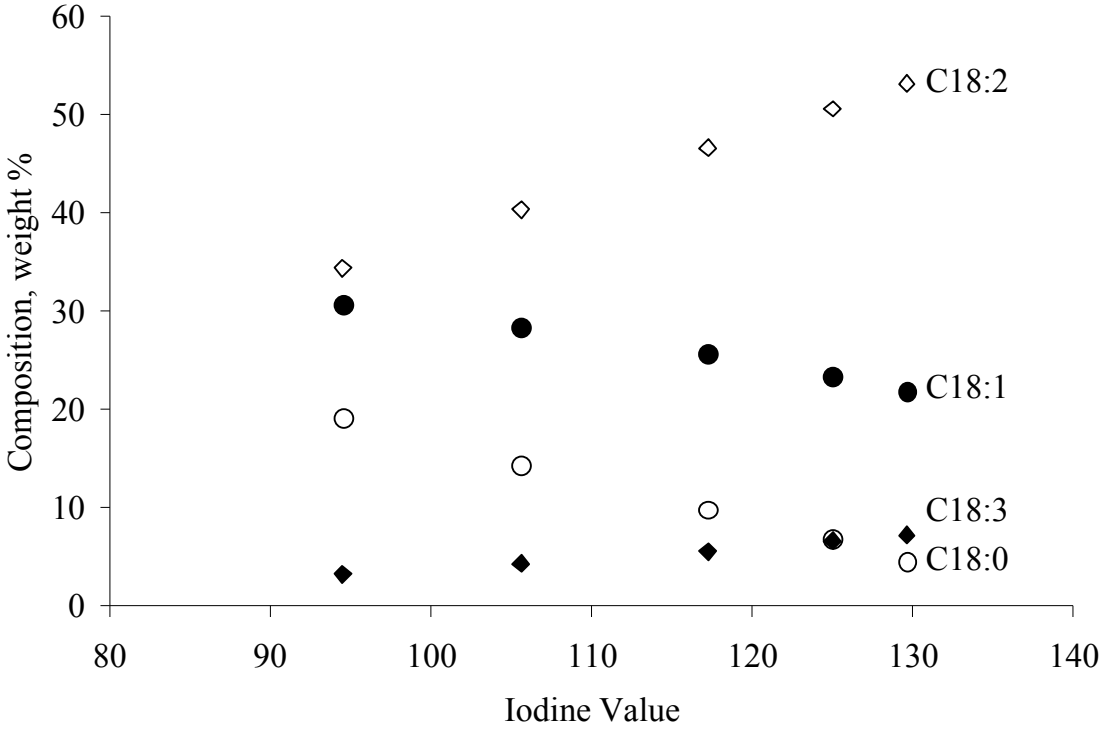

Figure B-12: Composition of soybean oil using platinum decorated polymeric membrane. Reaction conditions: 70 °C, 50 psig hydrogen pressure.

Table B-7: Properties of membrane used for hydrogenation run.

H_2 flux [GPU]	Ideal gas selectivity $\alpha_{H2/N2}$	H_2 flux [GPU]	Ideal gas selectivity $\alpha_{H2/N2}$	Catalyst (Sputtering time , s)
Before sputtering		*After sputtering*		Pt (6)
11	121	4	141	

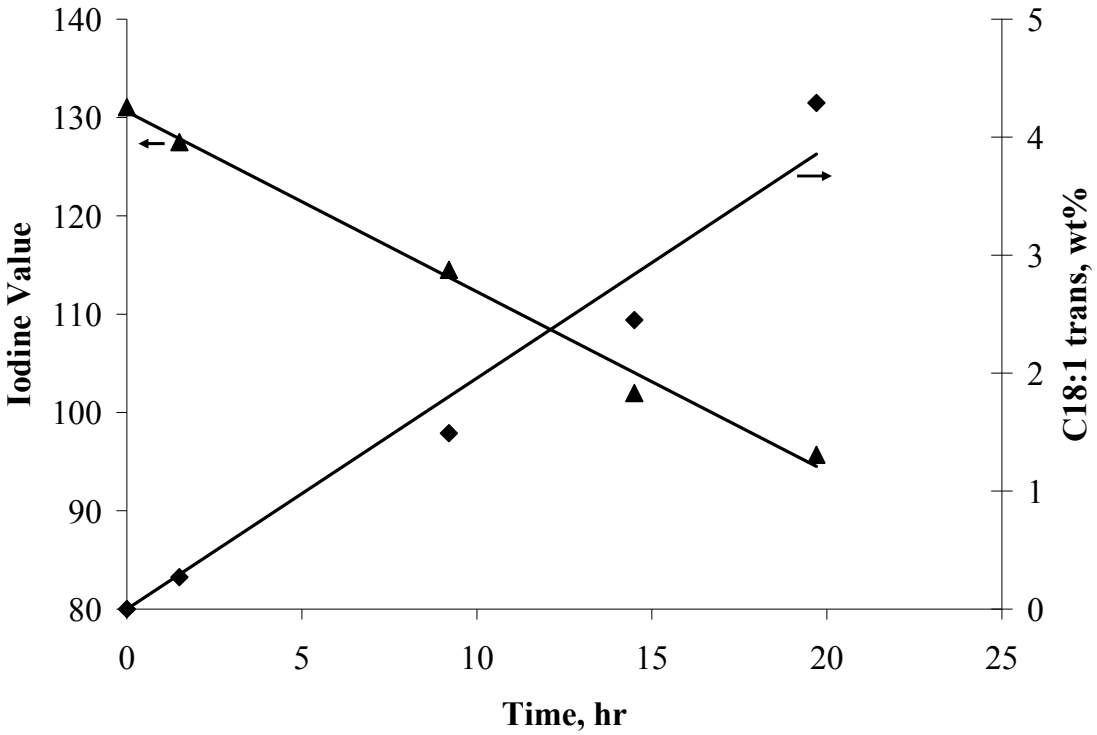

Figure B-13: TFA formation during hydrogenation of soybean oil using platinum decorated polymeric membrane. Reaction conditions: 70 °C, 50 psig hydrogen pressure.

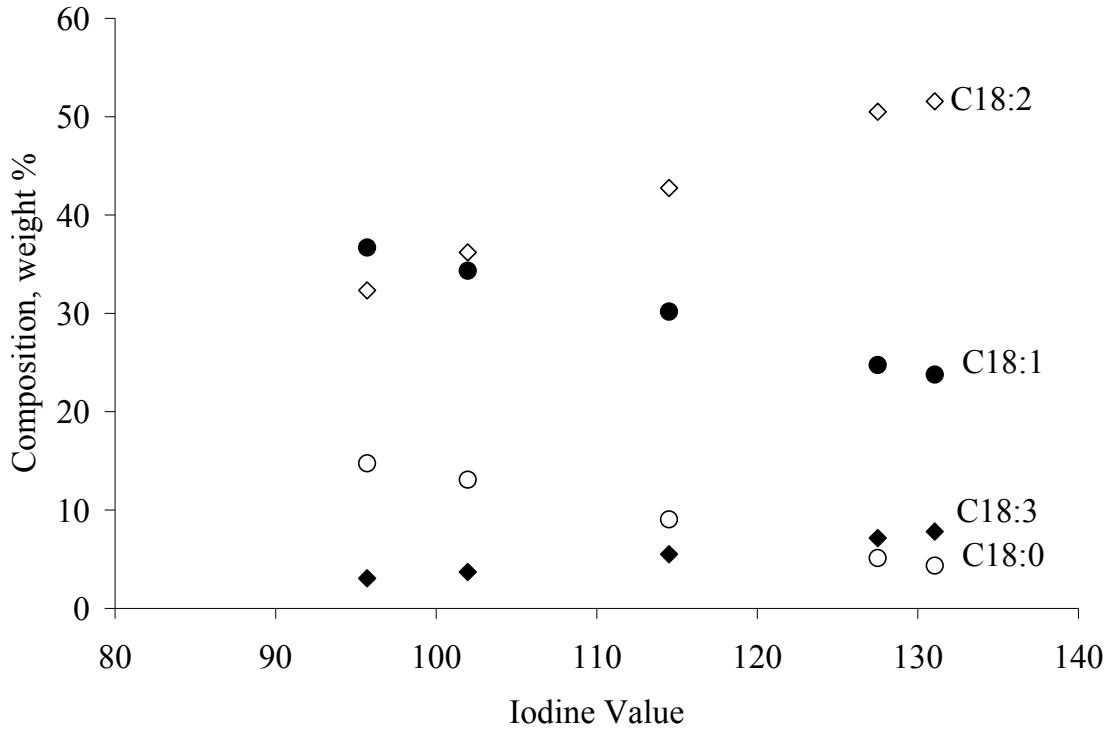

Figure B-14: Composition of soybean oil using platinum decorated polymeric membrane. Reaction conditions: 70 °C, 50 psig hydrogen pressure.

Table B-8: Properties of membrane used for hydrogenation run.

H_2 flux [GPU]	Ideal gas selectivity $\alpha_{H2/N2}$	H_2 flux [GPU]	Ideal gas selectivity $\alpha_{H2/N2}$	Catalyst (Sputtering time , s)
Before sputtering		*After sputtering*		Pt (6)
24	136	15	196	

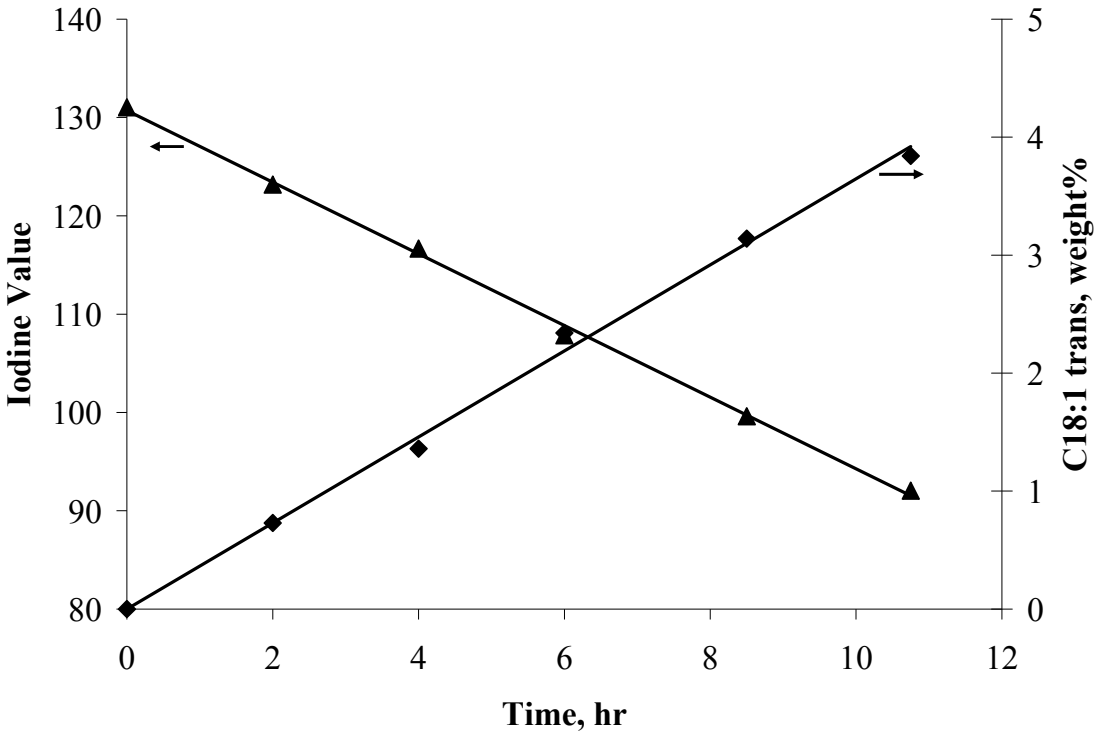

Figure B-15: TFA formation during hydrogenation of soybean oil using platinum decorated polymeric membrane. Reaction conditions: 70 °C, 50 psig hydrogen pressure.

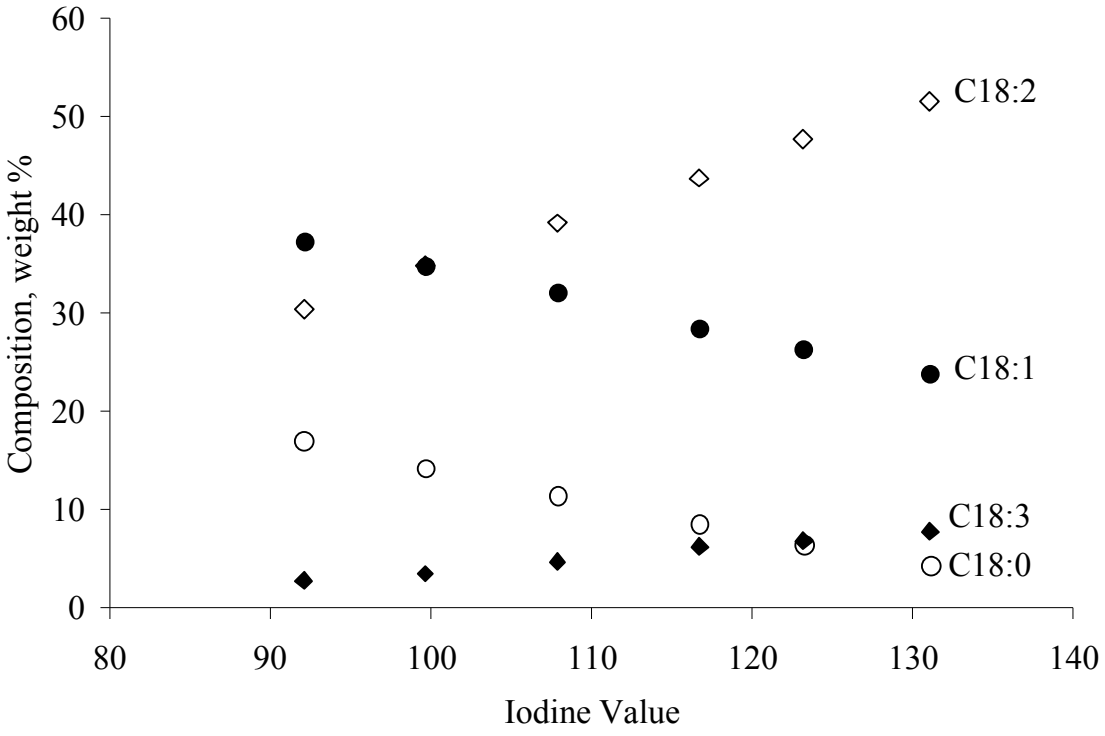

Figure B-16: Composition of soybean oil using platinum decorated polymeric membrane. Reaction conditions: 70 °C, 50 psig hydrogen pressure.

Table B-9: Properties of membrane used for hydrogenation run.

H_2 flux [GPU]	Ideal gas selectivity $\alpha_{H2/N2}$	H_2 flux [GPU]	Ideal gas selectivity $\alpha_{H2/N2}$	Catalyst (Sputtering time , s)
Before sputtering		*After sputtering*		Pt (6)
17	20	14	19	

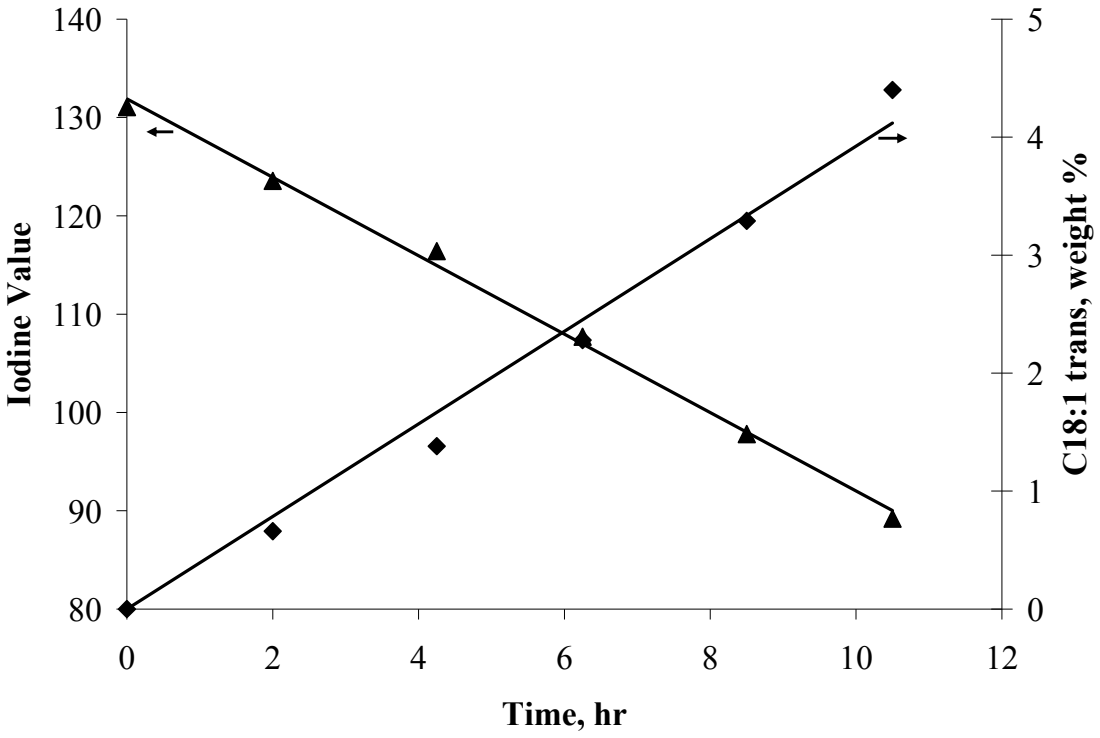

Figure B-17: TFA formation during hydrogenation of soybean oil using platinum decorated polymeric membrane. Reaction conditions: 70 °C, 50 psig hydrogen pressure.

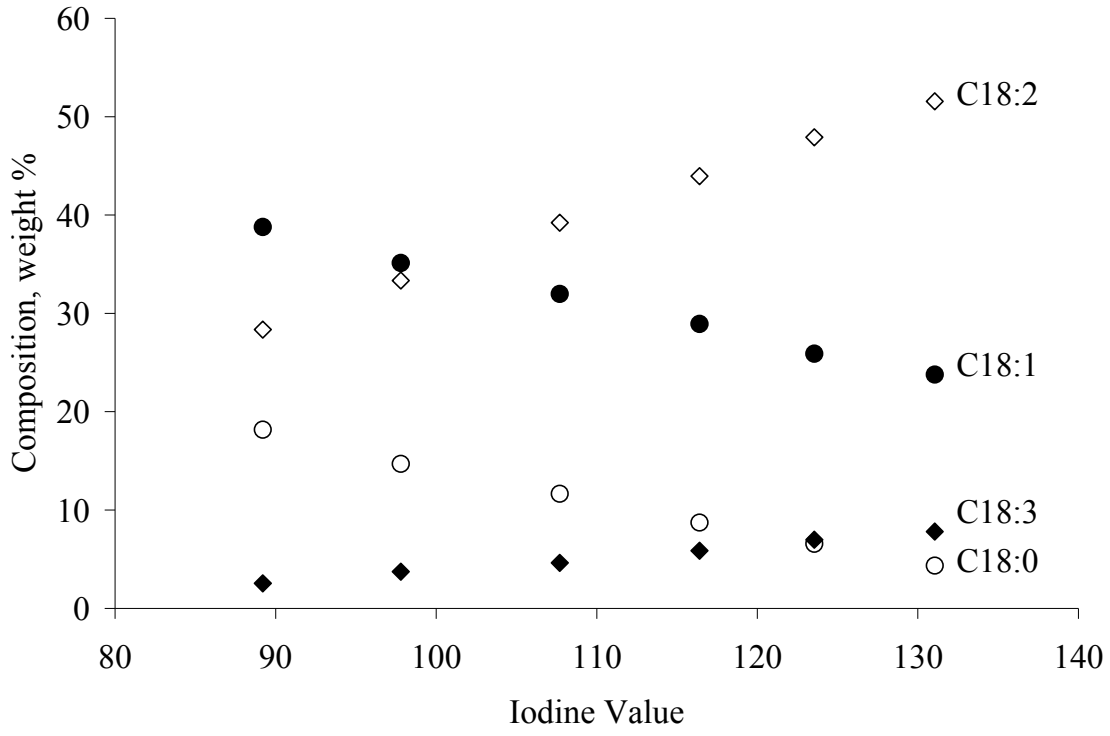

Figure B-18: Composition of soybean oil using platinum decorated polymeric membrane. Reaction conditions: 70 °C, 50 psig hydrogen pressure.

Table B-10: Properties of membrane used for hydrogenation run.

H_2 flux [GPU]	Ideal gas selectivity $\alpha_{H2/N2}$	H_2 flux [GPU]	Ideal gas selectivity $\alpha_{H2/N2}$	Catalyst (Sputtering time , s)
Before sputtering		*After sputtering*		
21	125	6	183	Pt (6)

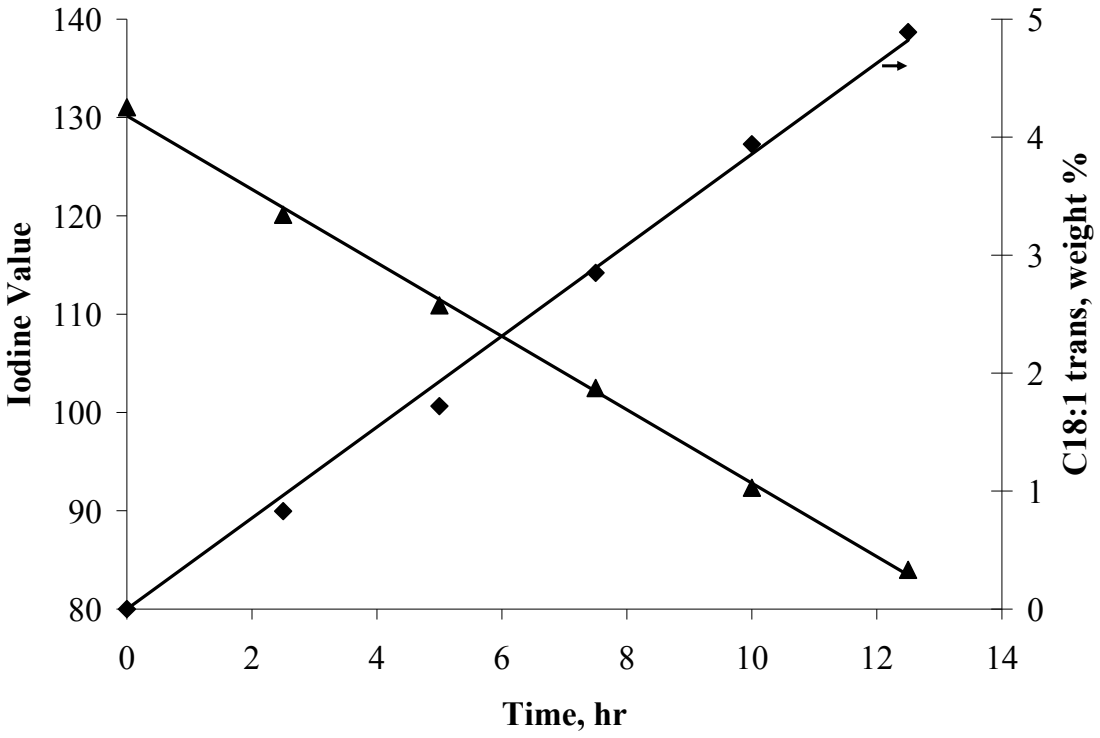

Figure B-19: TFA formation during hydrogenation of soybean oil using platinum decorated polymeric membrane. Reaction conditions: 70 °C, 50 psig hydrogen pressure.

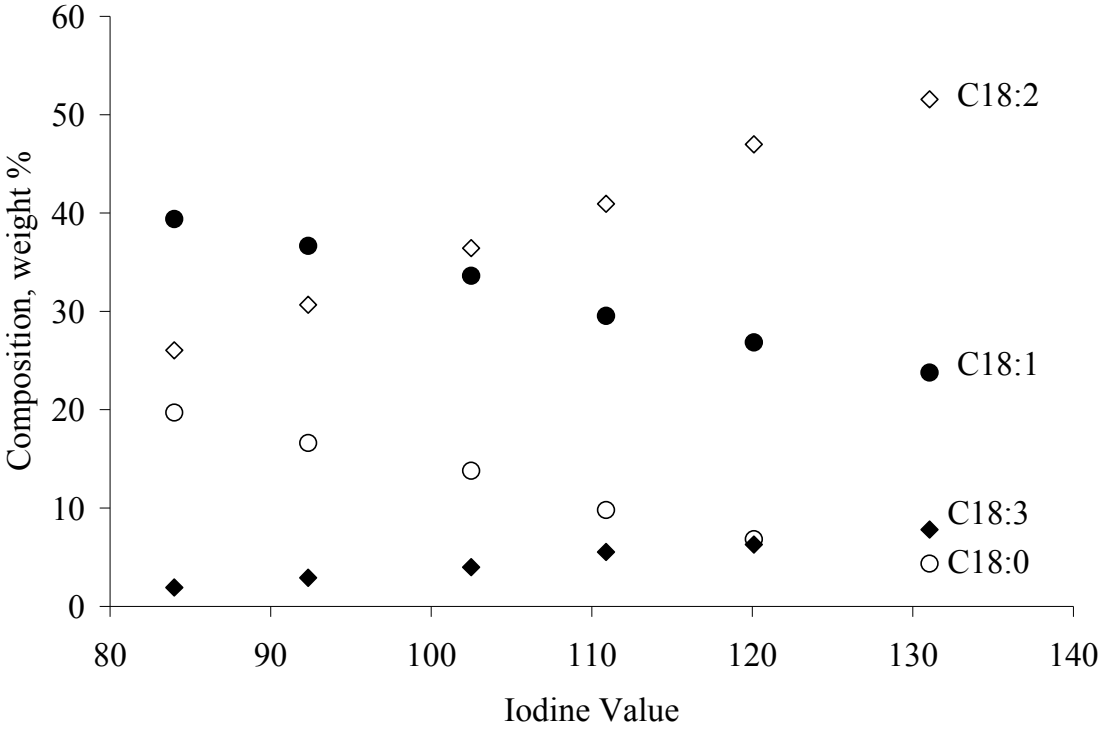

Figure B-20: Composition of soybean oil using platinum decorated polymeric membrane. Reaction conditions: 70 °C, 50 psig hydrogen pressure.

Table B-11: Properties of membrane used for hydrogenation run.

H_2 flux [GPU]	Ideal gas selectivity $\alpha_{H2/N2}$	H_2 flux [GPU]	Ideal gas selectivity $\alpha_{H2/N2}$	Catalyst (Sputtering time , s)
Before sputtering		*After sputtering*		Pt (6)
77	17	19	5	

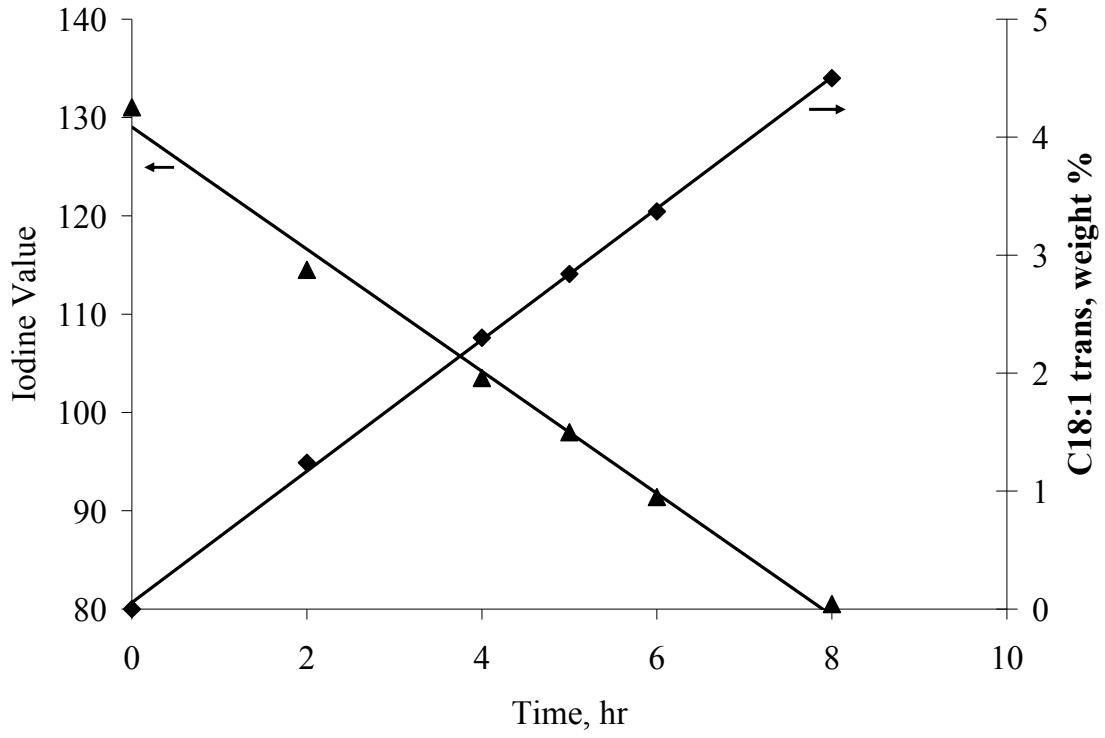

Figure B-21: TFA formation during hydrogenation of soybean oil using platinum decorated polymeric membrane. Reaction conditions: 70 °C, 50 psig hydrogen pressure.

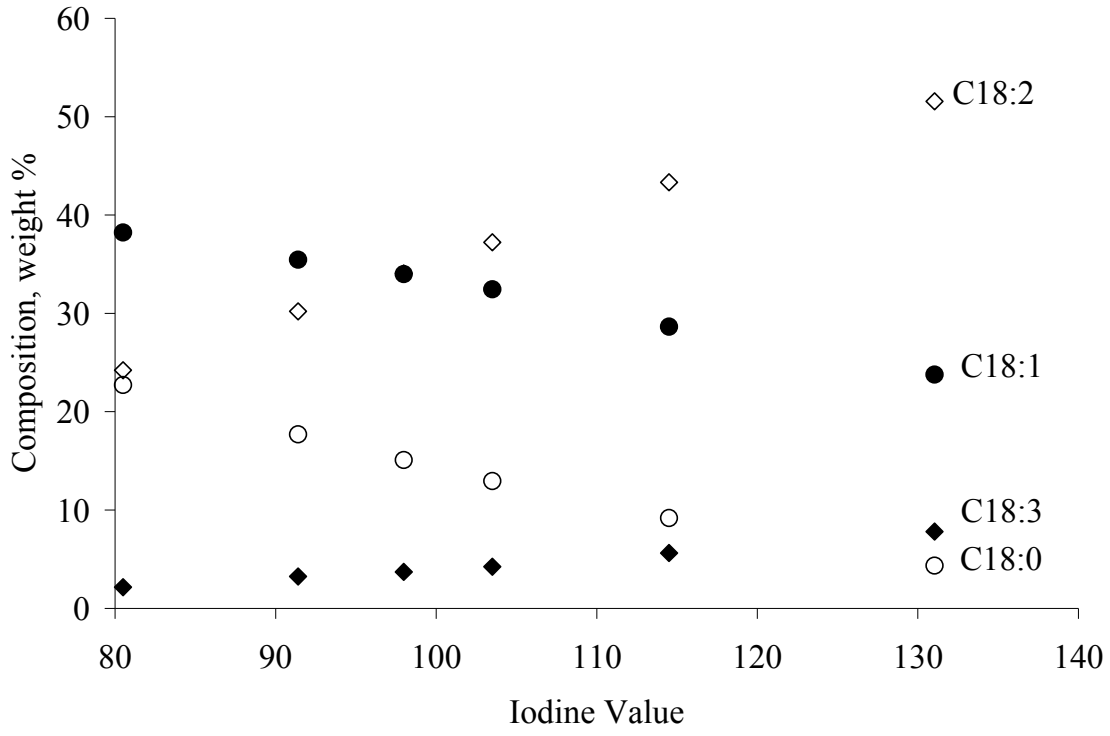

Figure B-22: Composition of soybean oil using platinum decorated polymeric membrane. Reaction conditions: 70 °C, 50 psig hydrogen pressure.

Table B-12: Properties of membrane used for hydrogenation run.

H_2 flux [GPU]	Ideal gas selectivity $\alpha_{H2/N2}$	H_2 flux [GPU]	Ideal gas selectivity $\alpha_{H2/N2}$	Catalyst (Sputtering time , s)
Before sputtering		*After sputtering*		Pt (3)
29	147	8	222	

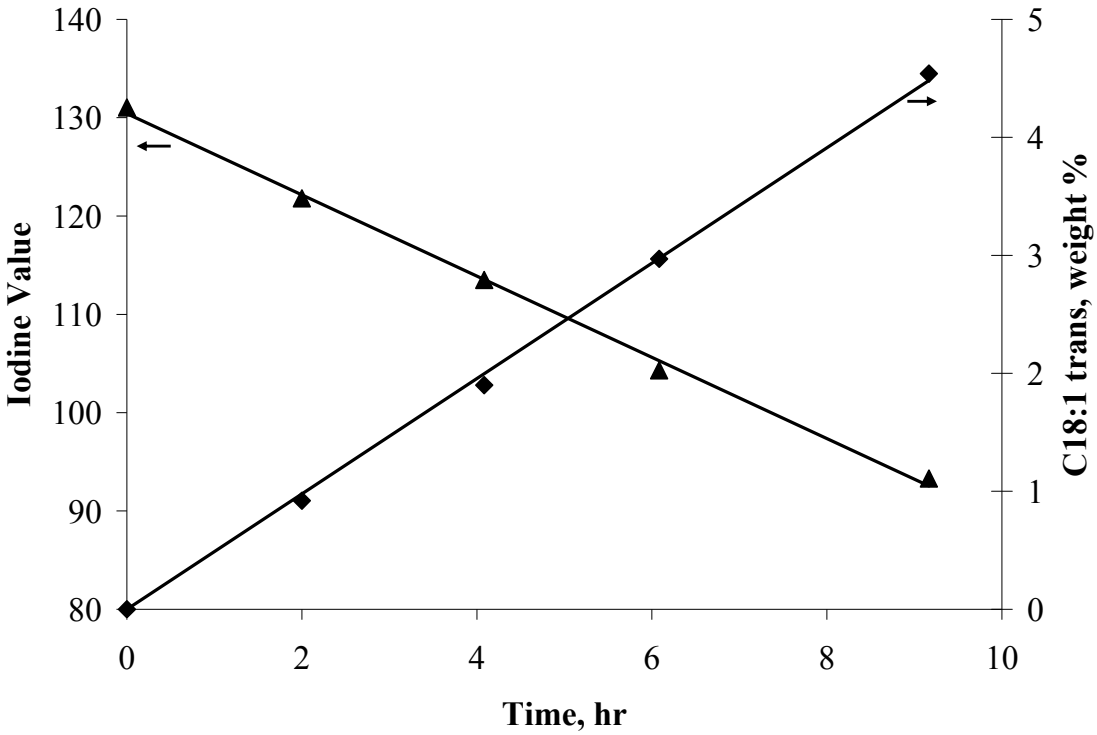

Figure B-23: TFA formation during hydrogenation of soybean oil using platinum decorated polymeric membrane. Reaction conditions: 70 °C, 50 psig hydrogen pressure.

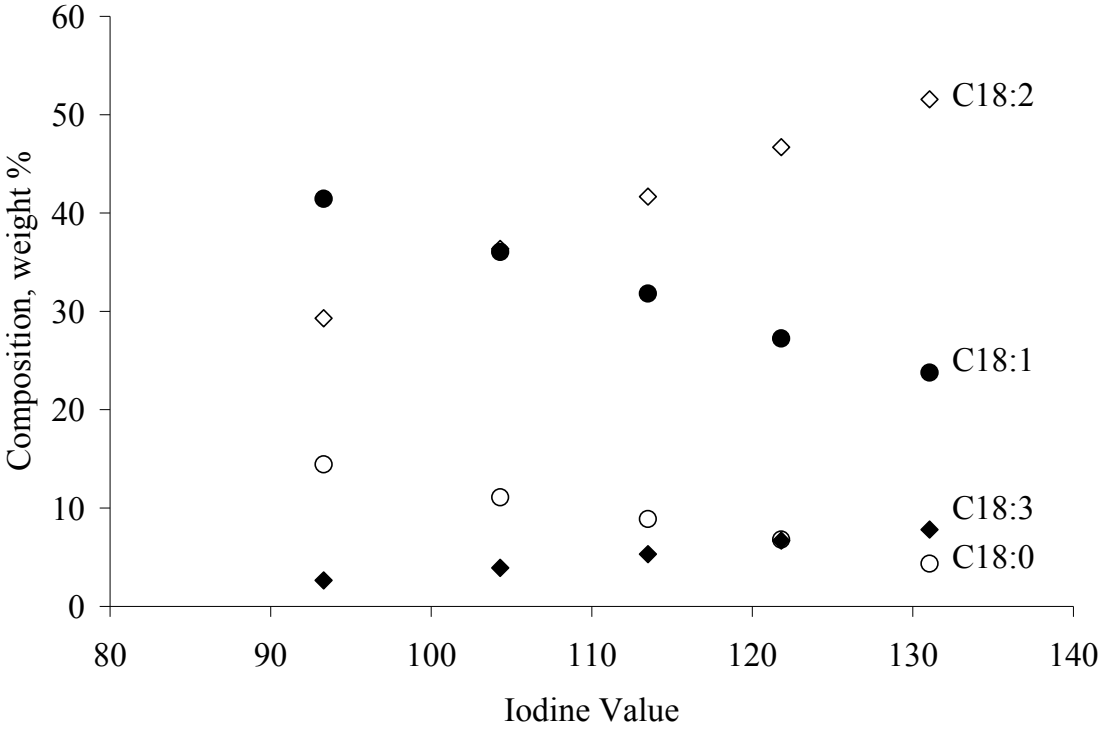

Figure B-24: Composition of soybean oil using platinum decorated polymeric membrane. Reaction conditions: 70 °C, 50 psig hydrogen pressure.

Table B-13: Properties of membrane used for hydrogenation run.

H_2 flux [GPU]	Ideal gas selectivity $\alpha_{H2/N2}$	H_2 flux [GPU]	Ideal gas selectivity $\alpha_{H2/N2}$	Catalyst (Sputtering time , s)
Before sputtering		*After sputtering*		Pt (3)
35	169	15	201	

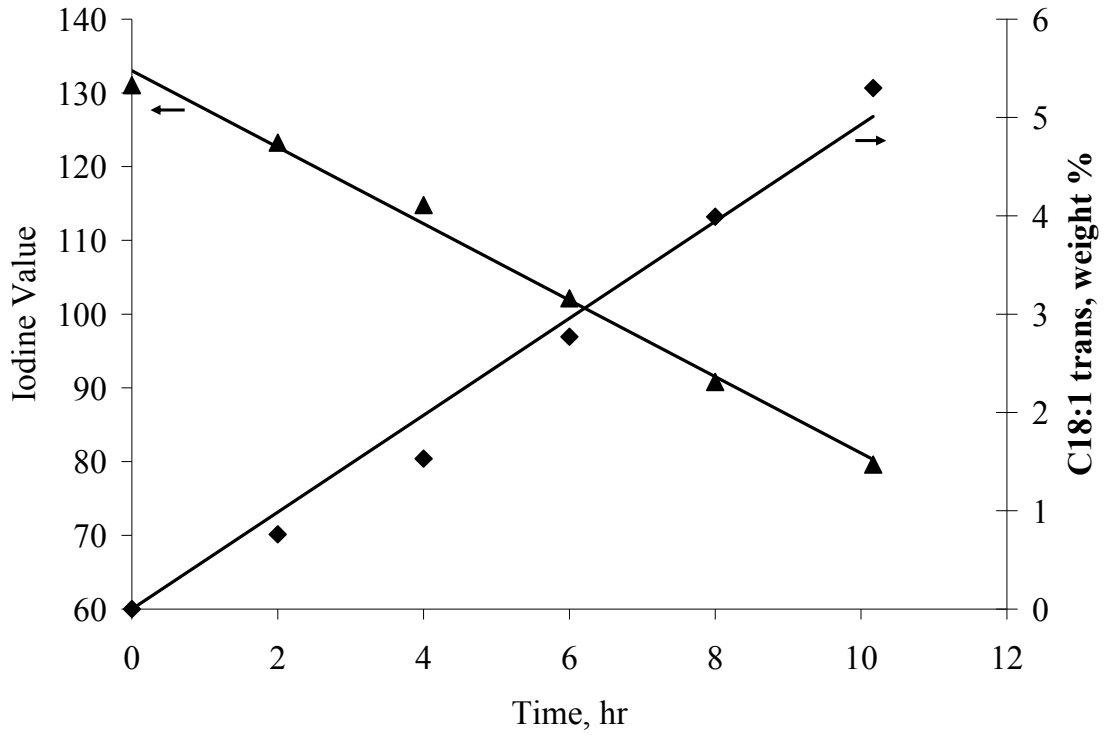

Figure B-25: TFA formation during hydrogenation of soybean oil using platinum decorated polymeric membrane. Reaction conditions: 70 °C, 50 psig hydrogen pressure.

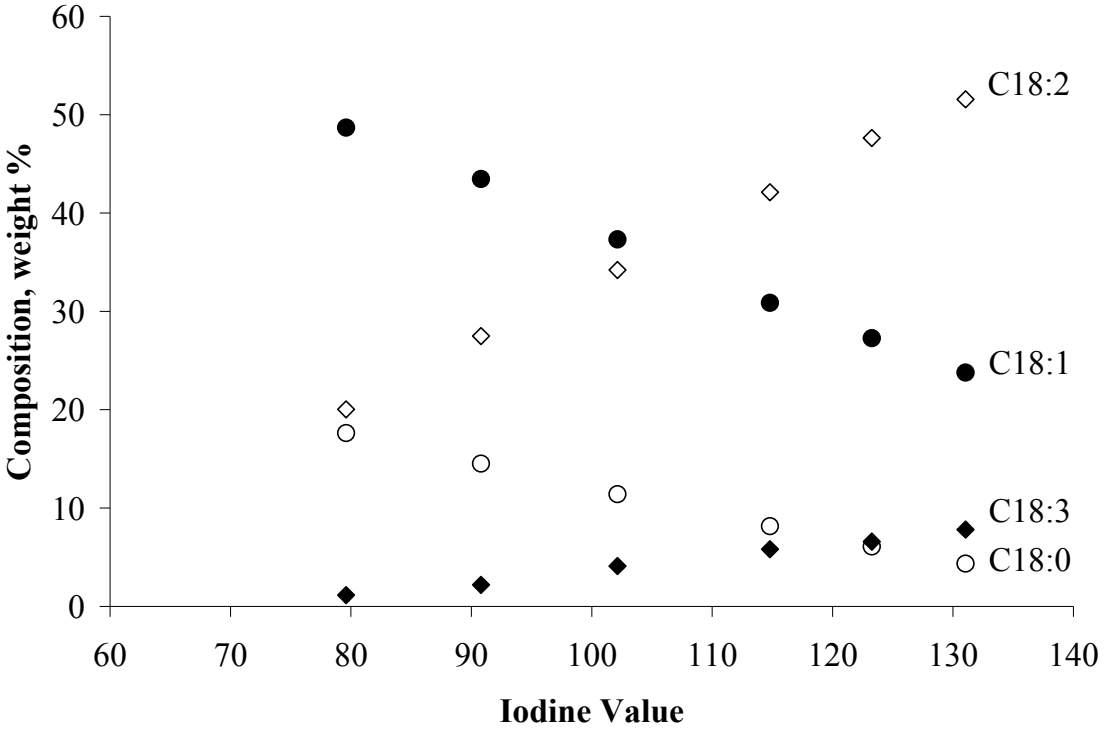

Figure B-26: Composition of soybean oil using platinum decorated polymeric membrane. Reaction conditions: 70 °C, 50 psig hydrogen pressure.

Table B-14: Properties of membrane used for hydrogenation run.

H_2 flux [GPU]	Ideal gas selectivity $\alpha_{H2/N2}$	H_2 flux [GPU]	Ideal gas selectivity $\alpha_{H2/N2}$	Catalyst (Sputtering time , s)
Before sputtering		*After sputtering*		Pt (3)
38	13	13	4	

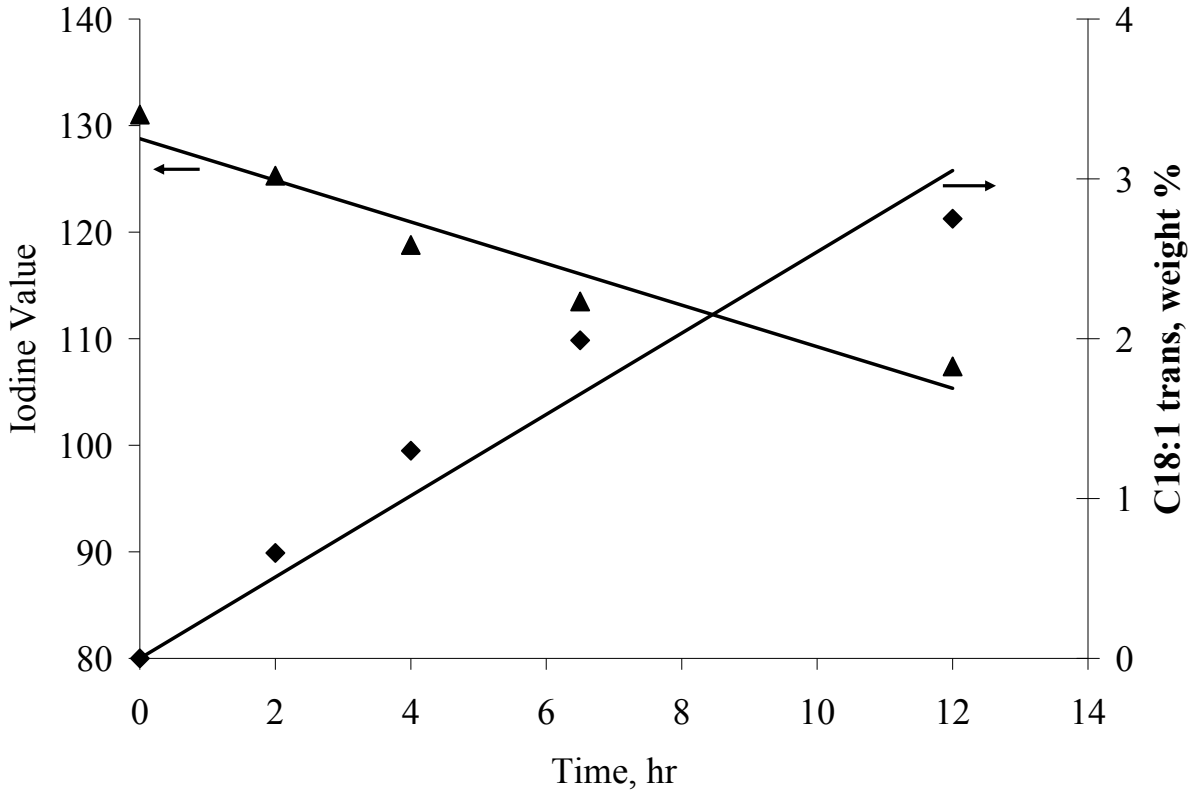

Figure B-27: TFA formation during hydrogenation of soybean oil using platinum decorated polymeric membrane. Reaction conditions: 70 °C, 50 psig hydrogen pressure.

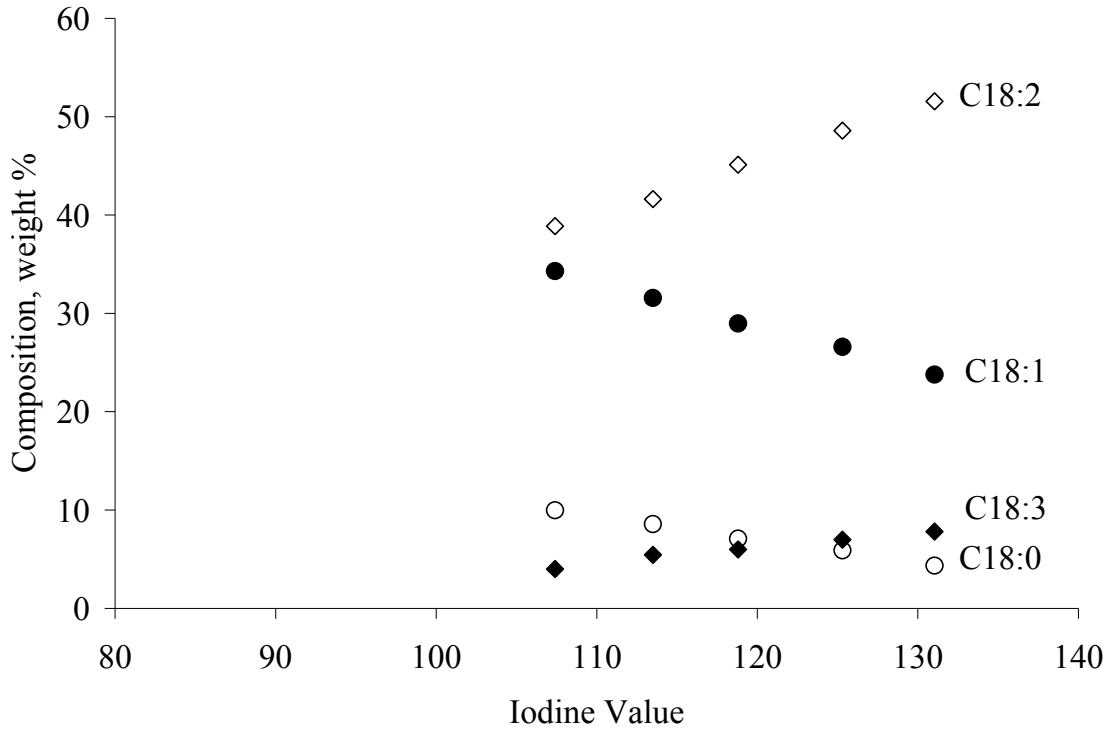

Figure B-28: Composition of soybean oil using platinum decorated polymeric membrane. Reaction conditions: 70 °C, 50 psig hydrogen pressure.

Table B-15: Properties of membrane used for hydrogenation run.

H_2 flux [GPU]	**Ideal gas selectivity $\alpha_{H2/N2}$**	**H_2 flux [GPU]**	**Ideal gas selectivity $\alpha_{H2/N2}$**	**Catalyst (Sputtering time , s)**
Before sputtering		*After sputtering*		
40	27	22	14	Pt (3)

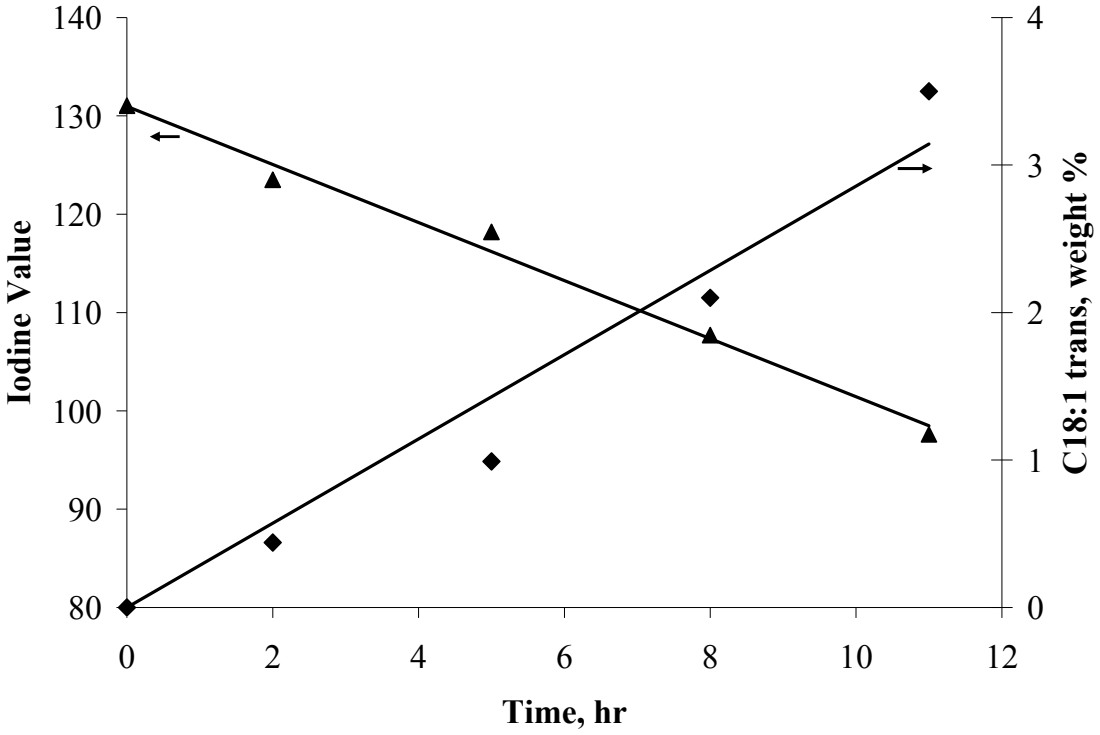

Figure B-29: TFA formation during hydrogenation of soybean oil using platinum decorated polymeric membrane. Reaction conditions: 70 °C, 50 psig hydrogen pressure.

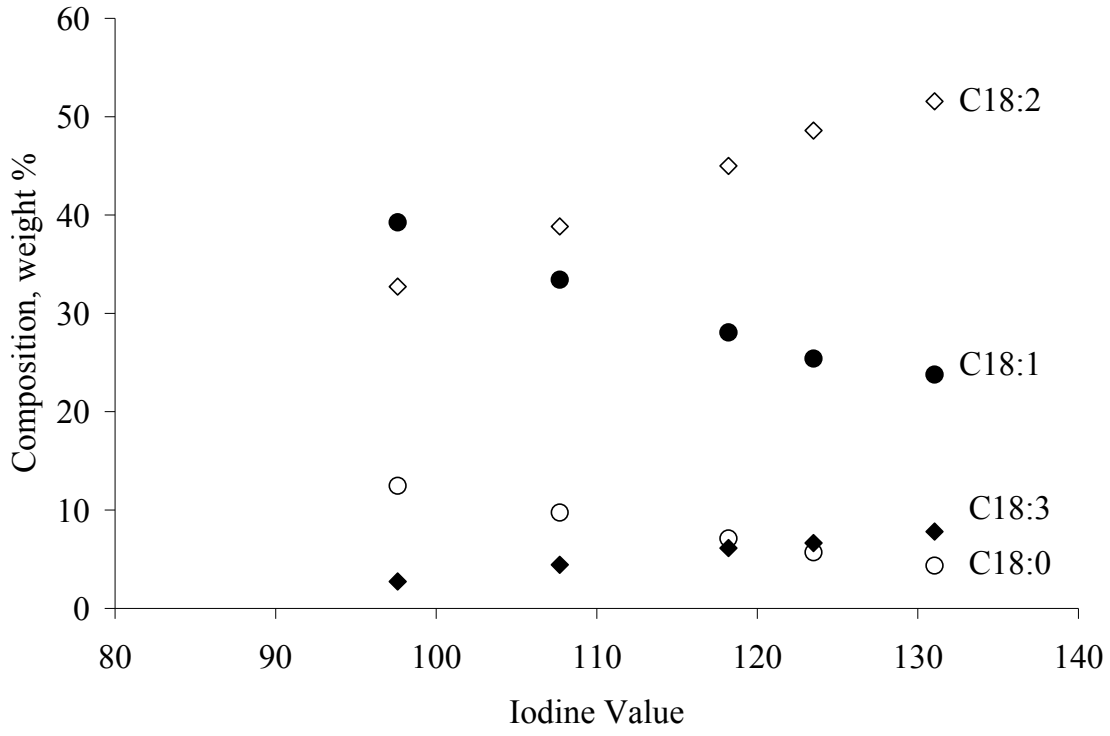

Figure B-30: Composition of soybean oil using platinum decorated polymeric membrane. Reaction conditions: 70 °C, 50 psig hydrogen pressure.

Table B-16: Properties of membrane used for hydrogenation run.

H_2 flux [GPU]	Ideal gas selectivity $\alpha_{H2/N2}$	H_2 flux [GPU]	Ideal gas selectivity $\alpha_{H2/N2}$	Catalyst (Sputtering time , s)
Before sputtering		*After sputtering*		Pt (9)
27	71	4	18	

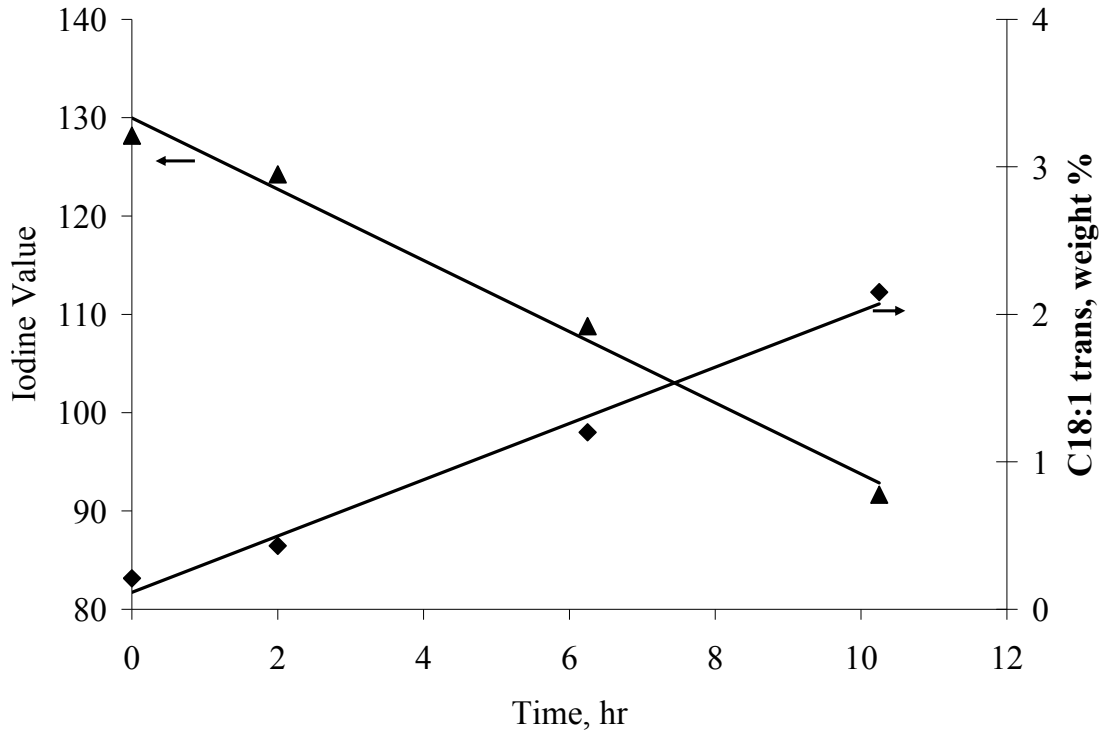

Figure B-31: TFA formation during hydrogenation of soybean oil using platinum decorated polymeric membrane. Reaction conditions: 60 °C, 50 psig hydrogen pressure.

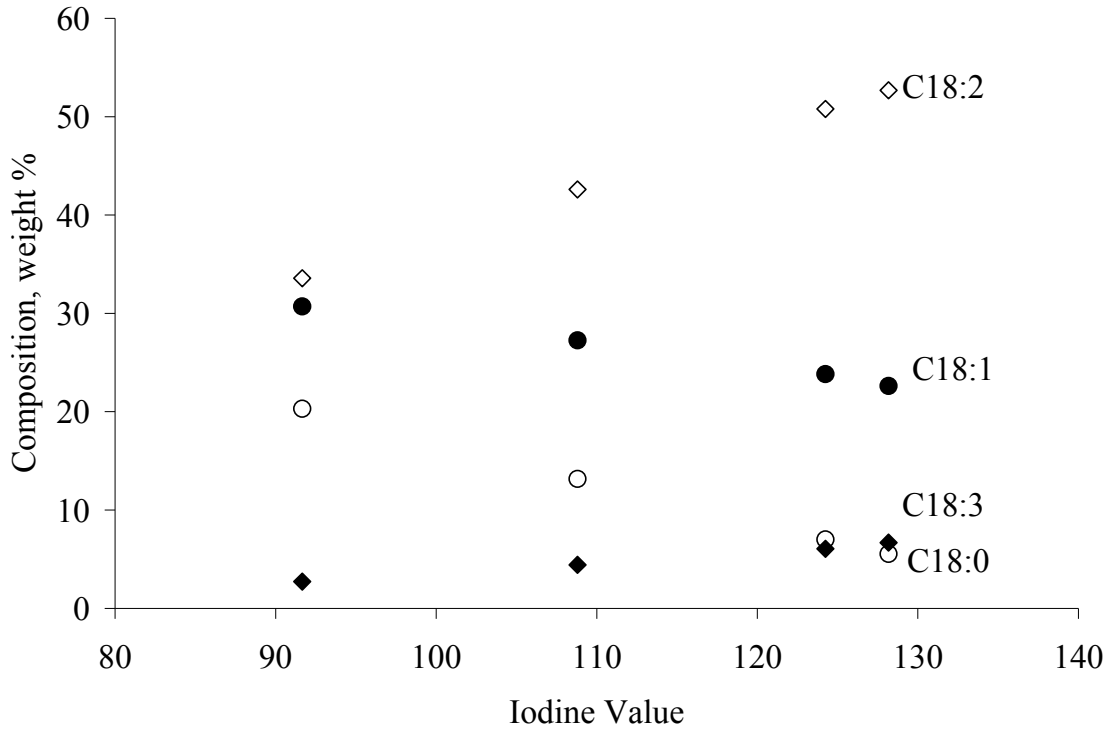

Figure B-32: Composition of soybean oil using platinum decorated polymeric membrane. Reaction conditions: 60 °C, 50 psig hydrogen pressure.

Table B-17: Properties of membrane used for hydrogenation run.

H_2 flux [GPU]	Ideal gas selectivity $\alpha_{H2/N2}$	H_2 flux [GPU]	Ideal gas selectivity $\alpha_{H2/N2}$	Catalyst (Sputtering time , s)
Before sputtering		*After sputtering*		Pt (9)
71	18	46	65	

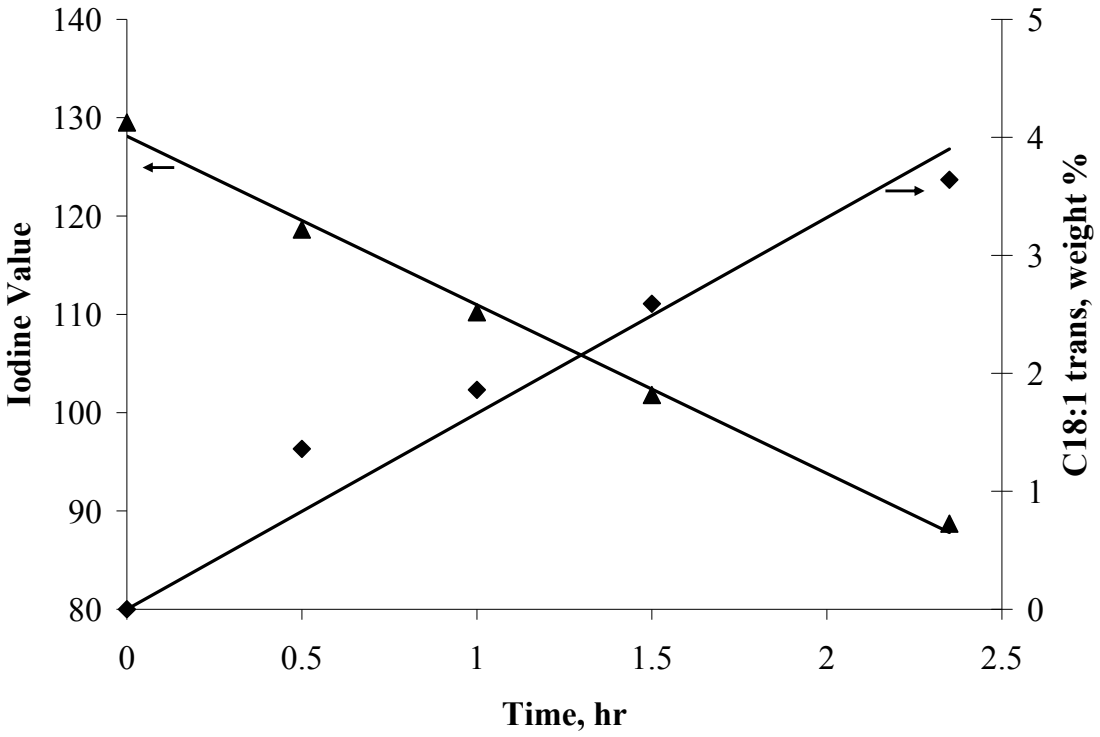

Figure B-33: TFA formation during hydrogenation of soybean oil using platinum decorated polymeric membrane. Reaction conditions: 90 °C, 50 psig hydrogen pressure.

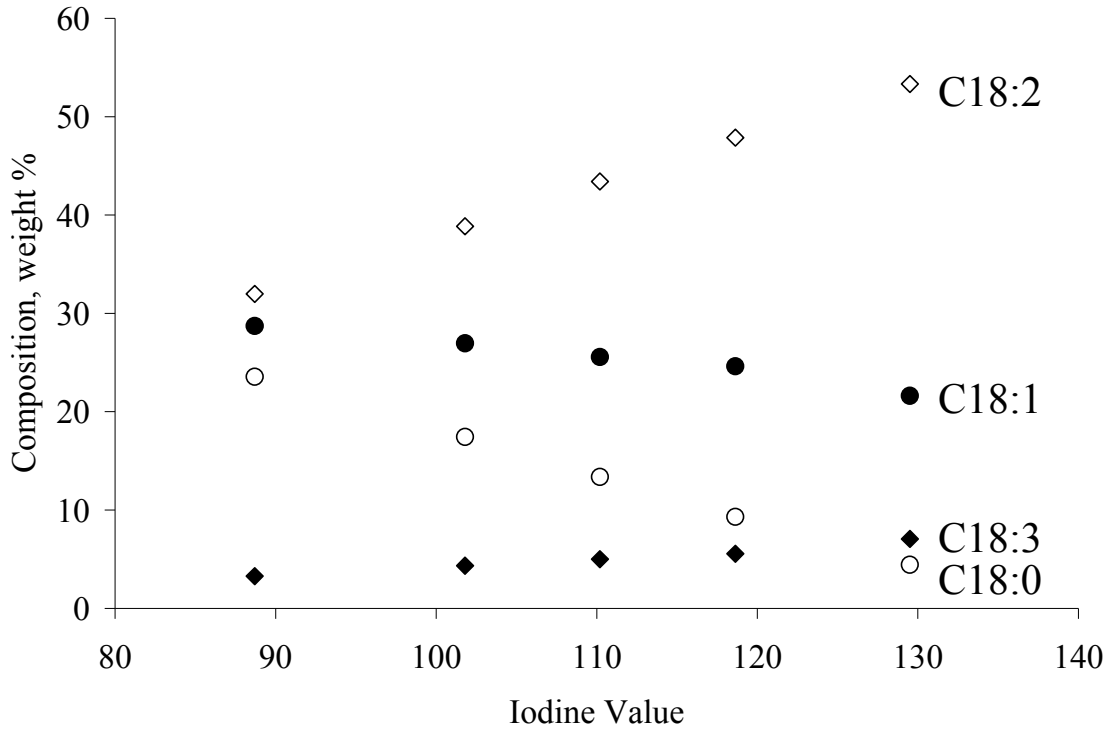

Figure B-34: Composition of soybean oil using platinum decorated polymeric membrane. Reaction conditions: 90 °C, 50 psig hydrogen pressure.